

---

Wayne State University Dissertations

---

January 2019

## Functional Characterization Of Accessory Proteins And Novel Activities In Direct And Indirect Trna Aminoacylation

Udumbara Menike Rathnayake  
Wayne State University, rathnayake.udumbara@gmail.com

Follow this and additional works at: [https://digitalcommons.wayne.edu/oa\\_dissertations](https://digitalcommons.wayne.edu/oa_dissertations)

 Part of the [Biochemistry Commons](#), and the [Chemistry Commons](#)

---

### Recommended Citation

Rathnayake, Udumbara Menike, "Functional Characterization Of Accessory Proteins And Novel Activities In Direct And Indirect Trna Aminoacylation" (2019). *Wayne State University Dissertations*. 2244.  
[https://digitalcommons.wayne.edu/oa\\_dissertations/2244](https://digitalcommons.wayne.edu/oa_dissertations/2244)

This Open Access Dissertation is brought to you for free and open access by DigitalCommons@WayneState. It has been accepted for inclusion in Wayne State University Dissertations by an authorized administrator of DigitalCommons@WayneState.

**FUNCTIONAL CHARACTERIZATION OF ACCESSORY PROTEINS AND NOVEL  
ACTIVITIES IN DIRECT AND INDIRECT TRNA AMINOACYLATION**

by

**UDUMBARA MENIKE RATHNAYAKE**

**DISSERTATION**

Submitted to the Graduate School

of Wayne State University,

Detroit, Michigan

in partial fulfillment of the requirements

for the degree of

**DOCTOR OF PHILOSOPHY**

2019

MAJOR: CHEMISTRY (Biochemistry)

Approved by:

---

Advisor

Date

---

---

---

## **DEDICATION**

This dissertation is dedicated to my mother (Mrs. Kusuma Munasinghe), my father (Mr. Premakumara Rathnyake), my husband (Mr. Harsha Amarasekara), and my lovely daughter (Anuki Amarasekara). Thank you for your endless love, support, guidance, and sacrifice.

## ACKNOWLEDGMENTS

First and foremost, I would like to express my sincere gratitude to my advisor, Professor Tamara L. Hendrickson, for her continuous support, guidance, and encouragement during my graduate studies at Wayne State University. I really appreciate the excellent atmosphere she created in our lab that encouraged me to develop and mature into the scientist I am today. Without her infectious personality, rewarding guidance, and constant encouragement, I would never have been able to succeed in my life at Wayne State University. Especially, thank you for being like a mother and a dear friend in my life at times when I needed my family and friends. It was such a great privilege to work under your guidance. With my deepest gratitude, I sincerely thank you and I wish you all the very best for your future.

I would like to extend my sincere gratitude to my dissertation committee, Professor Andrew L. Feig, Professor Claudio N. Verani, and Professor Steven M. Firestine for their time, consideration, invaluable support, and comments given throughout my studies. I am also thankful to Professor Andrew L. Feig, Professor Ashok S. Bhagwat, Professor Christine S. Chow, Professor Mary Kay Pflum, and Professor Thomas H. Linz for allowing me to use equipment in their labs. I would also like to thank Professor Young-Hoon Ahn for writing recommendation letters on my behalf. I would like to thank Wayne State University and personal donors for providing funding to pursue my Ph.D. Further, I would like to thank Dr. Kelly Sheppard, Dr. Babak Javid, and Dr. Takuya Ueda for providing tRNA and aaRS clones.

My greatest appreciation and sincere gratitude also go to all past Hendrickson group members. I especially thank, Dr. Gayathri Silva, Dr. Dilani Gamage, and Dr.

Sandamali Ekanayaka, who were always there for me as my closest sisters during my struggles and frustrations. Thank you, Dr. Liangjun Zhao and Dr. Shirin Fathima for all the assistance during my early years at Wayne State University. I am also thankful to all the past undergraduates who work with me during my time in Hendrickson lab. Thank you, Suwimon Suebka and Rongjun Caliburn Cai, for visiting us and sharing your experience and knowledge with me. Special thank goes to Dr. Travis Ness and Dr. Whitney Wood for their support, motivation, lookout, and friendship during the last seven years of my life. Thank you for being my family.

My greatest gratitude goes to all my Sri Lankan friends for your love and friendship in a country far away from our motherland.

I would like to express my gratitude to my parents, my sisters, my in-laws, my relatives, and my friends for believing in me, loving me and supporting me throughout my entire life. Last but not least, I am utterly grateful to my loving husband and my daughter for their kindness, motivation, and all the sacrifices they have made during this time. It is your endless love and belief in me that made me the person I am today. Thank you so much for being a part of my life.

## TABLE OF CONTENTS

DEDICATION .....	ii
ACKNOWLEDGMENTS .....	iii
LIST OF TABLES .....	xi
LIST OF FIGURES .....	xii
LIST OF ABBREVIATIONS .....	xv
CHAPTER 1 .....	1
1.1 Protein biosynthesis machinery in bacteria .....	1
1.2 Aminoacyl-tRNA synthetases (aaRSs): mechanisms, classifications, and editing activities .....	3
1.2.1 Mechanism of aminoacylation .....	3
1.2.2 Classification of aaRSs .....	4
1.2.3 aaRSs editing activities .....	6
1.3 Direct and indirect tRNA aminoacylation .....	7
1.3.2 Indirect tRNA aminoacylation pathways .....	8
1.4 Discriminating and non-discriminating AspRS .....	12
1.5 GatCAB, bacterial glutamine-dependent amidotransferase .....	14
1.6 Macromolecular transamidosome complexes in indirect tRNA aminoacylation ...	17
1.6.1 The Asn-transamidosome .....	18
1.6.2 The Gln-transamidosome .....	21
1.6.3 Asn-transamidosomes versus Gln-transamidosomes: Current understanding and future directions .....	23

1.7 Inducing mistranslation as a stress response by disrupting indirect tRNA aminoacylation .....	24
1.8 Hp0100, a component of the <i>H. pylori</i> Asn-transamidosome .....	27
1.9 Hp0100 and the truncated ortholog Sa2591 and queuosine biosynthesis .....	32
1.10 Dissertation research .....	34
CHAPTER 2 .....	36
2.1 Introduction .....	36
2.2 Results .....	37
2.2.1 Several putative accessory proteins are co-purified with <i>M. smegmatis</i> GatCAB constructs .....	37
2.2.2 Overexpression of GatCAB in <i>M. smegmatis</i> results in the co-purification of ND-AspRS and ND-GluRS .....	39
2.2.3 The substrate specificity conundrum of <i>M. smegmatis</i> ND-AspRS .....	42
2.2.4 ND-AspRS and GatCAB assemble into an Asn-transamidosome .....	44
2.3 Discussion .....	45
2.4 Materials and Methods .....	47
2.4.1 Materials .....	47
2.4.2 Overexpression and purification of <i>M. smegmatis</i> GatCAB, GatB, and GatCA .....	47
2.4.3 Overexpression and purification of <i>M. smegmatis</i> ND-AspRS and ND-GluRS .....	49
2.4.4 <i>In vivo</i> expression and purification of tRNAs .....	49
2.4.5 Aminoacylation assays with purified GatCAB .....	49
2.4.6 Aminoacylation assays with purified recombinant <i>M. smegmatis</i> ND-AspRS and ND-GluRS from <i>E. coli</i> .....	50

2.4.7 Mass spectrometric analysis of co-purified protein bands from <i>M. smegmatis</i> GatCAB purification .....	50
2.4.8 Transamidosome assembly analysis by electrophoretic mobility shift assays	50
CHAPTER 3 .....	52
3.1 Introduction .....	52
3.2 Results .....	57
3.2.1 <i>H. pylori</i> ND-AspRS appears to aminoacylate <i>H. pylori</i> tRNA <sup>Gln</sup> with aspartate and glutamate.....	57
3.2.2 <i>H. pylori</i> ND-AspRS aminoacylates <i>E. coli</i> tRNA <sup>Glu</sup> with glutamate to produce Glu-tRNA <sup>Glu</sup> .....	62
3.2.3 Glu-tRNA <sup>Glu</sup> production is common among bacterial non-discriminating and discriminating AspRSs.....	66
3.3 Discussion.....	68
3.4 Materials and Methods.....	72
3.4.1 Materials.....	72
3.4.2 Overexpression and purification of aaRSs.....	72
3.4.3 <i>In vivo</i> transcription and purification of tRNAs .....	74
3.4.4 Initial rate aminoacylation assays .....	74
3.4.5 Extended aminoacylation assays (90 min) by aaRSs .....	75
3.4.6 Acid gel electrophoresis and Northern blot analysis .....	75
CHAPTER 4 .....	77
4.1 Introduction .....	77
4.2 Results .....	79



4.2.1 Cloning, overexpression and purification of untagged Hp0100.....	81
4.2.2 Cloning, and overexpression of GST-Thrombin-Hp0100.....	82
4.2.3 Cloning, overexpression and purification of His <sub>6</sub> -TEV-Hp0100.....	83
4.2.4 Cloning, overexpression and purification of His <sub>6</sub> -SUMO-TEV-Hp0100.....	86
4.3 Discussion.....	87
4.4 Materials and Methods.....	89
4.4.1 Materials .....	89
4.4.2 Cloning of untagged WT and mutant Hp0100.....	90
4.4.2 Overexpression and purification of untagged WT Hp0100 .....	91
4.4.3 Cloning and overexpression of GST-Hp0100 .....	92
4.4.4 Cloning, overexpression and purification of His <sub>6</sub> -TEV-Hp0100.....	93
4.4.5 Cloning and overexpression of His <sub>6</sub> -SUMO-TEV-Hp0100.....	96
CHAPTER 5 .....	98
5.1 Introduction .....	98
5.2 Results.....	103
5.2.1 Sa2591 does not affect the GatCAB-catalyzed transamidation of <i>in vitro</i> transcribed <i>S. aureus</i> Asp-tRNA <sup>Asn</sup> to Asn-tRNA <sup>Asn</sup> .....	103
5.2.2 <i>S. aureus</i> GatCAB does not transaminate <i>H. pylori</i> Asp-tRNA <sup>Asn</sup> .....	106
5.3 Discussion.....	107
5.4 Materials and Methods.....	109
5.4.1 Materials.....	109
5.4.2 Overexpression and purification of <i>S. aureus</i> Sa2591.....	110

5.4.3 Overexpression and purification of <i>S. aureus</i> ND-AspRS.....	111
5.4.4 Overexpression and purification of <i>S. aureus</i> GatCAB.....	111
5.4.5 <i>In vitro</i> transcription and quantification of <i>S. aureus</i> tRNA <sup>Asn</sup> .....	112
5.4.6 <sup>32</sup> P/nuclease P1 GatCAB transamidation assays .....	113
CHAPTER 6.....	115
6.1 Introduction .....	115
6.2 The components of the indirect tRNA aminoacylation pathway of <i>M. smegmatis</i> assemble into an Asn-transamidosome.....	118
6.3 <i>M. smegmatis</i> GatCAB co-purified with other putative accessory proteins .....	119
6.4 Some bacterial AspRSs exhibits GluRS like activity .....	119
6.5 Hp0100 and Sa2591 are involved in indirect tRNA aminoacylation and exhibit different activities under different growth conditions .....	120
APPENDIX A.....	124
A.1 Introduction.....	124
A.2 Results.....	125
A.3 Discussion .....	128
A.4 Materials and Methods .....	130
A.4.1 Materials.....	130
A.4.2 Overexpression and purification of WT GatCAB and D185 mutants .....	131
A.4.3 <i>In vivo</i> transcription and purification of <i>H. pylori</i> tRNA <sup>Gln</sup> .....	131
A.4.4 <sup>32</sup> P/nuclease P1 GatCAB transamidation assays.....	132
APPENDIX B.....	133
REFERENCES.....	138

ABSTRACT ..... 160

AUTOBIOGRAPHIC STATEMENT ..... 162

## LIST OF TABLES

Table 1.1. Main features of the two classes of aaRSs. ....	5
Table 1.2. The two classes of aaRSs. ....	5
Table 1.3. AsnRS, AsnS and GlnRS gene distribution of <i>H. pylori</i> , <i>M. smegmatis</i> , and <i>S. aureus</i> . ....	11
Table 1.4. AspRS, AsnRS, AsnS and GatCAB gene distribution in bacteria. ....	13
Table 1.5. Asn-transamidosome complexes. ....	20
Table 1.6. Gln-transamidosome complexes. ....	22
Table 3.1. Summary of mutagenesis studies of AspRSs and ND-AspRSs anticodon-binding domains. ....	55
Table 3.2. The tRNA specific oligonucleotide sequences used in Northern blot analyses .....	76
Table 4.1. Plasmids encoding different variations of Hp0100. ....	80
Table 4.2. Oligonucleotide sequence used in LIC. ....	96
Table A.1. Initial rates for transamidation of WT and D185 GatCAB variants with NH <sub>4</sub> Cl as ammonia donor. ....	127

## LIST OF FIGURES

Figure 1.1. Bacterial protein translation.....	2
Figure 1.2. Aminoacylation of tRNAs.....	3
Figure 1.3. Aminoacylation and editing activity of the aaRSs.....	8
Figure 1.4. Direct and indirect biosynthesis of Asn-tRNA <sup>Asn</sup> and Gln-tRNA <sup>Gln</sup> in bacteria. .....	11
Figure 1.5. The three reactions catalyzed by GatCAB. ....	15
Figure 1.6. Mutations in GatCAB cause mistranslation and induce RSPR in <i>Mycobacteria</i> . ....	27
Figure 1.7. Yeast-2-hybrid interaction profile of Hp0100. ....	28
Figure 1.8. Proposed <i>H. pylori</i> Asn-transamidosome cycle.....	29
Figure 1.9. Hp0100 accelerates GatCAB-catalyzed transamidation of misacylated tRNAs. ....	30
Figure 1.10. Hp0100 contains two distinct ATPase active sites, which are activated by misacylated Asp-tRNA <sup>Asn</sup> and Glu-tRNA <sup>Gln</sup> . ....	31
Figure 1.11. The putative metal-binding motif of Hp0100.....	32
Figure 1.12. The final three steps in queuosine biosynthesis.....	34
Figure 2.1. Putative accessory proteins co-purify with GatCAB.....	39
Figure 2.2. SDS-PAGE gel analysis of GatCAB purification.....	40
Figure 2.3. <i>M. smegmatis</i> ND-AspRS and ND-GluRS co-purify with the overexpressed GatCAB in <i>M. smegmatis</i> cell line.....	41
Figure 2.4. <i>M. smegmatis</i> ND-AspRS and ND-GluRS assemble into a transamidosomes(s) with GatCAB. ....	42
Figure 2.5. <i>M. smegmatis</i> ND-AspRS aminoacylates at least one tRNA with glutamate. .....	44
Figure 2.6. Transamidosome evaluation by native gel electrophoresis. ....	45
Figure 3.1. Canonical roles of AspRS and ND-AspRS.....	53

Figure 3.2. Anticodon-binding domains of the archaeal-type and bacterial-type AspRSs..	56
Figure 3.3. Extended <i>H. pylori</i> tRNA <sup>Asn</sup> or tRNA <sup>Gln</sup> aminoacylation assays with <i>H. pylori</i> ND-AspRS and GluRS2 with aspartate versus glutamate. ....	59
Figure 3.4. Extended <i>M. smegmatis</i> tRNA <sup>Asn</sup> or tRNA <sup>Gln</sup> aminoacylation assays with <i>M. smegmatis</i> ND-AspRS and ND-GluRS with aspartate versus glutamate.....	60
Figure 3.5. <i>H. pylori</i> ND-AspRS shows unexpected aminoacylation activity with overexpressed <i>H. pylori</i> tRNA <sup>Gln</sup> suggesting cross-reactivity with <i>E. coli</i> tRNA. ....	61
Figure 3.6. <i>H. pylori</i> ND-AspRS aminoacylates <i>E. coli</i> tRNA <sup>Glu</sup> with glutamate producing Glu-tRNA <sup>Glu</sup> .....	63
Figure 3.7. SDS-PAGE of purified aaRSs. ....	64
Figure 3.8. <i>H. pylori</i> ND-AspRS attaches glutamate to an <i>E. coli</i> tRNA. ....	65
Figure 3.9. Extended total <i>E. coli</i> tRNA aminoacylation assays with <i>H. pylori</i> ND-AspRS and GluRS2 with aspartate versus glutamate. ....	65
Figure 3.10. Extended total <i>E. coli</i> tRNA aminoacylation assays with <i>M. smegmatis</i> ND-AspRS and ND-GluRS with aspartate versus glutamate. ....	66
Figure 3.11. Some bacterial AspRS's aminoacylate <i>E. coli</i> tRNA <sup>Glu</sup> with glutamate producing Glu-tRNA <sup>Glu</sup> .....	67
Figure 3.12. Sequence and secondary structure of <i>E. coli</i> tRNAs.....	71
Figure 4.1. Purification optimization of untagged Hp0100 protein.....	82
Figure 4.2. SDS-PAGE analysis of the overexpression of GST-thrombin-Hp0100 in <i>E. coli</i> BL21(DE3)-RIL.....	83
Figure 4.3. SDS-PAGE analysis of the overexpression of His <sub>6</sub> -TEV-codon optimized Hp0100 (pUD010) in <i>E. coli</i> DH5 $\alpha$ .....	85
Figure 4.4. SDS-PAGE analysis of His <sub>6</sub> -TEV-Hp0100 (pUD010) purification.....	86
Figure 4.5. SDS-PAGE analysis of overexpression of SUMO tagged Hp0100 in <i>E. coli</i> BL21(DE3)-RIL cell line. ....	87
Figure 5.1. Sequence similarities between Hp0100 and two putative truncated orthologs Sa2591 and Ng0682.....	100
Figure 5.2. Structural similarities between Hp0100.....	101

Figure 5.3. <i>E. coli</i> AspRS co-purifies with Sa2591. ....	101
Figure 5.4. Sa2591 is an ATPase that is activated by misacylated tRNAs. ....	103
Figure 5.5. Schematic representation of P1 nuclease transamidation assay. ....	105
Figure 5.6. Sa2591 does not affect Asn-tRNA <sup>Asn</sup> production by GatCAB. ....	105
Figure 5.7. <i>H. pylori</i> Asp-tRNA <sup>Asn</sup> is a poor substrate for <i>S. aureus</i> GatCAB. ....	106
Figure 6.1. Hp0100 is a multi-functional protein. ....	118
Figure 6.2. Schematic representation of the role of Hp0100 and Sa2591 under different growth conditions. ....	123
Figure A.1. The use of glutamine as an ammonia source for WT and D185 GatCAB mutants. ....	126
Figure A.2. The use of ammonium chloride as an ammonia source for WT and D185 GatCAB mutants. ....	127

## LIST OF ABBREVIATIONS

aa-AMP	Aminoacyl-AMP
aaRS	Aminoacyl-tRNA synthetase
aa-tRNA	Aminoacyl-tRNA
ADT	Adenosine diphosphate
AMP	Adenosine monophosphate
AsnRS	Asparaginyl-tRNA synthetase
AsnS	Asparagine synthetase
AspRS	Aspartyl-tRNA synthetase
ATP	Adenosine triphosphate
D	Discriminating
DNA	Deoxyribonucleic acid
DUF	Domain of unknown function
<i>E. coli</i>	<i>Escherichia coli</i>
EF-Tu	Elongation factor Tu
GatCAB	Asp-tRNA <sup>Asn</sup> /Glu-tRNA <sup>Gln</sup> amidotransferase
GlnRS	Glutaminyl-tRNA synthetase
GluRS	Glutamyl-tRNA synthetase
GTP	Guanosine triphosphate



<i>H. pylori</i>	<i>Helicobacter pylori</i>
<i>M. smegmatis</i>	<i>Mycobacterium smegmatis</i>
<i>M. tuberculosis</i>	<i>Mycobacterium tuberculosis</i>
mRNA	Messenger RNA
<i>N. gonorrhoeae</i>	<i>Neisseria gonorrhoeae</i>
NAD <sup>+</sup>	Nicotinamide adenine dinucleotide (oxidized)
NADH	Nicotinamide adenine dinucleotide (reduced)
ND	Non-discriminating
oQ	Epoxyqueuosine
PreQ <sub>1</sub>	7-Aminomethyl-7-deazaguanine
Q	Queuosine
QueA	S-Adenosylmethionine ribosyltransferase-isomerase
QueG	Cobalamine-dependent epoxyqueuosine reductase
RNA	Ribonucleic acid
<i>S. aureus</i>	<i>Staphylococcus aureus</i>
<i>T. thermophilus</i>	<i>Thermus thermophilus</i>
tRNA	Transfer RNA

## CHAPTER 1

### INTRODUCTION

#### INDIRECT BIOSYNTHESIS OF ASN-TRNA<sup>ASN</sup> AND GLN-TRNA<sup>GLN</sup> IN BACTERIA

Some parts of this chapter have been reproduced with permission from Rathnayake, U. M. \*; Wood, W. N. \*; and Hendrickson, T. L. Indirect tRNA aminoacylation during accurate translation and phenotypic mistranslation. *Curr. Opin. Chem. Biol.* **2017**, *41*, 114-122. \*

These authors contributed equally and are listed in alphabetical order. Copyright © 2017, Elsevier, reprinted with permission.

#### 1.1 Protein biosynthesis machinery in bacteria

Protein translation is a central, important process in living organisms. First, the genetic information stored in DNA is transcribed to messenger RNA (mRNA), which is then decoded by the ribosome to generate a specific amino acid sequence (1-2). Ribosomal protein translation has two phases (**Figure 1.1**). In phase I, the cognate tRNA is paired up with its cognate amino acid by a specific aminoacyl-tRNA synthetase (aaRS) to produce an aminoacyl-tRNA (aa-tRNA). During phase II, the aa-tRNA forms a ternary complex with elongation factor Tu (EF-Tu) and GTP and is loaded into the aminoacyl site (A site) of the ribosome via matching of the mRNA codons to the anticodon of tRNA. Next, peptide bond formation occurs between the amino acid on the tRNA in the A site of the ribosome with the growing polypeptide chain in the ribosome's peptidyl site (P site) (3). Finally, the fully translated peptide undergoes folding and post-translational modifications to yield a functional protein.

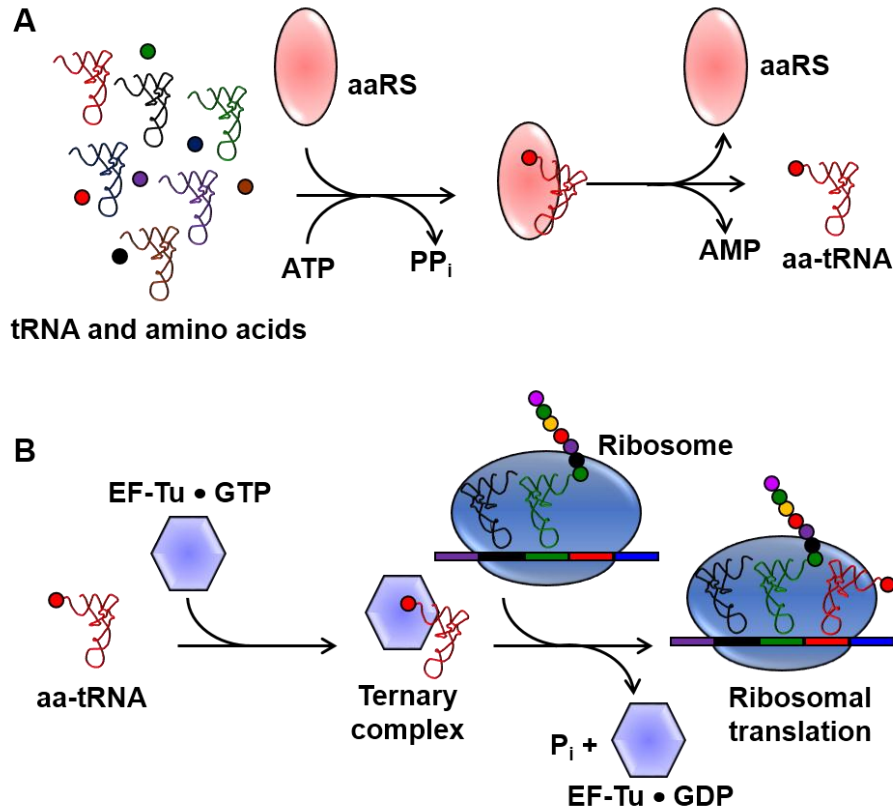


**Figure 1.1. Bacterial protein translation. (A)** Phase I of protein synthesis: tRNA is aminoacylated with its cognate amino acid in an ATP-dependent manner by the corresponding aaRS to produce an aa-tRNA. **(B)** Phase II of protein synthesis: aa-tRNA assembles in a ternary complex with EF-Tu and GTP and is loaded onto the ribosome for protein translation (3).

Protein translation is generally carried out with a high level of accuracy: Under low-stress conditions, only 1 out of every 10,000 mRNA codons is mistranslated (4-5). This error rate of translation results in ~15% of the proteome containing at least one misacylated amino acid under normal growth conditions (6-7). Many of these misacylated proteins are inactive and are degraded after translation. Nevertheless, a small subset of errors can be advantageous to an organism in stressful environments. This phenomenon will be discussed later in this chapter.

## 1.2 Aminoacyl-tRNA synthetases (aaRSs): mechanisms, classifications, and editing activities

As mentioned above, the aaRSs play a fundamental role in protein translation: these enzymes catalyze the aminoacylation of their cognate tRNA(s) with their cognate amino acid to produce a complete set of aa-tRNA.

### 1.2.1 Mechanism of aminoacylation

The synthesis of aa-tRNAs occurs in two steps: activation of the amino acid and linking of it to the cognate tRNA (**Figure 1.2**). To achieve tRNA aminoacylation, an aaRS first reacts its cognate amino acid with ATP to generate an enzyme-bound aminoacyl-adenylate (aa-AMP). In some cases, this step requires binding of tRNA to the aaRS (8-10). Next, the 2' or 3' hydroxyl group of the 3' adenosine (A76) of the tRNA reacts with this high-energy aminoacyl-adenylate intermediate to produce the aa-tRNA.

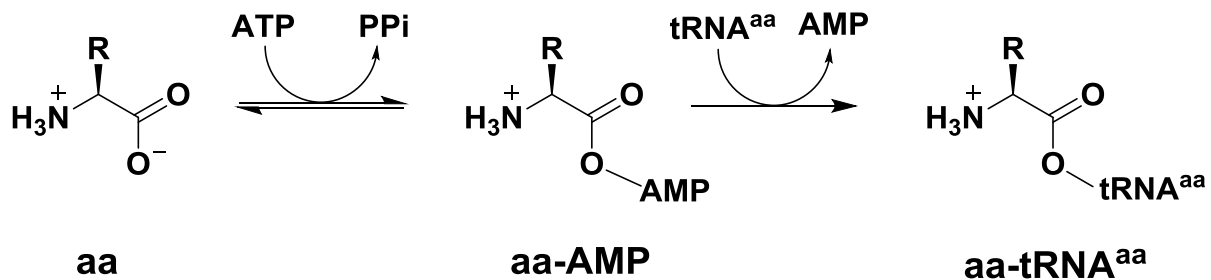


**Figure 1.2. Aminoacylation of tRNAs.** During tRNA aminoacylation, an aaRS reacts its substrate amino acid with ATP to generate a high-energy aa-AMP intermediate. Then, either the 2' or the 3' hydroxyl group of the 3' adenosine of the tRNA reacts with the aa-AMP to produce the cognate aa-tRNA.

### 1.2.2 Classification of aaRSs

The aaRSs are categorized into two distinct classes: class I and class II. The active site of class I aaRSs contains an alternating  $\alpha$ -helical and  $\beta$ -sheet arrangement (a Rossmann fold), while class II aaRSs have a seven-stranded antiparallel  $\beta$ -sheet fold. The class I aaRSs share HIGH and KMSKS signature motifs. Class II aaRSs contains three signature motifs called motif 1, 2 and 3. Class I aaRSs use their two signature sequences to recognize ATP and ATP is recognized in an extended conformation. Class II uses motifs 2 and 3 to bind ATP in a bent configuration. Class I aaRSs are typically monomeric, whereas class II enzymes tend to be dimeric and oligomerization is driven by the motif 1 sequence. In class I aaRSs, tRNA aminoacylation typically occurs at the 2' hydroxyl group of the terminal (A76) tRNA. In contrast, esterification occurs at the 3' hydroxyl group of the terminal tRNA in class II enzymes. The class I aaRSs binds the acceptor stem of the tRNA on the minor groove side and class II aaRSs binds on the major groove side (11-14). These differences among the class I and class II aaRSs are summarized in **Table 1.1**. The two classes of aaRSs can be further divided into subclasses based on their structural and functional peculiarities (**Table 1.2**).

**Table 1.1. Main features of the two classes of aaRSs.**

	<b>Class I</b>	<b>Class II</b>
<b>Conserved signature motifs<sup>1</sup></b>	<ul style="list-style-type: none"> <li>• HiGh</li> <li>• kmSKs</li> </ul>	<ul style="list-style-type: none"> <li>• motif 1: gΦxxΦxxP</li> <li>• motif 2: fRxe</li> <li>• motif 3: gxgxxgfd/eR</li> </ul>
<b>Active site fold</b>	Rossmann fold	Antiparallel β-sheets
<b>ATP binding</b>	Extended	Bent
<b>tRNA recognition</b>	Minor groove	Major groove
<b>Aminoacylation site</b>	2' hydroxyl group	3' hydroxyl group

<sup>1</sup> Lower case letters represent less conserved residues and Φ indicates a requirement for a hydrophobic amino acid.

**Table 1.2. The two classes of aaRSs.**

<b>Class I</b>	<b>Class II</b>
<b>Class Ia</b>	<b>Class IIa</b>
ArgRS	AlaRS <sup>1</sup>
CysRS	GlyRS <sup>1</sup>
IleRS	HisRS
LeuRS	ProRS
MetRS	SerRS
ValRS	ThrRS
<b>Class Ib</b>	<b>Class IIb</b>
GluRS	AspRS
GlnRS	AsnRS
LysRS <sup>2</sup>	LysRS <sup>2</sup>
<b>Class Ic</b>	<b>Class IIc</b>
TrpRS	PheRS
TryRS	

<sup>1</sup> AlaRS and GlyRS have been classified as class IIa (12) by some and as class IIc by others (11, 15). Here we represent it as class IIa according to reference (12).

<sup>2</sup> LysRS can be classified into both classes. Class I LysRS is found in a few bacteria and mainly in archaea (12).

### 1.2.3 aaRSs editing activities

Generally, protein synthesis needs to be carried out with high accuracy and fidelity. The aaRSs play an important part in this regard by discriminating between the cognate and noncognate amino acid and tRNA substrates. Errors in amino acid recognition by the aaRSs is higher than that of tRNA recognition (11), due to the size and complexity differences between amino acid and tRNAs. While amino acids are smaller and less complex in nature, tRNAs are bigger and contain greater structural diversity. For example, arginyl-tRNA synthetase (ArgRS) can discriminate its cognate tRNA<sup>Arg</sup> over tRNA<sup>Asp</sup> by about 10,000-fold (16). In contrast, isoleucyl-tRNA synthetase (IleRS) can only discriminate its cognate amino acid isoleucine from its noncognate amino acid substrate valine by ~ 180-fold (17-19). However, mistakes in amino acid recognition are not typically carried into proteins because of proofreading mechanisms.

Both class I and class II aaRSs exhibits proofreading/editing mechanisms called pre- and post-transfer editing (**Figure 1.3**) (11, 15, 20). These activities eliminate the non-cognate amino acids that are used during aminoacylation. Pre-transfer editing is the hydrolysis of the noncognate aa-AMP intermediate. Pre-transfer editing can occur in three different ways: enzyme-catalyzed hydrolysis; tRNA-mediated, enzyme-catalyzed hydrolysis; and non-enzymatic hydrolysis of the aa-AMP after release from the enzyme (21). If the noncognate amino acid is transferred to the tRNA, then the 3' end of the misacylated aa-tRNA is translocated into the editing site of the aaRS (typically ~25-30 Å away from the active site) where it undergoes enzyme-catalyzed hydrolysis (post-transfer editing) (22-24).

The lower errors observed in the recognition of a non-cognate tRNAs by aaRSs is accomplished by several mechanisms. tRNAs contain several structural elements called identity elements that are used by the aaRS to favor specific recognition of the cognate tRNA. Some tRNAs also contain anti-determinants that acts as negative elements and prevent tRNA binding to non-cognate aaRSs (7, 15, 25). Post-transcriptionally modified nucleotides, such as queuosine and 2-thiouridine, also play important roles in tRNA selection (26-27).

### 1.3 Direct and indirect tRNA aminoacylation

When the aaRSs were first discovered, it was believed that there would always be 20 aaRSs in each organism, with one enzyme for each aa-tRNA isoacceptor set. However, this rule of 20 aaRSs for 20 amino acids is only true in the cytoplasm of eukaryotes (e.g. yeast (28) and humans (29)) and some microorganisms (e.g. *Escherichia coli* (*E. coli*) (30)). This phenomenon is not true for most bacteria (31), most archaea (32) and eukaryotic organelles (chloroplasts, mitochondria) (33). Organisms that diverge from this rule follow an indirect tRNA aminoacylation pathway and utilize noncanonical aaRSs to compensate for the activity of missing, canonical aaRSs.

#### 1.3.1 Direct tRNA aminoacylation pathway

The organisms that contain a full set of 20 aaRSs can directly aminoacylate all tRNAs with their cognate amino acids to produce a complete set of aa-tRNAs. For example, glutamyl-tRNA synthetase (GlnRS) aminoacylates tRNA<sup>Gln</sup> with glutamine to produce Gln-tRNA<sup>Gln</sup> directly, and asparaginyl-tRNA synthetase (AsnRS) can pair up tRNA<sup>Asn</sup> with asparagine to produce Asn-tRNA<sup>Asn</sup> (**Figure 1.4A and B, top arrows**).



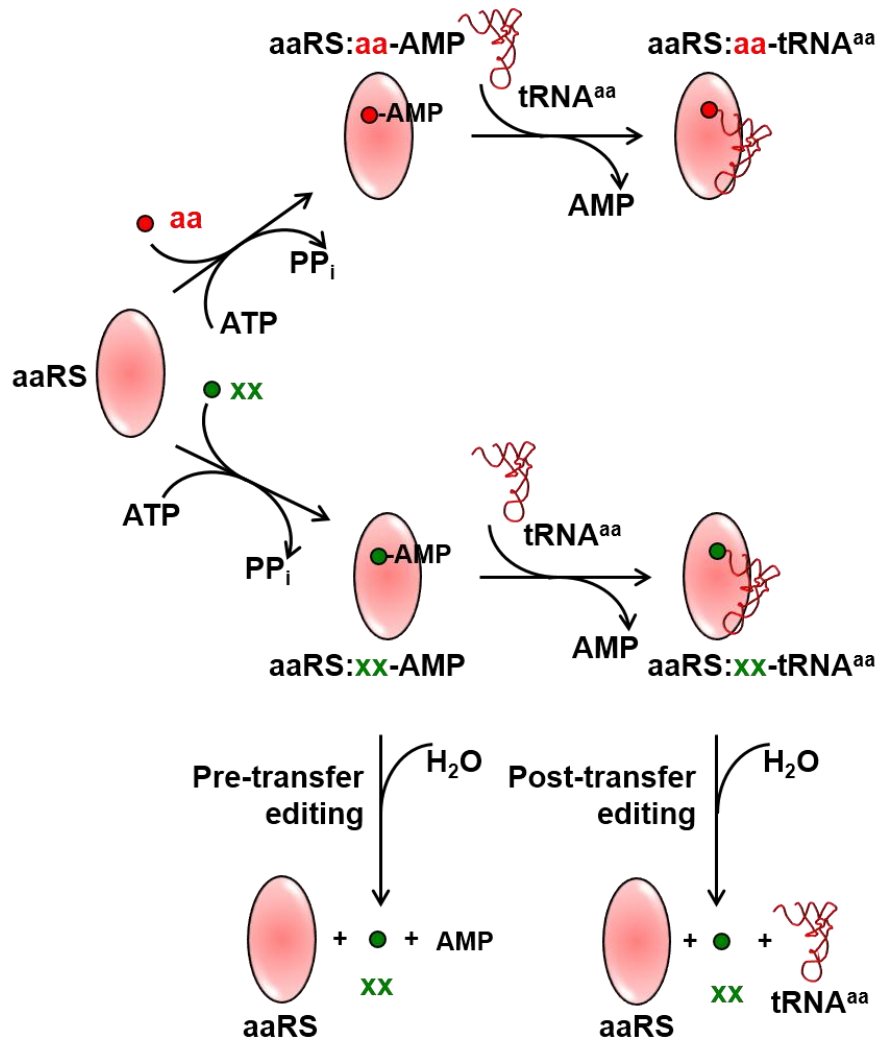


**Figure 1.3. Aminoacylation and editing activity of the aaRSs.** aaRSs aminoacylate their cognate tRNA<sup>aa</sup> with their cognate amino acid (aa) to produce aa-tRNA<sup>aa</sup>. Usually, the aaRSs can select their cognate substrates from a substrate pool that contains similar, non-cognate species. Occasionally, non-cognate amino acids (xx) are misactivated by an aaRS. In these cases, the non-cognate amino acid (xx) can be removed by hydrolysis of the xx-AMP (pre-transfer editing) or the xx-tRNA (post-transfer editing).

### 1.3.2 Indirect tRNA aminoacylation pathways

Organisms that do not have a full set of aaRSs utilize an indirect biosynthesis pathway to produce the aa-tRNAs that correspond to the missing aaRSs. In these species, additional enzymes are required to generate these cognate aa-tRNA pairs. AsnRS, GlnRS, and cysteinyl-tRNA synthetase (CysRS) are the aaRSs that are known

to be missing from different microorganisms, and AsnRS and GlnRS are actually quite uncommon among microorganisms (34). Thus, indirect biosynthesis pathways are used to generate Asn-tRNA<sup>Asn</sup>, Gln-tRNA<sup>Gln</sup>, and Cys-tRNA<sup>Cys</sup> (35-39). Further, indirect pathways are also used in producing non-standard aa-tRNAs, such as selenocysteinyl-tRNA<sup>Sec</sup> and pyrrolysyl-tRNA<sup>Pyl</sup> (34).

### 1.3.2.1 Indirect biosynthesis of Gln-tRNA<sup>Gln</sup>

Indirect tRNA aminoacylation was first discovered in *Bacillus subtilis* (*B. subtilis*) in the late 1960s (40). *B. subtilis* lacks GlnRS and cannot directly produce Gln-tRNA<sup>Gln</sup> (**Figure 1.4B, top arrow**). (40-42) Instead, Gln-tRNA<sup>Gln</sup> is synthesized via the indirect tRNA aminoacylation pathway. First, tRNA<sup>Gln</sup> is misacylated with glutamate to produce Glu-tRNA<sup>Gln</sup>. This reaction is catalyzed by a non-discriminating glutamyl-tRNA synthetase (ND-GluRS) or GluRS2 (a tRNA<sup>Gln</sup>-specific GluRS) (40-42). Next, this misacylated intermediate Glu-tRNA<sup>Gln</sup> is transamidated by an amidotransferase called AdT (GatCAB or GatDE, described in further detail below) to generate Gln-tRNA<sup>Gln</sup> (**Figure 1.4B, bottom arrow**) (34, 37-38, 43). ND-GluRS can glutamylate both tRNA<sup>Gln</sup> and tRNA<sup>Glu</sup> with glutamate to produce Glu-tRNA<sup>Gln</sup> and Glu-tRNA<sup>Glu</sup>, respectively. Some organisms contain two divergent glutamyl-tRNA synthetases: GluRS1 and GluRS2 (41-42). For example, in *Helicobacter pylori* (*H. pylori*), GluRS1 acts as a discriminating GluRS and aminoacylates tRNA<sup>Glu</sup> to generate Glu-tRNA<sup>Glu</sup>. In contrast, GluRS2 is used specifically in the indirect biosynthesis of Gln-tRNA<sup>Gln</sup>, and it misacylates tRNA<sup>Gln</sup> with glutamate to produce Glu-tRNA<sup>Gln</sup>; GluRS2 does not produce Glu-tRNA<sup>Glu</sup> (42).

### 1.3.2.2 Indirect biosynthesis of Asn-tRNA<sup>Asn</sup>

The indirect biosynthesis of Asn-tRNA<sup>Asn</sup> is analogous to the above-mentioned indirect production of Gln-tRNA<sup>Gln</sup> pathway. In organisms that lack AsnRS and/or asparagine synthetase (AsnS), non-discriminating aspartyl-tRNA synthetase (ND-AspRS) aminoacylates both tRNA<sup>Asp</sup> and tRNA<sup>Asn</sup> with aspartate to produce Asp-tRNA<sup>Asp</sup> and Asp-tRNA<sup>Asn</sup>, respectively (35, 43). The misacylated Asp-tRNA<sup>Asn</sup> is then converted to Asn-tRNA<sup>Asn</sup> by AdT (**Figure 1.4A, bottom arrow**) (34, 37, 44-45). In some species, which lack AsnS, this indirect pathway is the sole biosynthetic route to asparagine.

Since AsnRS is more abundant than GlnRS, the indirect biosynthesis of Asn-tRNA<sup>Asn</sup> is less common in organisms compared to the corresponding pathway producing Gln-tRNA<sup>Gln</sup> (16). Further, compared to Gln-tRNA<sup>Gln</sup> biosynthesis, in the indirect production of Asn-tRNA<sup>Asn</sup>, the second step is only catalyzed by GatCAB, as the intermediate Asp-tRNA<sup>Asn</sup> cannot be recognized by GatDE (38).

The work presented in this dissertation is focused on three different pathogenic bacteria: *H. pylori*, *Mycobacterium smegmatis* (*M. smegmatis*), and *Staphylococcus aureus* (*S. aureus*). These organisms all utilize indirect tRNA aminoacylation to produce both Asn-tRNA<sup>Asn</sup> and Gln-tRNA<sup>Gln</sup> (46-48). *H. pylori* and *M. smegmatis* lack genes encoding both GlnRS and AsnRS and use indirect tRNA aminoacylation to produce both Asn-tRNA<sup>Asn</sup> and Gln-tRNA<sup>Gln</sup> (42, 49-50). Since *H. pylori* do not contain a functional AsnS, this pathway is also essential as a source of asparagine. In contrast, *S. aureus* lacks GlnRS and AsnS but has AsnRS. Thus *S. aureus* produces Gln-tRNA<sup>Gln</sup> by indirect tRNA aminoacylation only but can produce Asn-tRNA<sup>Asn</sup> directly and indirectly. The latter

pathway is necessary for asparagine biosynthesis (51). **Table 1.3** summarize the gene distribution of these organisms.

**Table 1.3. AsnRS, AsnS and GlnRS gene distribution of *H. pylori*, *M. smegmatis*, and *S. aureus*.**

Organism	AsnRS	AsnS	GlnRS
<i>H. pylori</i>	x	x	x
<i>M. smegmatis</i>	x	✓	x
<i>S. aureus</i>	✓	x	x

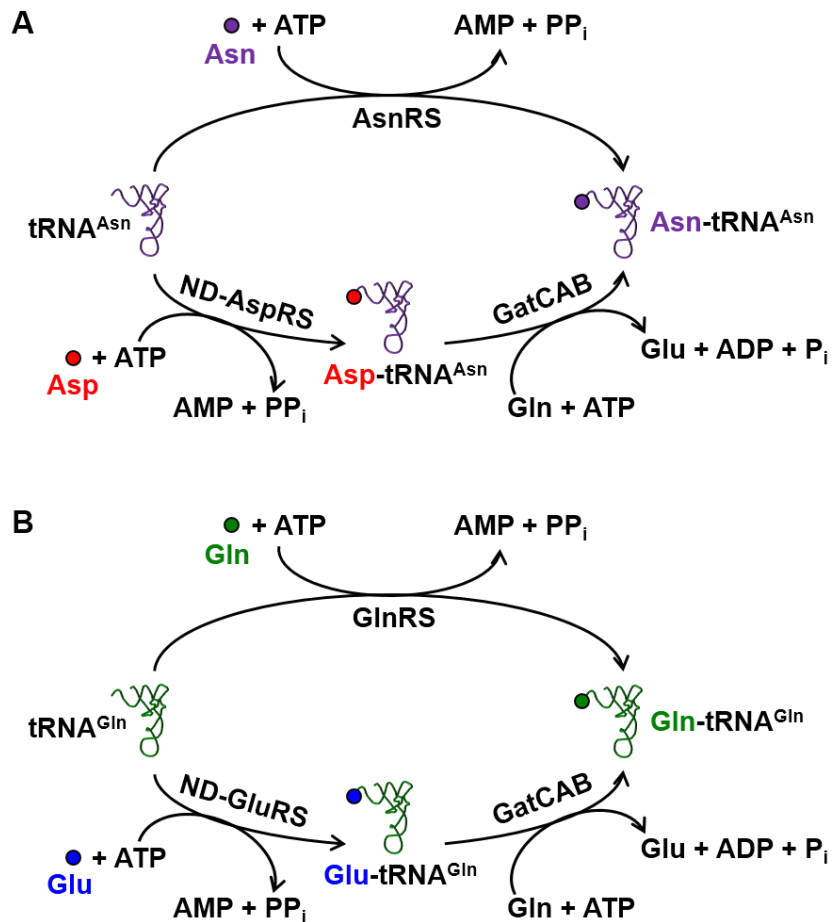


**Figure 1.4. Direct and indirect biosynthesis of Asn-tRNA<sup>Asn</sup> and Gln-tRNA<sup>Gln</sup> in bacteria. (A) Biosynthesis of Asn-tRNA<sup>Asn</sup>: direct biosynthesis (top arrow), and GatCAB-catalyzed indirect biosynthesis (bottom arrow). (B) Biosynthesis of Gln-tRNA<sup>Gln</sup>: direct biosynthesis (top arrow), and GatCAB-catalyzed indirect biosynthesis (bottom arrow). ND stands for non-discriminating.**

## 1.4 Discriminating and non-discriminating AspRS

In chapter 3, we discuss our discovery of an unusual and unexpected behavior in some bacterial AspRSs, namely the fact that these enzymes can produce Glu-tRNA<sup>Glu</sup>. This section of the introduction will focus more on the gene distribution of AspRSs in bacteria and the reactions catalyzed by AspRS and ND-AspRS.

Based on their tRNA substrate specificities, AspRS is found in two forms: discriminating, which produces Asp-tRNA<sup>Asp</sup> (16, 52), and non-discriminating, which produces both Asp-tRNA<sup>Asp</sup> and Asp-tRNA<sup>Asn</sup> (35, 43, 52). In the latter case, the misacylated Asp-tRNA<sup>Asn</sup> is converted to Asn-tRNA<sup>Asn</sup> by GatCAB (36-37). Most organisms contain one genetic copy of AspRS, defined to be either discriminating (as in *E. coli* (53)) or non-discriminating (as in *H. pylori* (49), *M. smegmatis* (50), *S. aureus* (51)). However, some contain two different copies of AspRS, wherein one is typically discriminating and the other is non-discriminating (e.g. *Thermus thermophilus* (*T. thermophilus* (54)), *Deinococcus radiodurans* (*D. radiodurans* (45)), and *Clostridium acetobutylicum* (*C. acetobutylicum* (55)). In these cases, the long bacterial-type AspRS is discriminating and catalyzes the synthesis of Asp-tRNA<sup>Asp</sup>. The additional AspRS is non-discriminating and produces both Asp-tRNA<sup>Asn</sup> along with Asp-tRNA<sup>Asp</sup>. The ND-AspRS is of archaeal origin and was acquired through horizontal gene transfer (56). **Table 1.4** list examples of bacteria with different types of AspRSs and the major Asn-tRNA<sup>Asn</sup> biosynthesis pathway in these organisms.

**Table 1.4. AspRS, AsnRS, AsnS and GatCAB gene distribution in bacteria.**

Organism	AspRS <sup>1</sup>	AsnRS	AsnS	GatCAB	Notes	Ref.
<i>Escherichia coli</i>	D	+	+	-	• Utilizes direct route to produce Asn-tRNA <sup>Asn</sup>	(53)
<i>Lactobacillus bulgaricus</i>	D	+	+	+	• AspRS is discriminating even in the presence of AdT	(57)
<i>Bacillus subtilis</i>	ND	+	+	+	• AspRS is non-discriminating although organisms have AsnRS and AsnS • Utilize both direct and indirect routes to synthesize Asn-tRNA <sup>Asn</sup>	(56)
<i>Bacillus halodurans</i>						
<i>Staphylococcus aureus</i>	ND	+	-	+	• Synthesize asparagine from Asp-tRNA <sup>Asn</sup>	(51)
<i>Legionella pneumophila</i>						(58)
<i>Bdellovibrio bacteovorvus</i>						
<i>Mycobacterium tuberculosis</i>	ND	-	+	+	• Uses indirect tRNA aminoacylation to produce Asn-tRNA <sup>Asn</sup>	(50)
<i>Mycobacterium smegmatis</i>						
<i>Pseudomonas aeruginosa</i>	ND	-	-	+	• Asparagine biosynthesis is tRNA dependent	(59)
<i>Helicobacter pylori</i>						(49)
<i>Thermus thermophilus</i>	1 D 1 ND	+	-	+	• Contain multiple copies of AspRS • Long bacterial-type AspRS is discriminating • Additional AspRS is non-discriminating and of archaeal origin	(54)
<i>Deinococcus radiodurans</i>	1 D 1 ND					(45)
<i>Clostridium acetobutylicum</i>	1 D 2 ND					(55)

<sup>1</sup> The nature of AspRS is represented as follows: D is for discriminating and ND is for non-discriminating.

## 1.5 GatCAB, bacterial glutamine-dependent amidotransferase

In organisms that use the indirect tRNA aminoacylation pathway, the misacylated intermediates Asp-tRNA<sup>Asn</sup> and Glu-tRNA<sup>Gln</sup> need to be transamidated to Asn-tRNA<sup>Asn</sup> and Gln-tRNA<sup>Gln</sup>, respectively. AdT catalyzes the efficient conversion of these misacylated tRNAs to their correctly acylated forms (34). AdT can be found in two different forms: the heterotrimeric GatCAB in bacteria, some archaea, and in some organelles (36, 44, 60-61) and the heterodimeric GatDE, which is confined to archaea (38, 61-62). While GatCAB is bi-functional and catalyzes the amidation of both Asp-tRNA<sup>Asn</sup> and Glu-tRNA<sup>Gln</sup> into Asn-tRNA<sup>Asn</sup> and Gln-tRNA<sup>Gln</sup> respectively, GatDE is mono-functional and only catalyzes the conversion of Glu-tRNA<sup>Gln</sup> into Gln-tRNA<sup>Gln</sup> (61). Since we study the bacterial indirect tRNA aminoacylation systems, henceforth we will emphasize the structure and mechanism of the bacterial GatCAB.

As mentioned above, bacterial GatCAB can recognize both Asp-tRNA<sup>Asn</sup> and Glu-tRNA<sup>Gln</sup> and transamidate these into Asn-tRNA<sup>Asn</sup> and Gln-tRNA<sup>Gln</sup> using glutamine as an ammonia donor (34, 36). The bacterial GatCAB is a heterotrimeric protein composed of three subunits: GatA, GatB, and GatC, with two active sites located in GatA and GatB that are ~40 Å apart (60). GatCAB achieves transamidation by catalyzing three discrete reactions: glutamine hydrolysis, phosphorylation of misacylated tRNA, and transamidation of the phosphorylated misacylated tRNA into correctly aminoacylated tRNA (**Figure 1.5, shown only for Gln-tRNA<sup>Gln</sup> biosynthesis**). GatA hydrolyzes glutamine to produce glutamate and ammonia (**Figure 1.5A**). The ammonia is then delivered to the active site of GatB through an ammonia tunnel (which will be discussed in detail later). The GatB subunit catalyzes ATP-dependent phosphorylation of Asp-

tRNA<sup>Asn</sup> and Glu-tRNA<sup>Gln</sup> to phosphoryl-Asp-tRNA<sup>Asn</sup> and phosphoryl-Glu-tRNA<sup>Gln</sup> (**Figure 1.5B**) (63-64). Next, GatB catalyzes the transamidation of these two phosphorylated tRNAs to produce Asn-tRNA<sup>Asn</sup> or Gln-tRNA<sup>Gln</sup> using the ammonia produced by GatA (**Figure 1.5C**) (36).

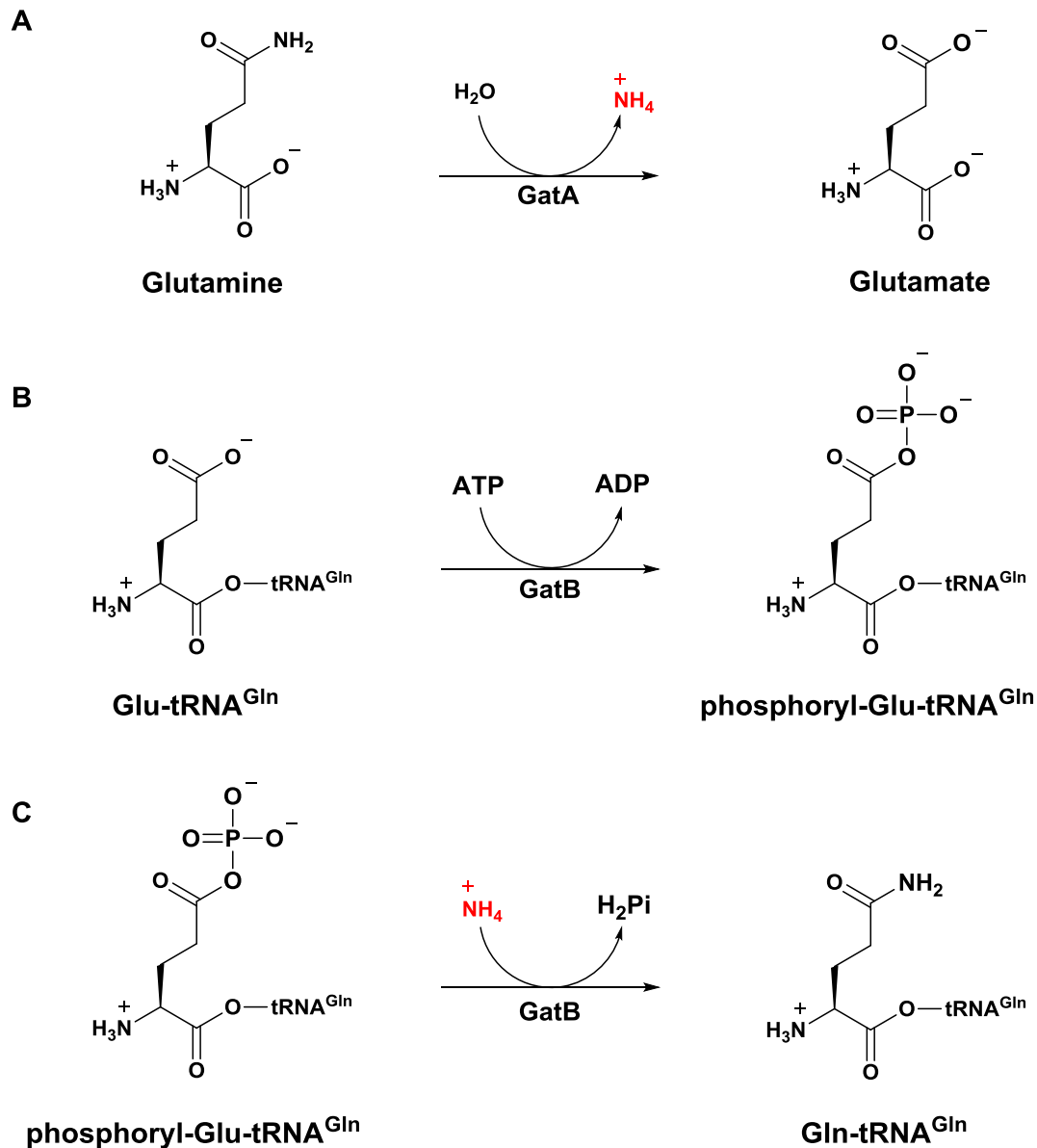


**Figure 1.5. The three reactions catalyzed by GatCAB.** Reactions are only shown for Gln-tRNA<sup>Gln</sup> production. **(A)** Glutamine hydrolysis by GatA to produce glutamate and ammonia. **(B)** Phosphorylation of Glu-tRNA<sup>Gln</sup> to phosphoryl-Glu-tRNA<sup>Gln</sup>, by GatB. **(C)** Transamidation of phosphoryl-Glu-tRNA<sup>Gln</sup> to Gln-tRNA<sup>Gln</sup> by GatB using the ammonia generated by GatA.



Many glutamine-dependent aminotransferases (GATs) contains molecular tunnels to deliver the ammonia produced in their glutaminase active sites to downstream transamidase active sites. Most of the ammonia tunnels reported so far are largely hydrophobic (65-68) and assumed to deliver ammonia in its neutral, deprotonated form by passive transportation (69). In contrast, GatCAB's ammonia tunnel is largely hydrophilic, lined with polar ionic amino acids, and populated with ordered water molecules (60).

Using the *S. aureus* GatCAB crystal structure, two ammonia tunnels have been proposed: tunnel I (60) and tunnel II (70). Tunnel I is lined with conserved acid/base residues and it has been proposed that ammonia delivery occurs through a series of protonation and deprotonation steps (60). Tunnel II (70) is slightly different from than tunnel I. These two tunnels have different paths starting at a highly conserved aspartate in GatA. While tunnel I is lined with hydrophilic amino acids, the top of tunnel II is lined with hydrophobic residues. The two tunnels merge into one  $\sim 10$  Å past the active site of GatA, and the rest of the tunnel is hydrophilic in nature. Mutational work on *H. pylori* GatCAB (71) and free energy calculations with *S. aureus* GatCAB (72) suggest that tunnel I is more functionally relevant than tunnel II.

A kinetic analysis of tunnel I mutants in *H. pylori* GatCAB with molecular dynamics simulations using *S. aureus* GatCAB indicate apparent domain-domain communication between GatA and GatB (71). Recent work characterizing the conserved aspartate (D185A) in *H. pylori*, located only in tunnel I, further support the idea that tunnel I is the physiologically relevant tunnel (73). D185A and D185N GatCAB mutants completely disrupted transamidase activity with lower glutaminase activity and kinase activity

compared to WT GatCAB. In comparison, the D185E mutant had wild-type activity. These results demonstrated that D185 is integral to ammonia transport in GatCAB and is the first example of an acid/base residue in an ammonia tunnel (73).

### 1.6 Macromolecular transamidosome complexes in indirect tRNA aminoacylation

Elongation factor Tu (EF-Tu) plays an important role in maintaining the fidelity of protein biosynthesis by differentiating against the misacylated Asp-tRNA<sup>Asn</sup> and Glu-tRNA<sup>Gln</sup> in favor of the cognate Asn-tRNA<sup>Asn</sup> and Gln-tRNA<sup>Gln</sup> (74). However, discrimination by EF-Tu is not sufficient to prevent aspartate and glutamate misincorporation into proteins at asparagine and glutamine codons, respectively (50, 74-76). Thus, additional mechanisms to sequester both misacylated tRNAs from EF-Tu and the ribosome must exist. The most straightforward solution is to deliver each misacylated tRNA directly from its misacylating aaRS to GatCAB (33). In fact, it is now clear that an Asn-transamidosome, composed of ND-AspRS, GatCAB, and either tRNA<sup>Asn</sup> (77-78) or a protein called Hp0100 (79), is critical for efficient Asn-tRNA<sup>Asn</sup> production and sequestration of Asp-tRNA<sup>Asn</sup> away from EF-Tu and the ribosome. These complexes have been predominantly characterized *in vitro*, however, their stability and ease of formation support their *in vivo* importance. Evidence also exists for the formation of an analogous Gln-transamidosome (80-81), although a clear demonstration of functional relevance has remained elusive. **Tables 1.5** and **1.6** and the following sections describe our current understanding of the formation and function of Asn-transamidosome and Gln-transamidosome complexes.

### 1.6.1 The Asn-transamidosome

The first Asn-transamidosome was reconstituted *in vitro* from *T. thermophilus* components (77). The crystal structure of this complex contains two dimeric ND-AspRS, two copies of GatCAB, and four copies of tRNA<sup>Asn</sup> (82). Assembly of the *T. thermophilus* Asn-transamidosome requires tRNA<sup>Asn</sup>. Two copies of tRNA<sup>Asn</sup> are productively bound to the GatB active site, while the other two serve as scaffolds for the complex. Based on this structure, the authors proposed a convincing model for simple rotation of the 3' acceptor end of tRNA<sup>Asn</sup> to allow the transfer of Asp-tRNA<sup>Asn</sup> from the ND-AspRS active site to the GatB transamidation active site without dissociation from the complex, thus sequestering Asp-tRNA<sup>Asn</sup> from EF-Tu and the ribosome. Consistent with this model for sequestration, this Asn-transamidosome complex protects the labile ester of Asp-tRNA<sup>Asn</sup> (1.4–2-fold) from hydrolysis (77).

A crystal structure of the *Pseudomonas aeruginosa* (*P. aeruginosa*) Asn-transamidosome has also been reported (78). The *P. aeruginosa* structure is different from that of *T. thermophilus*, even though both require tRNA<sup>Asn</sup> to assemble. The *P. aeruginosa* Asn-transamidosome contains two copies of GatCAB, two copies of tRNA<sup>Asn</sup>, and one copy of the ND-AspRS homodimer. In this case, both tRNAs are bound productively to the two GatB active sites. The differences in these two structures likely arise from the evolutionary origin of their respective ND-AspRSs: *T. thermophilus* uses an archaeal-type ND-AspRS (77), whereas *P. aeruginosa* uses a bacterial type (78). The bacterial-type ND-AspRS contains a GAD domain that is missing in the archaeal-type enzyme. This *P. aeruginosa* GAD domain forces GatCAB into a different position than that observed in the *T. thermophilus* structure (78). It is also possible that some of these

structural differences reflect adaptation to the different optimal growth temperatures of these two organisms (37 °C vs. 65 °C).

The *H. pylori* Asn-transamidosome has been characterized *in vitro* (79, 83), but a crystal structure of this complex has not yet been reported. This complex is also distinct from those of *T. thermophilus* and *P. aeruginosa*. Initial characterization demonstrated the formation of a more dynamic, tRNA<sup>Asn</sup>-dependent, *H. pylori* Asn-transamidosome (83). The size of this complex, and consequently its overall integrity, was sensitive to the presence or absence of different substrates for indirect tRNA aminoacylation (e.g. L-aspartate, L-glutamine, and ATP). A subsequent study showed that a novel protein partner called Hp0100 drives the formation of a stable *H. pylori* Asn-transamidosome, even in the absence of tRNA<sup>Asn</sup>. The addition of Hp0100 increases the rate of GatCAB-catalyzed transamidation of Asp-tRNA<sup>Asn</sup> to Asn-tRNA<sup>Asn</sup> by approximately 35-fold but has no effect on ND-AspRS activity (79). It is not clear yet why only some bacteria have incorporated Hp0100 into the Asn-transamidosome, displacing a requirement for tRNA<sup>Asn</sup> for complex assembly. The identification of Hp0100 raises the tantalizing possibility that other proteins involved in indirect tRNA aminoacylation remain undiscovered.

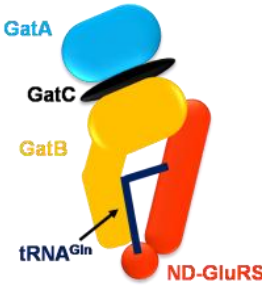
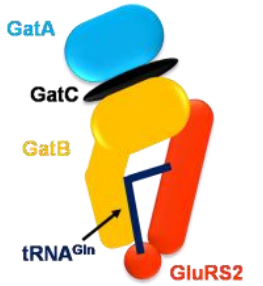
**Table 1.5. Asn-transamidosome complexes. (Cartoons adapted from that given in reference (78)).**

Organism	<i>T. thermophilus</i>	<i>H. pylori</i>	<i>P. aeruginosa</i>
Structure			
Composition	<ul style="list-style-type: none"> <li>• 2 ND-AspRS dimers</li> <li>• 2 GatCAB</li> <li>• 4 tRNA<sup>Asn</sup></li> </ul>	<ul style="list-style-type: none"> <li>• ND-AspRS</li> <li>• GatCAB</li> <li>• Hp0100</li> <li>• Complex stoichiometry unknown</li> </ul>	<ul style="list-style-type: none"> <li>• 1 dimeric ND-AspRS</li> <li>• 2 GatCAB</li> <li>• 2 tRNA<sup>Asn</sup></li> </ul>
Additional information and observations	tRNA <sup>Asn</sup> -dependent	tRNA <sup>Asn</sup> -independent	tRNA <sup>Asn</sup> -dependent
	Only two ND-AspRS monomers are active at a given time (out of four)	No effect on ND-AspRS activity	Both ND-AspRS monomers are active
	Complex increases ND-AspRS activity	Hp0100 had no effect on ND-AspRS activity	Complex increases ND-AspRS activity
	Decreases GatCAB activity with Asp-tRNA <sup>Asn</sup>	Hp0100 increases GatCAB activity with Asp-tRNA <sup>Asn</sup>	ND
	Protects Asp-tRNA <sup>Asn</sup> and Asn-tRNA <sup>Asn</sup> from hydrolysis	ND	Rapidly releases Asn-tRNA <sup>Asn</sup>
	Four tRNA <sup>Asn</sup> are bound in two forms: catalytic and scaffold	tRNA stoichiometry is unknown	Two tRNA <sup>Asn</sup> are bound in productive conformations
	Crystal structure available	ND	Crystal structure available
References	(77, 82)	(79, 83)	(78)

### 1.6.2 The Gln-transamidosome

With the demonstration of different, functional Asn-transamidosome complexes, it is logical to assume that an analogous Gln-transamidosome is also important for sequestering Glu-tRNA<sup>Gln</sup> from EF-Tu and ribosomes and/or promoting efficient production of Gln-tRNA<sup>Gln</sup>. However, to date, the characterization of Gln-transamidosomes has proven to be more challenging. *In vitro* characterization of a bacterial transamidosome from *Thermotoga maritima* (*T. maritima*) has been reported to be tRNA<sup>Gln</sup>-dependent (81). In an electrophoretic mobility shift assay, Gln-transamidosome formation was observed upon equimolar titration of both ND-GluRS and GatCAB (0–100  $\mu$ M) with constant tRNA<sup>Gln</sup> (2  $\mu$ M). A crystal structure of this complex was obtained by expressing the GatC subunit of GatCAB and ND-GluRS as a single polypeptide chain, connected by a short peptide linker. In this structure, the tRNA<sup>Gln</sup> is bound to ND-GluRS in a manner suitable for aminoacylation but not transamidation (81). Thus, this structure does not offer the same satisfying explanation for facile transfer of Glu-tRNA<sup>Gln</sup> from ND-GluRS to GatCAB that is observed in the *T. thermophilus* Asn-transamidosome structure. Efforts to isolate a functional, *H. pylori* Gln-transamidosome identified a narrow range of tRNA<sup>Gln</sup> concentrations where complex formation was observed, suggesting that this complex is highly dynamic (80).

Table 1.6. Gln-transamidosome complexes. (Cartoons adapted from that given in reference (78)).

<i>Organism</i>	<i>T. maritima</i>	<i>H. pylori</i>
<b>Structure</b>		
<b>Composition</b>	<ul style="list-style-type: none"> <li>• 1 ND-GluRS</li> <li>• 1 GatCAB</li> <li>• 1 tRNA<sup>Gln</sup></li> </ul>	<ul style="list-style-type: none"> <li>• 1 GluRS2</li> <li>• 1 GatCAB</li> <li>• 1 tRNA<sup>Gln</sup></li> </ul>
<b>Additional information and observations</b>	tRNA <sup>Gln</sup> -dependent	tRNA <sup>Gln</sup> -dependent
	ND-GluRS is functionally bound to tRNA <sup>Gln</sup>	Complex assembly forms over a small range of tRNA <sup>Gln</sup> concentrations
	GatCAB is bound to tRNA <sup>Gln</sup> in a non-productive conformation	ND
	No apparent mechanism for Glu-tRNA <sup>Gln</sup> transfer between enzymes	ND
	GatC and ND-GluRS are covalently linked in the crystal structure	ND
<b>References</b>	(81)	(80)

### 1.6.3 Asn-transamidosomes versus Gln-transamidosomes: Current understanding and future directions

The Gln-transamidosomes characterized to date (80-81) appear to be generally less stable and more dynamic than known Asn-transamidosomes (77-79, 82-83). Further, in the structure of the *T. thermophilus* Asn-transamidosome, Asp-tRNA<sup>Asn</sup> is positioned for facile transfer from the catalytic site of ND-AspRS to the GatB transamidation site, without disruption of the complex (82). This transfer is achievable because ND-AspRS and GatCAB recognize different faces of the acceptor stem of tRNA<sup>Asn</sup>, with ND-AspRS binding from the major groove side and GatCAB from the minor groove side (82). This elegant solution cannot be achieved in a complex between ND-GluRS (or GluRS2) and GatCAB, because these enzymes all bind the minor groove face of tRNA<sup>Gln</sup> and consequently compete for recognition of this substrate (81). With the current Gln-transamidosome structure available, it seems that these complexes must either dissociate or go through a series of undefined movements to facilitate sequestration and transamidation of Glu-tRNA<sup>Gln</sup> (81).

The utilization of Asn-transamidosome complexes in bacteria provides a tidy solution for maintaining accuracy at asparagine codons in organisms that lack AsnRS. Careful work characterizing Gln-transamidosome complexes *in vitro* has also led to important insight, but without as satisfying a conclusion, because a mechanism for sequestering Glu-tRNA<sup>Gln</sup> and transferring it from ND-GluRS to GatCAB has not yet emerged. In this regard, the possibility that other currently unknown proteins may drive Gln-transamidosome assembly, analogous to the role played by Hp0100 in the *H. pylori* Asn-transamidosome (79), might provide an answer. Moreover, the likelihood of the



formation of a larger complex containing both ND-AspRS and ND-GluRS, with GatCAB and either or both tRNAs has not yet been investigated. Little is known about the dynamics of GatCAB *in vivo* as it works concomitantly to produce both Asn-tRNA<sup>Asn</sup> and Gln-tRNA<sup>Gln</sup>. Does this enzyme exist simultaneously in two distinct Asn-transamidosome and Gln-transamidosome complexes? Or, is there a mega Asn/Gln-transamidosome in species that lack both AsnRS and GlnRS? The mechanisms through which this dual action is achieved are certain to prove interesting.

### **1.7 Inducing mistranslation as a stress response by disrupting indirect tRNA aminoacylation**

Evidence is accumulating that bacteria can induce mistranslation under times of stress, such that heterogeneous proteins are formed (84-85). Many of these proteins are inactive and degraded. However, a small subpopulation of mutated proteins may exhibit new functions within this statistical proteome, which can be advantageous to an organism, particularly if they provide an immediate persistence or survival mechanism against a given environmental stress. Because indirect tRNA aminoacylation proceeds via two misacylated tRNA intermediates, Asp-tRNA<sup>Asn</sup> and Glu-tRNA<sup>Gln</sup>, the possibility that mistranslation at asparagine and/or glutamine codons would be upregulated under stress conditions has recently received attention with interesting results.

The first hint that mistranslation at asparagine and glutamine codons could provide a phenotypic advantage came from work in *M. smegmatis* (50). *M. smegmatis* tRNA<sup>Asp</sup> and tRNA<sup>Glu</sup> were mutated to contain asparagine and glutamine anticodons. The tRNA<sup>Asp</sup> anticodon was mutated from <sup>34</sup>CUG to <sup>34</sup>UUG. Two tRNA<sup>Glu</sup> isoacceptors were mutated, from <sup>34</sup>CUC to <sup>34</sup>GUC and from <sup>34</sup>CUU to <sup>34</sup>GUU. The *Mycobacteria* lack genes for both

AsnRS and GlnRS; and, ND-AspRS and ND-GluRS were capable of misacylating these mutant tRNAs to produce Asp-tRNA<sup>Asp(34UUU)</sup>, Glu-tRNA<sup>Glu(34GUC)</sup>, and Glu-tRNA<sup>Glu(34GUU)</sup>. When these tRNAs were overexpressed, tolerance of cell cultures to the antibiotic rifampicin increased by nearly three orders of magnitude. Only weak tolerance against isoniazid and no tolerance to ciprofloxacin was noted. This rifampicin tolerance was traced to alterations in RNA polymerase (RNAP) activity, which showed diminished antibiotic sensitivity to rifampicin. The authors proposed that mistranslation of glutamate to glutamine and/or aspartate to asparagine in the rifampicin resistance-determining region (RRDR) of the  $\beta$ -subunit of RNAP led to this specific tolerance to rifampicin. These results were the first to suggest that indirect tRNA aminoacylation could be perturbed to promote mistranslation as a method to achieve specific phenotypic responses against antibiotics (50).

The experiments above used a strain of *M. smegmatis* that had been modified to overexpress non-native tRNA hybrids (tRNA<sup>Asp</sup> with an asparagine codon and two different tRNA<sup>Glu</sup> isoacceptors, both with glutamine codons) (50). A connection between indirect tRNA aminoacylation, mistranslation, and phenotypic resistance was discovered in *M. smegmatis* and clinical strains of *Mycobacterium tuberculosis* (*M. tuberculosis*) (76). The application of two clever, *in vivo*, forward genetic screens for mistranslation at asparagine and glutamine codons (using native tRNAs) led to the identification of three mutations in GatA (A10T, V405D, and a three-residue deletion DTAL295–297, *M. smegmatis* numbering) that induced increased tolerance to rifampicin even when transplanted into clean genetic backgrounds. A database search of clinically relevant strains and analysis of clinical samples identified additional GatA mutations in *M.*

*tuberculosis* (P143T, A9T, G444S, and K61N, *M. tuberculosis* numbering) that also showed increased rifampicin tolerance. Exhaustive characterization of these mutations from both organisms clearly demonstrated higher levels of mistranslation and rifampicin-specific phenotypic resistance (RSPR) (**Figure 1.6**). The authors postulated that this RSPR is due to specific mistranslation of aspartate for asparagine at N434 in the  $\beta$ -subunit of *M. smegmatis* RNAP (N437 in *M. tuberculosis* RNAP), a position known to be important for rifampicin binding (76). In our opinion, the importance of this work cannot be overstated as it offers the first direct evidence for coopting of indirect tRNA aminoacylation to promote mistranslation in response to stress in a critically important human pathogen. It seems probable that similar phenotypic response mechanisms are used outside of the *Mycobacteria*, although this possibility remains to be seen.

The above work led to the identification of five mutations and a small deletion in GatA, all of which increase the ability of mycobacteria to resist rifampicin (76). Remarkably, these mutations are all found on the surface of GatA far from its active site or interactions with either GatB or GatC. These mutations decrease the stability of GatA and GatB *in vivo* leading Javid and coworkers to propose that they induce mistranslation by disrupting the GatCAB heterotrimeric complex (76). It is also possible that they perturb GatCAB activity or disrupt the formation of either the Asn-transamidosome or Gln-transamidosome. Additional characterization of these mutations to determine their functional consequences will certainly provide further insight into their mechanism(s) of action.

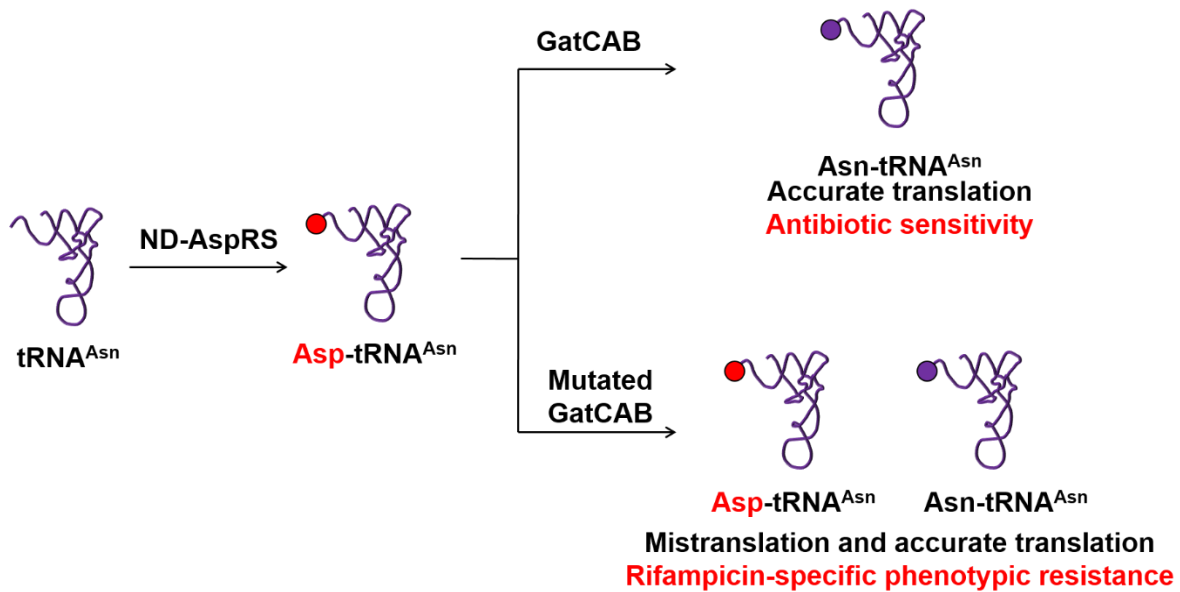
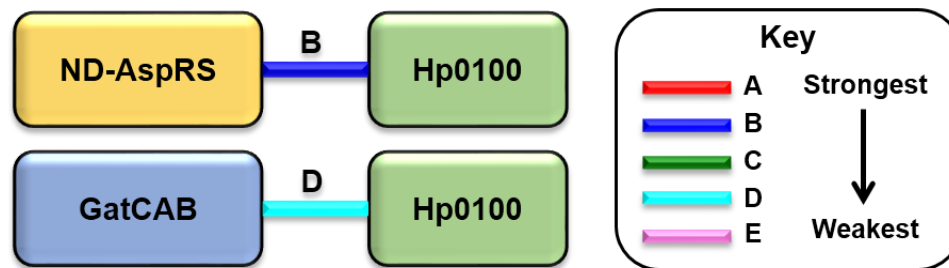


Figure 1.6. **Mutations in GatCAB cause mistranslation and induce RSPR in *Mycobacteria*.** Mutations in GatCAB were identified that increase mistranslation at asparagine and glutamine codons (shown for asparagine only). This mistranslation leads to increased tolerance to rifampicin.

### 1.8 Hp0100, a component of the *H. pylori* Asn-transamidosome

After years of research dedicated to characterizing the *H. pylori* Asn-transamidosome composed of  $tRNA^{Asn}$ , ND-AspRS, and GatCAB were unsuccessful (80, 83), in an effort to find an alternative strategy for Asn-transamidosome assembly and function, data-mining of a published yeast-two-hybrid (Y2H) interaction profile of the *H. pylori* proteome led our lab to discover a protein of unknown function called Hp0100 (79, 86). In this interaction profile, the likelihood of a protein-protein interaction being physiologically relevant was given a letter score: a score of A indicates an interaction that is likely to be physiologically important, and a score of E was given to observed interactions that were predicted to be artifactual. In this screen, Hp0100 showed a B level interaction with ND-AspRS and a weak, D level interaction with GatCAB (**Figure 1.7**). Since ND-AspRS and GatCAB are closely-intertwined functional components of the

indirect tRNA aminoacylation pathway and Hp0100 shows interactions with both proteins, our lab further investigated Hp0100 as a possible protein partner in the formation of a transamidosome complex in *H. pylori*.



**Figure 1.7. Yeast-2-hybrid interaction profile of Hp0100.** Hp0100 show a B level interaction with ND-AspRS and a D level interaction with GatCAB. Data acquired from (86).

Dr. Gayathri Silva demonstrated that Hp0100 is an essential component of a tRNA independent Asn-transamidosome in *H. pylori* (**Figure 1.8**) (79, 87). In the proposed catalytic Asn-transamidosome cycle, ND-AspRS, GatCAB, and Hp0100 first assemble into a stable apo-transamidosome. A holo-transamidosome is formed that includes tRNA<sup>Asn</sup>. ND-AspRS aminoacylates tRNA<sup>Asn</sup> to form misacylated Asp-tRNA<sup>Asn</sup>, which is then converted to Asn-tRNA<sup>Asn</sup> by GatCAB. Finally, the correctly aminoacylated Asn-tRNA<sup>Asn</sup> is released to regenerate the apo-transamidosome (79).

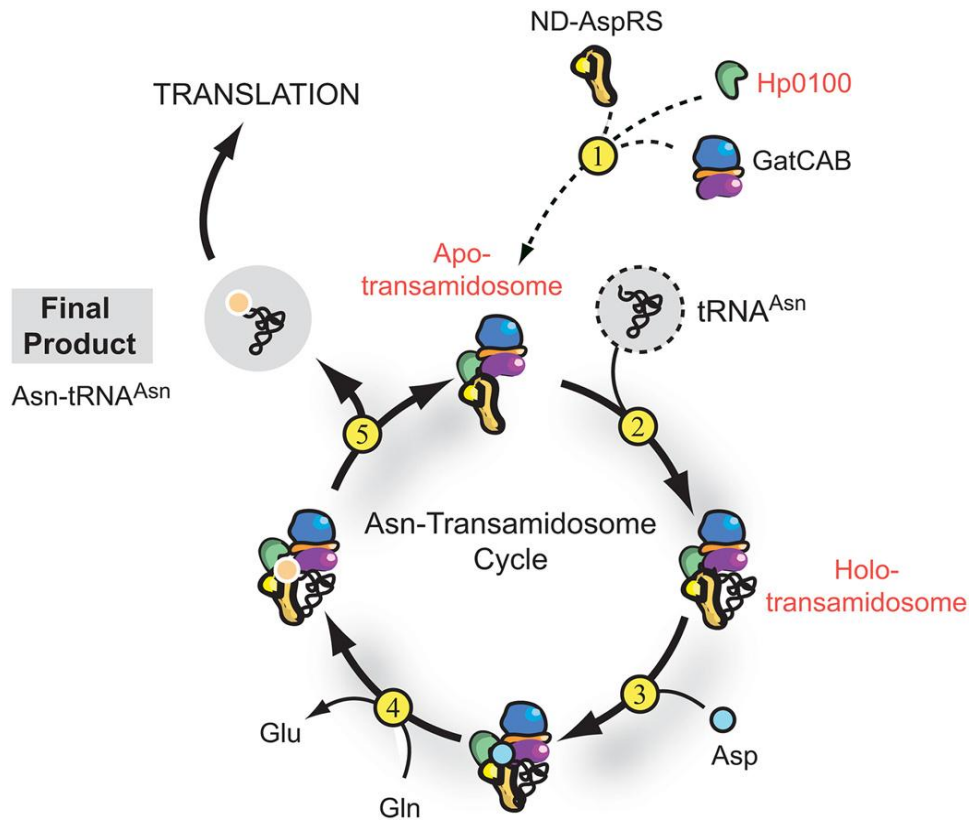


**Figure 1.8. Proposed *H. pylori* Asn-transamidosome cycle.** GatCAB, ND-AspRS, and Hp0100 assemble into an apo-transamidosome and tRNA<sup>Asn</sup> is recruited to form the holo-transamidosome. After the production of misacylated Asp-tRNA<sup>Asn</sup> by ND-AspRS, the product gets transamidated by GatCAB and released as Asn-tRNA<sup>Asn</sup> from the complex regenerating the apo-transamidosome. Figure regenerated with permission from the Journal of Biological Chemistry (79).

Further, Dr. Silva found that Hp0100 enhances the GatCAB-catalyzed transamidation of both Asp-tRNA<sup>Asn</sup> and Glu-tRNA<sup>Gln</sup>: the addition of Hp0100 to GatCAB reactions enhances the observed rate of Asp-tRNA<sup>Asn</sup> transamidation to Asn-tRNA<sup>Asn</sup> by ~35 fold (79) and of Glu-tRNA<sup>Gln</sup> to Gln-tRNA<sup>Gln</sup> by ~3 fold (87) (**Figure 1.9**). Hp0100 does not impact ND-AspRS aminoacylation activity (87).

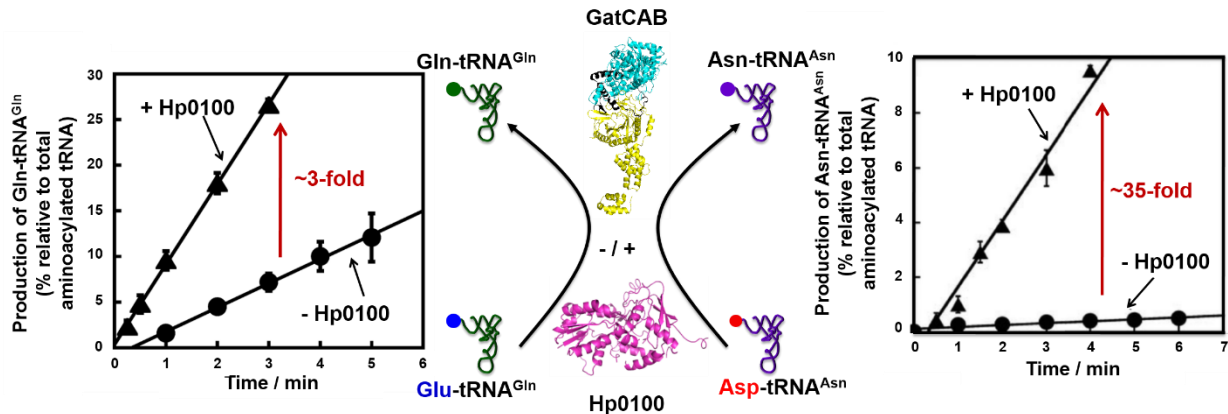


**Figure 1.9. Hp0100 accelerates GatCAB-catalyzed transamidation of misacylated tRNAs.** Hp0100 accelerates the transamidation of Glu-tRNA<sup>Gln</sup> to Gln-tRNA<sup>Gln</sup> by ~3-fold (left) (87) and Asp-tRNA<sup>Asn</sup> to Asn-tRNA<sup>Asn</sup> by GatCAB by ~35-fold (right) (79). Figure provided by Dr. Gayathri Silva.

Conserved domain analysis identified two putative ATPase domains, one built from an  $\alpha$ -adenosine nucleotide hydrolase (AANH) domain and the second from a P-loop motif (**Figure 1.10A**) (88). Encouragingly, the model structure of Hp0100 (generated by Rosetta (89)) was built from the argininosuccinate synthetase structure that also contains an AANH domain (90-91). AANH domain proteins contain an alpha-beta-alpha fold and generally hydrolyze ATP to AMP and PP<sub>i</sub> (88, 90). P-loop proteins have a consensus sequence of GXXXXGK[S/T] and hydrolyze ATP to ADP and Pi (92-93). Using TLC and an enzyme-coupled assay specific for ADP detection, Dr. Silva discovered that Hp0100 hydrolyzes ATP to ADP and Pi, and this ATP hydrolysis is enhanced in the presence of either Asp-tRNA<sup>Asn</sup> or Glu-tRNA<sup>Gln</sup> (**Figure 1.10B**) (87). Analysis of point mutations in the two ATPase domains demonstrated that both ATPase sites are catalytically active and AANH domain activity is specifically accelerated by Glu-tRNA<sup>Gln</sup>, while the P-loop responds to Asp-tRNA<sup>Asn</sup> (**Figure 1.10C**) (87). Hp0100 is the first example of an ATPase with two different active sites that are activated by two different misacylated tRNAs.

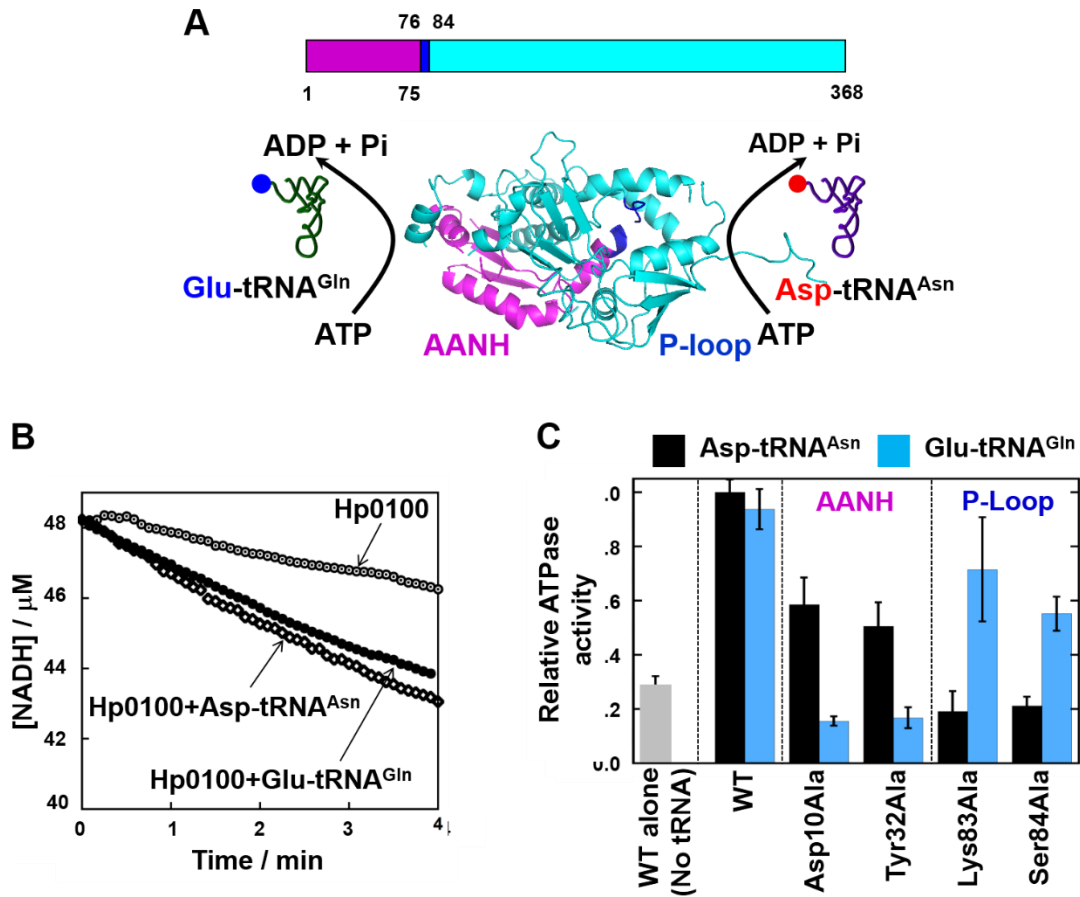


**Figure 1.10. Hp0100 contains two distinct ATPase active sites, which are activated by misacylated Asp-tRNA<sup>Asn</sup> and Glu-tRNA<sup>Gln</sup>.** (A) Hp0100 is an ATPase with an AANH domain (magenta, residues 1-75) and a P-loop motif (blue, residue 76-84). A Rosetta model of Hp0100 is shown with the AANH domain in magenta and the P-loop in blue. (B) Hp0100 exhibits ATPase activity in the presence of misacylated tRNAs. An enzyme-coupled assay was used to monitor ADP production via NADH oxidation to NAD<sup>+</sup>. (C) Mutations in the AANH domain affect Hp0100's Glu-tRNA<sup>Gln</sup>-dependent ATPase activity and its Asp-tRNA<sup>Asn</sup>-dependent ATPase activity is sensitive to mutants in the P-loop (87). Figure provided by Dr. Gayathri Silva.

Further, sequence analysis and the predicted model structure suggest that Hp0100 also contains several, clustered, conserved cysteine residues, including a possible metal binding motif with a CXXC signature sequence in the P-loop ATPase domain (**Figure 1.11**). Initial metal binding studies showed that Hp0100 preferentially binds divalent metal ions such as Fe(II), Zn(II) and Ni(II).



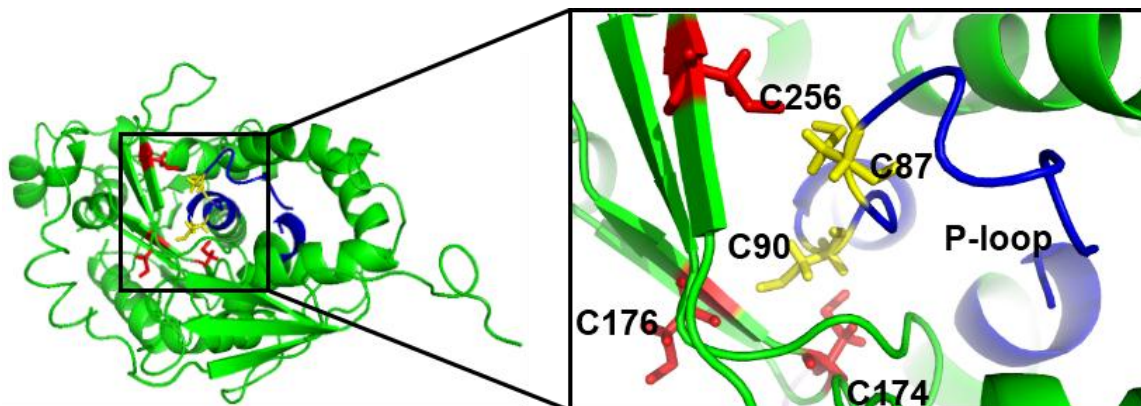


**Figure 1.11. The putative metal-binding motif of Hp0100.** Yellow: conserved Cysteine residues in the CXXC motif. Red: Conserved Cysteine residues proximal to the CXXC motif.

Chapter 4 of this dissertation focuses on cloning overexpression and purification of Hp0100 protein constructs. Hp0100 difficult to reproducibly purify; consequently, we turned to orthologs of this enzyme for further characterization. Full length Hp0100 is found in  $\epsilon$ -proteobacteria, however, truncated orthologs, composed of the N-terminal 2/3 of Hp0100 are found in other bacterial clades. Chapter 5 will summarize our preliminary characterization of a truncated Hp0100 ortholog from *S. aureus*, Sa2591.

### 1.9 Hp0100 and the truncated ortholog Sa2591 and queuosine biosynthesis

Queuosine is a modified guanosine base that is found in the first anticodon position of tRNA<sup>Asp</sup>, tRNA<sup>Asn</sup>, tRNA<sup>His</sup>, and tRNA<sup>Tyr</sup> (94-96). Even though queuosine is found in both bacteria and eukaryotes, only bacteria are capable of biosynthesizing this modified base; eukaryotes obtained it from their environment (94). The biosynthesis of queuosine is a multistep process, where the first few steps occur on free guanosine triphosphate (GTP), and the last three steps on the target tRNA (**Figure 1.12**). (97-98) After GTP is converted into preQ<sub>1</sub>, transfer RNA-guanine transglycosylase (TGT) catalyze the transfer of preQ<sub>1</sub> onto its specific tRNA. PreQ<sub>1</sub> is converted to epoxyqueuosine (oQ) by an S-

adenosylmethionine ribosyltransferase-isomerase enzyme called QueA. The last step in queuosine biosynthesis is the reduction of epoxyqueuosine to queuosine (Q) by a cobalamine-dependent epoxyqueuosine reductase, QueG.

Some bacteria that biosynthesize queuosine contain TGT and QueA but lack QueG. Recently, through comparative genomics, a group of proteins of unknown function (DUF208) was identified as a putative epoxyqueuosine reductase. Both Hp0100 and Sa2591 are DUF208 family members (**Figure 1.12, last step**). Overexpression of Hp0100 and Sa2591 restored queuosine biosynthesis in a  $\Delta$ QueG *E. coli* strain (99), indicating that these enzymes also have epoxyqueuosine reductase activity. We hypothesize that these proteins have this activity when they are not associated with the transamidosome.

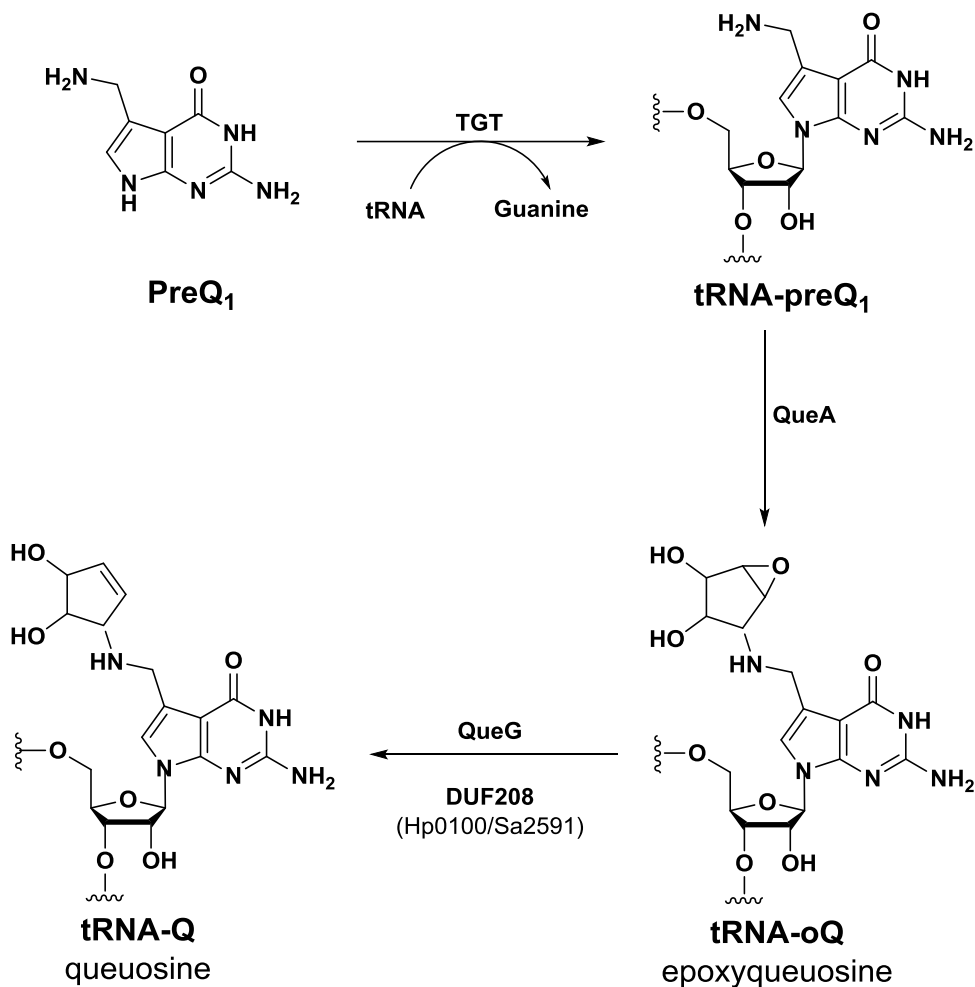


**Figure 1.12. The final three steps in queuosine biosynthesis.** TGT catalyzes the exchange of guanine 34 with preQ<sub>1</sub> in target tRNAs. QueA catalyzes the conversion of PreQ<sub>1</sub> into epoxyqueuosine. This intermediate is then reduced to queuosine by QueG or QueH. In organisms that lack QueG, the epoxyqueuosine reduction is catalyzed by DUF208 family proteins, such as Hp0100 and Sa2591. These proteins have been renamed QueH.

### 1.10 Dissertation research

This dissertation research is focused on broadening our understanding of bacterial indirect tRNA aminoacylation pathways by characterization and elucidation of novel activities of accessory proteins involved in this pathway. We hypothesize that accessory proteins regulate transamidosome assembly in response to the environment. Under favorable growth conditions, these proteins may promote stable assembly of the

transamidosome and Asn-tRNA<sup>Asn</sup> and/or Gln-tRNA<sup>Gln</sup> formation. But under unfavorable conditions, they may detach from the transamidosome, leading to its disassembly and the release of misacylated Asp-tRNA<sup>Asn</sup> and/or Glu-tRNA<sup>Gln</sup>. These misacylated tRNAs maybe incorporated into the proteome, providing conditions beneficial for the survival of the organism.

Chapter 2 discusses the first isolation of an *M. smegmatis* transamidosome. Chapter 3 focuses on the discovery of an unexpected enzymatic activity of bacterial AspRSs. We demonstrate that some bacterial AspRSs are capable of acting as a GluRS and produce Glu-tRNA<sup>Glu</sup>. Chapter 4 summarizes our efforts to clone, overexpress, and purify Hp0100 without a His<sub>6</sub>-tag. In chapter 5, the preliminary characterization of a truncated ortholog of Hpo100 called Sa2591 from *S. aureus* is presented.

## CHAPTER 2

### ***M. SMEGMATIS* TRANSAMIDOSOME ASSEMBLY**

#### **2.1 Introduction**

In many organisms, a set of 20 aaRSs ensures the accurate aminoacylation of tRNA and safeguards the fidelity of protein synthesis. However, many bacteria don't have a full set of aaRSs (15). In fact, most microorganisms lack AsnRS and/or GlnRS, and consequently, rely on a two-step, indirect aminoacylation pathway to produce Asn-tRNA<sup>Asn</sup> and Gln-tRNA<sup>Gln</sup> (34, 36-37, 43). This pathway proceeds via the misacylation of tRNA<sup>Asn</sup> and tRNA<sup>Gln</sup> to form Asp-tRNA<sup>Asn</sup> and Glu-tRNA<sup>Gln</sup>, respectively. These reactions are catalyzed by ND-AspRS and ND-GluRS (35, 43, 100). Next, a specific amidotransferase, GatCAB in bacteria, converts these misacylated tRNAs into their correctly aminoacylated forms (Asn-tRNA<sup>Asn</sup> and Gln-tRNA<sup>Gln</sup>) (34, 37). The central hub of the indirect tRNA aminoacylation pathway for Asn-tRNA<sup>Asn</sup> production is a macromolecular complex called the Asn-transamidosome, which brings the misacylating ND-AspRS and the correcting enzyme GatCAB together either via tRNA (77-78, 82, 101-102) or another protein partner called Hp0100 (79). In comparison to the reported Asn-transamidosomes (77-79, 82), to date, examples of analogous Gln-transamidosomes (80-81) are less stable and more dynamic in nature and their physiological relevance remains in doubt.

Evidence is accumulating that mistranslation is beneficial to organisms under certain conditions, e.g. tolerance to antibiotics (76) and antifungals (103), amino acid stress (104), oxidative stress (105-107), and growth temperature variations (108). The *Mycobacteria* are the only organisms in which a clear connection between indirect tRNA

aminoacylation and asparagine to aspartate mistranslation has been demonstrated (76). *M. tuberculosis* (the pathogenic bacterium that causes tuberculosis) and *M. smegmatis* (a benign, close relative of *M. tuberculosis*) lack genes encoding for either AsnRS or GlnRS. Thus, they use the indirect tRNA aminoacylation pathway to produce both Asn-tRNA<sup>Asn</sup> and Gln-tRNA<sup>Gln</sup> (47, 76). In particular, natural mutations in the GatA subunit of GatCAB result in the mistranslation of aspartate at asparagine codons at low levels throughout the *Mycobacterial* proteome (76). Remarkably, a particular mistranslation event in RNA polymerase (RNAP) resulted in bacterial persistence and phenotypic rifampicin tolerance (76). This work was described in more detail in section 1.7 of Chapter 1.

The mutants in GatCAB that induce mistranslation are located on the surface of the GatA subunit rather than in the enzyme's active site. We hypothesized that these mutations may promote mistranslation by disrupting or destabilizing the Asn-transamidosome. However, to date, wild-type *Mycobacterial* transamidosome(s) remain uncharacterized. This chapter focuses on our efforts to isolate and characterize the *M. smegmatis* transamidosomes, including the identification of two putative accessory proteins that were co-purified with GatCAB by affinity chromatography.

## **2.2 Results**

### **2.2.1 Several putative accessory proteins are co-purified with *M. smegmatis* GatCAB constructs**

We overexpressed and purified different combinations of the GatCAB subunits with His<sub>6</sub>-tags as follows: GatB alone (His<sub>6</sub>-GatB); GatCA (GatA-His<sub>6</sub> with co-expressed GatC); and GatCAB (GatB-His<sub>6</sub> with co-expressed GatCA) in the *M. smegmatis mc*<sup>2</sup>-155.

Our aim was to characterize the Asn-transamidosome. However, upon purification under mild conditions, we observed several proteins that repeatedly co-purified specifically in the presence of GatA (**Figure 2.1**). Purification of GatB alone resulted in pure protein with no evidence of endogenous GatA co-purification (**Figure 2.1, panel A, lane 1**). In contrast, purification of GatCA resulted in co-purification of endogenous levels of GatB with multiple other co-purified proteins. A similar pattern of co-purification was observed when GatCAB was purified by Ni<sup>2+</sup>-affinity chromatography. Given that the *H. pylori* Asn-transamidosome requires Hp0100 for assembly (79) and the *Mycobacteria* lack an Hp0100 ortholog, we hypothesized that these proteins might be important for Asn-transamidosome assembly or function.

The two protein bands that were observed to co-purify with GatCA and GatCAB were subjected to in-gel trypsin digestion and analyzed by mass spectrometry at the WSU Proteomics Facility. These proteins were identified as MSMEG3950 (a universal stress protein (USP), upper band) and superoxide dismutase (SOD, lower band).

Ten unique peptides from the in-gel trypsin digestion covered 44% of the protein sequence of MSMEG3950 (**Figure 2.1B**). There are 14 USPs in *M. smegmatis* (47) and the ortholog of MSMEG3950 from *M. tuberculosis* Rv2683 has been characterized (109-110). Rv2683 is upregulated under hypoxic and nitrosative stress conditions. It is proposed that Rv2683 is involved in bacterial persistence (110). Thirty unique peptides were identified for SOD and covered 83% of the protein sequence (**Figure 2.1C**). The role of SOD in protecting cells against oxidative damage is well characterized (111). Any connection between MSMEG3950, SOD, and indirect tRNA aminoacylation is unknown

and further experiments are needed to verify that these interactions are physiologically relevant.

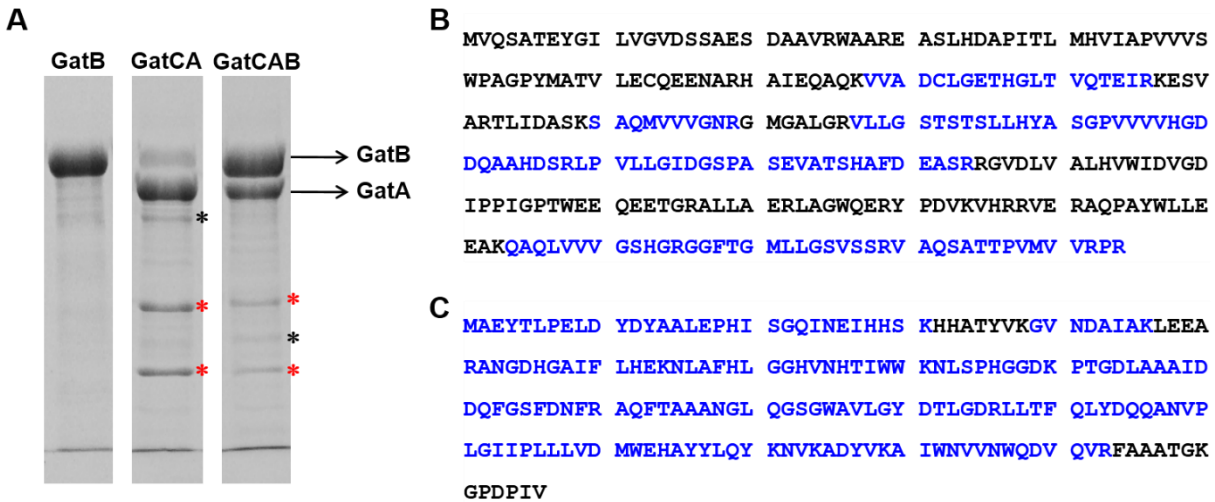


**Figure 2.1. Putative accessory proteins co-purify with GatCAB.** (A) SDS-PAGE gel showing the co-purification of accessory proteins with different GatCAB constructs from *M. smegmatis*. His<sub>6</sub>-GatB (lane 1), GatCA (GatA-His<sub>6</sub> with co-expressed GatC, lane 2), and GatCAB (GatB-His<sub>6</sub> with co-expressed GatCA, lane 3). Proteins of unknown identity that co-purified with GatA are labeled with asterisks. Red asterisks indicate those characterized by mass spectrometry. (B) Sequencing results of the top co-purified protein band highlighted with a red asterisk in A. This band was identified as MSMEG3950. The peptides highlighted in blue were observed by mass spectrometry. (C) The bottom band was identified as superoxide dismutase by mass spectrometry. Observed peptides are highlighted in blue.

### 2.2.2 Overexpression of GatCAB in *M. smegmatis* results in the co-purification of ND-AspRS and ND-GluRS

We also examined purified GatCAB for the co-purification of endogenous ND-AspRS or ND-GluRS as evidence of the formation of a stable transamidosomes. The protein samples were purified in two ways: Co<sup>+2</sup> affinity purification alone and Co<sup>+2</sup> affinity purification followed by size exclusion chromatography (SEC) (Figure 2.2). Neither ND-AspRS nor ND-GluRS was visible in protein gels after purification of GatCAB indicated



that they either did not co-purify or that co-purification occurred at levels too low to detect by SDS-PAGE gel.

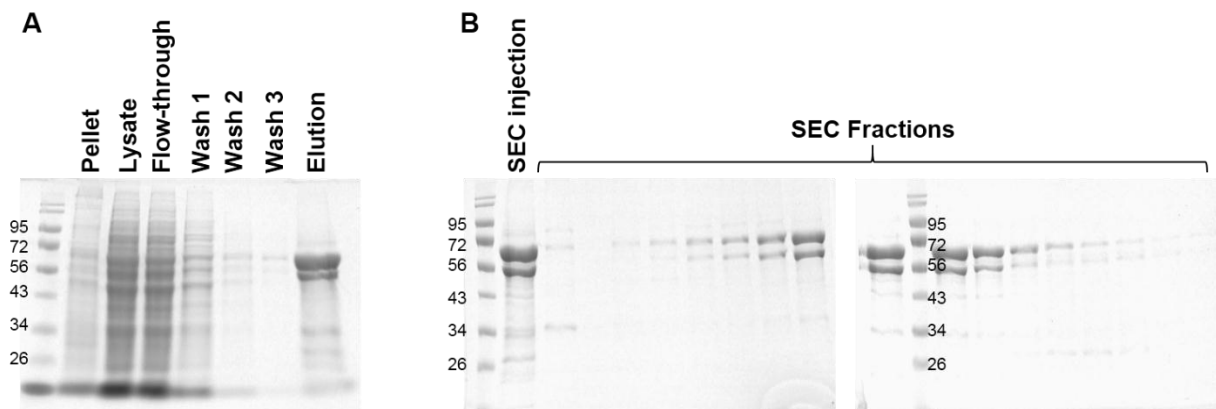


**Figure 2.2. SDS-PAGE gel analysis of GatCAB purification. (A)** SDS-PAGE gel showing Co<sup>2+</sup> affinity purification of overexpressed GatCAB from *M. smegmatis*. **(B)** SDS-PAGE gel showing an additional SEC purification of GatCAB.

We turned to aminoacylation assays to more sensitively assess GatCAB for the presence of co-purified ND-AspRS or ND-GluRS. As a control, we used an empty *M. smegmatis* cell line (without overexpression of GatCAB). The assays from the protein samples purified from Co<sup>2+</sup> affinity chromatographic purification (**Figure 2.2A, elution**) clearly indicated the co-purification of ND-AspRS and ND-GluRS with GatCAB (**Figure 2.3**). In these assays, the increase in the concentration of aa-tRNA<sup>aa</sup> indicates the presence of the corresponding aaRS. There levels of ND-AspRS purification with GatCAB are consistent with robust Asn-transamidosome formation (**Figure 2.3A**). These data represent the first demonstration of a functional *Mycobacterial* Asn-transamidosome.

Compared to ND-AspRS, assay results suggested that ND-GluRS only weakly co-purifies with GatCAB as part of a Gln-transamidosome (**Figure 2.3B**). These results are consistent with other reports that have suggested that the Gln-transamidosome is notably less stable than its Asn-transamidosome counterpart. Nevertheless, this observed

activity suggested that we had isolated a Gln-transamidosome for the first time from any bacterium. The empty *M. smegmatis* cell line was used as a control in both cases. The expectation was that neither ND-AspRS nor ND-GluRS activity would be evident in these assays following “purification” by  $\text{Co}^{2+}$ -affinity. Surprisingly, considerable aminoacylation activity was observed with this control in both cases suggesting that both aaRSs have some nascent affinity for  $\text{Co}^{2+}$  resin.

Analogous enzyme assays were carried out using GatCAB that had been purified by both  $\text{Co}^{+2}$  affinity and SEC in an effort to eliminate the challenges faced by the unexpected ND-AspRS and ND-GluRS activity observed in the control samples (**Figure 2.4**). The data more robustly demonstrate that both ND-AspRS and ND-GluRS co-purify with *M. smegmatis* GatCAB.

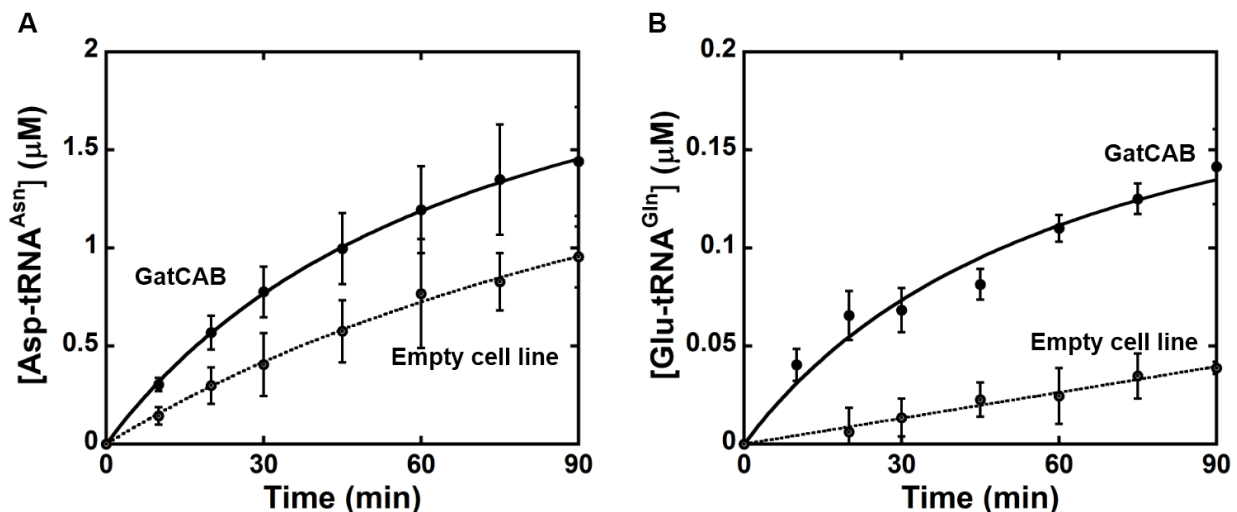


**Figure 2.3.** *M. smegmatis* ND-AspRS and ND-GluRS co-purify with the overexpressed GatCAB in *M. smegmatis* cell line. **(A)** Aminoacylation assays with *M. smegmatis* tRNA<sup>Asn</sup> and aspartate using the  $\text{Co}^{+2}$ -affinity purified GatCAB confirm the co-purification of ND-AspRS with GatCAB. **(B)** Aminoacylation assays with *M. smegmatis* tRNA<sup>Gln</sup> and glutamate using the  $\text{Co}^{+2}$ -affinity purified GatCAB confirm the co-purification of ND-GluRS with GatCAB. The empty *Mycobacterial* cell line was used as a control for comparison. Error bars represent the standard deviation from biological triplicates.

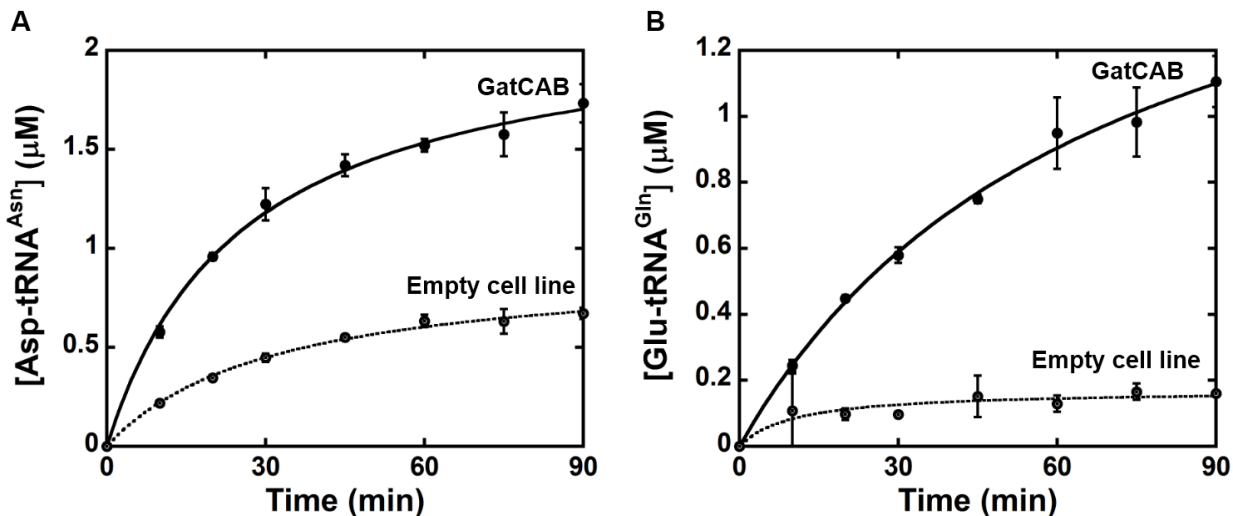


**Figure 2.4. *M. smegmatis* ND-AspRS and ND-GluRS assemble into a transamidosomes(s) with GatCAB.** (A) Aminoacylation assays with *M. smegmatis* tRNA<sup>Asn</sup> and aspartate with the Co<sup>+2</sup> affinity followed by SEC purified GatCAB confirmed the co-purification of ND-AspRS with GatCAB. (B) Aminoacylation assays with *M. smegmatis* tRNA<sup>Gln</sup> and glutamate with the Co<sup>+2</sup> affinity followed by SEC purified GatCAB confirmed the co-purification of ND-GluRS with GatCAB. Error bars represent the standard deviation from biological triplicates.

### 2.2.3 The substrate specificity conundrum of *M. smegmatis* ND-AspRS

An important remaining conundrum in the field of indirect tRNA aminoacylation is that we don't understand how GatCAB can exist in an Asn-transamidosome and still convert Glu-tRNA<sup>Gln</sup> into Gln-tRNA<sup>Gln</sup>. Some evidence suggests a Gln-transamidosome (80-81), but the physiological relevance of these reports remain unclear. The formation of a mega-transamidosome, composed of GatCAB, ND-AspRS, and ND-GluRS is difficult to envision sterically. Consequently, the results presented in Figure 2.4, which suggest that these three enzymes co-purify as a single complex, are particularly intriguing and merited more detailed analyses.

To verify that the aminoacylation of tRNA<sup>Asn</sup> and tRNA<sup>Gln</sup> is due to co-purified ND-AspRS and ND-GluRS respectively, we performed aminoacylation assays with purified, recombinant, *M. smegmatis* ND-AspRS and ND-GluRS for comparison (**Figure 2.6**). Both

of these enzymes are expected to be non-discriminating, however, their precise tRNA substrate specificities have never been reported. Consequently, our first step was to verify that both of these enzymes were capable of aminoacylating their non-cognate tRNA substrates: tRNA<sup>Asn</sup> for ND-AspRS and tRNA<sup>Gln</sup> for ND-GluRS. These assays were performed with the two *M. smegmatis* tRNAs, which had been overexpressed in *E. coli* and purified as total tRNA. Consequently, these tRNAs are enriched for the specific *M. smegmatis* isoacceptor of interest but they are contaminated with total *E. coli* tRNA.

As expected, *M. smegmatis* ND-GluRS is capable of producing Glu-tRNA<sup>Gln</sup>, but not Asp-tRNA<sup>Asn</sup> (**Figure 2.5, dash lines**), consistent with it being a canonical ND-GluRS. Similarly, ND-AspRS aminoacylates tRNA<sup>Asn</sup> with aspartate (**Figure 2.5A**), consistent with ND-AspRS activity. However, we were surprised to observe aminoacylation activity with *M. smegmatis* ND-AspRS, tRNA<sup>Gln</sup>, and glutamate (**Figure 2.5B**). This activity indicates that *M. smegmatis* ND-AspRS is capable of producing Glu-tRNA<sup>Gln</sup> or aminoacylating a contaminating *E. coli* tRNA with glutamate (**Figure 2.5B**). In Chapter 3, we further characterize this unexpected ND-AspRS activity and show that bacterial AspRSs (both discriminating and non-discriminating) have the ability to produce Glu-tRNA<sup>Glu</sup>. Unfortunately, this unexpected ND-AspRS activity with glutamate raises ambiguity with respect to the formation of an *M. smegmatis* Gln-transamidosome.

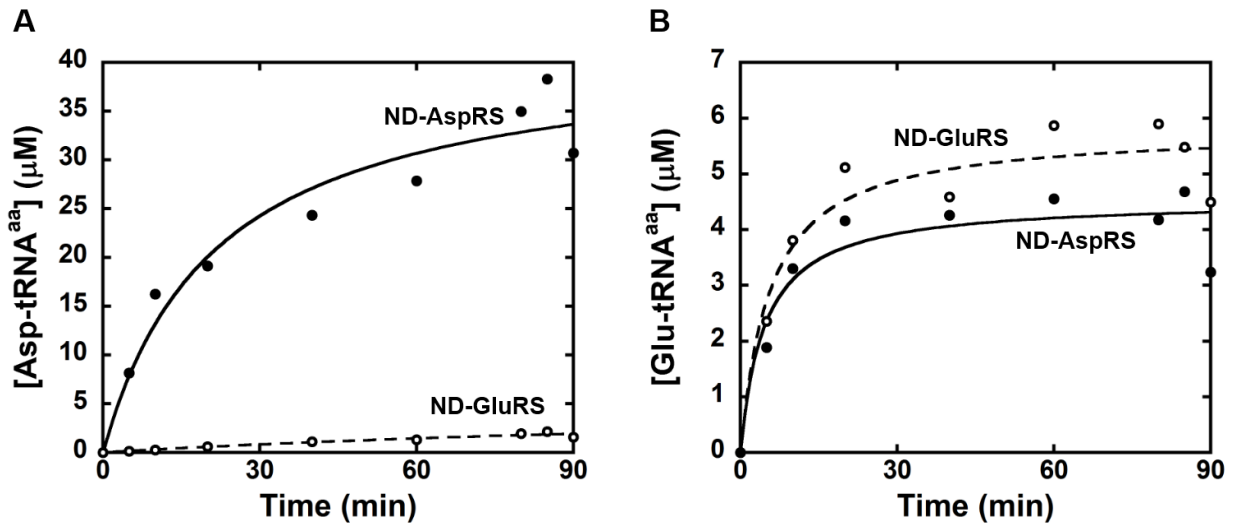


**Figure 2.5.** *M. smegmatis* ND-AspRS aminoacylates at least one tRNA with glutamate. **(A)** Aminoacylation of *M. smegmatis* tRNA<sup>Asn</sup> and/or *E. coli* tRNAs with aspartate by *M. smegmatis* ND-AspRS versus ND-GluRS. **(B)** Aminoacylation of *M. smegmatis* tRNA<sup>Gln</sup> and/or *E. coli* tRNAs with glutamate by *M. smegmatis* ND-AspRS and ND-GluRS.

#### 2.2.4 ND-AspRS and GatCAB assemble into an Asn-transamidosome

We also evaluated the possibility of Asn and/or Gln-transamidosome formation by native gel electrophoresis using overexpressed and purified ND-AspRS, ND-GluRS, and GatCAB (**Figure 2.6**). A faint upward shift is observed when ND-AspRS is incubated with increasing amounts of GatCAB (**Figure 2.6, lanes 7, 9, and 10, indicated with an asterisk**), suggesting weak Asn-transamidosome formation. Repeated attempts to better resolve this species, including the addition of tRNA<sup>Asn</sup>, were unsuccessful. No indication of complex formation between ND-GluRS and GatCAB was observed (**Figure 2.6, lane 5 and 8**). These results could indicate a requirement for tRNA and/or an accessory protein-like Hp0100 for robust transamidosomes assembly.

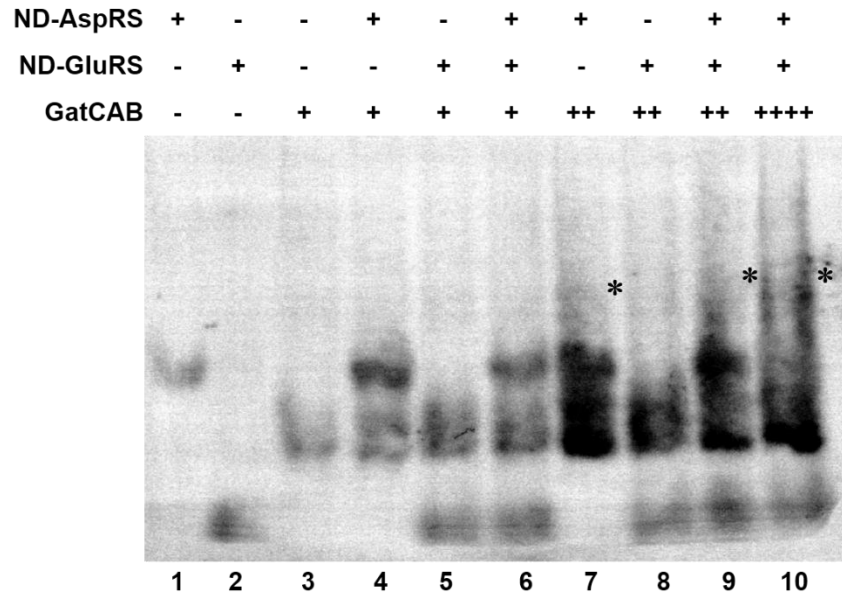


**Figure 2.6. Transamidosome evaluation by native gel electrophoresis.** The formation of Asn and/or Gln-transamidosome complexes was evaluated by native gel electrophoresis and anti-His<sub>6</sub> Western blots (ND-AspRS, ND-GluRS, and GatB were modified with His<sub>6</sub>-tags). The upward shift of bands indicated by asterisks suggests incomplete Asn-transamidosome assembly.

## 2.3 Discussion

*M. smegmatis* lacks genes for AsnRS and GlnRS, thus this bacterium requires indirect tRNA aminoacylation for the production of Asn-tRNA<sup>Asn</sup> and Gln-tRNA<sup>Gln</sup>. During indirect tRNA biosynthesis, it is important to sequester the misacylated intermediates Asp-tRNA<sup>Asn</sup> and Glu-tRNA<sup>Gln</sup> from the ribosome until they are converted to Asn-tRNA<sup>Asn</sup> and Gln-tRNA<sup>Gln</sup> by GatCAB. One such mechanism is the formation of a macromolecular complex called a transamidosome. The Asn-transamidosome bring together ND-AspRS and GatCAB via either tRNA<sup>Asn</sup> (77-78, 82, 101-102) or an accessory protein-like Hp0100 (79). The reported Gln-transamidosomes also depend on tRNA<sup>Gln</sup> but are more dynamic and less stable than their Asn-transamidosome counterparts (80-81). How Glu-tRNA<sup>Gln</sup> is transferred from ND-GluRS to GatCAB remains an open question in the field.

Here we have shown that purification of *M. smegmatis* GatCAB Co<sup>2+</sup>-affinity purification and SEC results in the co-purification of endogenous ND-AspRS (**Figure 2.3 and 2.4**), clearly indicating Asn-transamidosome formation. This complex was also assembled from its components and observed by native gel electrophoresis. Though aminoacylation assays confirm the co-purification of ND-AspRS and GatCAB, they do not provide details regarding the composition or the assembly of the transamidosome. Is the transamidosome tRNA-dependent or does it require another protein partner analogous to Hp100 for its assembly? These questions need to be addressed in the future.

Unfortunately, efforts to confirm co-purification of ND-GluRS with GatCAB were less clear. Aminoacylation assays suggested that low levels of ND-GluRS did accompany GatCAB through its purification; however, our discovery that *M. smegmatis* ND-AspRS can produce Glu-tRNA<sup>Glu</sup> introduces uncertainty into these results. Acid gel electrophoresis, combined with Northern blots, may prove useful to resolve this ambiguity. For the time being, the possibility of a functional Gln-transamidosome remains unresolved.

We have repeatedly observed several putative accessory proteins in our GatCAB purifications (**Figure 2.1**) and have identified two of these proteins as a USP, MSMEG3950, and SOD. These proteins were identified by in-gel trypsin digestion, followed by sequencing of the peptide fragments by mass spectrometry. USP and SOD are stress-related proteins (110-111). With the knowledge that mistranslation in *M. smegmatis* results in persistence and phenotypic rifampicin tolerance (76), and that mistranslation in other organisms can be beneficial under numerous stress-related conditions (76, 103-108), we speculate that these accessory proteins may disrupt or

contribute to the *M. smegmatis* transamidosome. This hypothesis, while intriguing, remains highly speculative at the present time. Additional experiments are needed to further explore these putative interactions.

In conclusion, we have characterized the *Mycobacterial* transamidosome and have identified two putative accessory proteins that may interact with the transamidosome, both of which are relevant to stress. Future experiments need to be carried out to assess the composition of the transamidosome under normal versus stress-inducing conditions.

## **2.4 Materials and Methods**

### **2.4.1 Materials**

Sodium dihydrogen phosphate ( $\text{NaH}_2\text{PO}_4$ ), magnesium chloride, Tween-80, and glucose were purchased from Sigma-Aldrich (St. Louis, MO). Ampicillin, kanamycin, chloramphenicol, hygromycin B, ethylenediaminetetraacetic acid (EDTA), isopropyl  $\beta$ -D-thiogalactopyranoside (IPTG), tris(hydroxymethyl) aminomethane (Tris), lysozyme, and phenylmethanesulfonyl fluoride (PMSF) were from Gold Biotechnology, Inc. (St. Louis, MO). Sodium chloride (NaCl) and glycine were purchased from Fisher Scientific (Hampton, NH). Mouse *anti*-His<sub>6</sub> tag antibody and goat *anti*-mouse IgG antibodies were purchased from BIO-RAD (Hercules, CA).

### **2.4.2 Overexpression and purification of *M. smegmatis* GatCAB, GatB, and GatCA**

*M. smegmatis* N-terminal His<sub>6</sub>-tagged GatB, C-terminus His<sub>6</sub>-tagged GatC with co-expressed GatA (GatCA), and C-terminal His<sub>6</sub>-tagged GatB co-expressed with GatCA (GatCAB) were overexpressed in *M. smegmatis* mc<sup>2</sup>-155 using vectors kindly provided by Dr. Babak Javid. The cultures were grown in Middlebrook 7H9 medium (0.8 L in a 4 L flask) supplemented with glycerol (0.2%), Tween-80 (0.05%), hygromycin B (50  $\mu\text{g/ml}$ ),



and anhydrotetracycline (50 ng/mL) starting with a saturated culture grown in the same medium supplemented with NaCl (0.85%), glucose (2%), and BSA (5%). The cultures were incubated at 37 °C, 200 rpm until the OD<sub>600</sub> reached between 1 and 2 (approximately 24-30 hours). The cells were harvested by centrifugation at 5,000 rpm for 15 min at 4 °C and the cell pellets were kept at -80 °C until ready to use.

The His<sub>6</sub>-tagged GatB and GatCA proteins were only purified by Co<sup>2+</sup> affinity chromatography. The His<sub>6</sub>-tagged GatCAB was purified by Co<sup>2+</sup>-affinity and SEC. In all three cases, for Co<sup>2+</sup>-affinity purification, the cell pellets were suspended in lysis buffer (50 mM NaH<sub>2</sub>PO<sub>4</sub> pH 7.4, 300 mM NaCl, 10 mM imidazole) and the cells were lysed with lysozyme (2 mg/mL) and sonication. Saturated PMSF (15 μL/mL) was added every 20 min to reduce proteolysis. The cell debris was separated from the lysate by centrifugation at 14,000 rpm for 30 min at 4 °C. Typically, a cell extract was added to a polyprep column that contained high-density cobalt agarose beads (~ 2 mL, Gold Biotechnology, Inc.) pre-washed with lysis buffer. The lysate was incubated with the resin by rotating at 4 °C for 1 hour. The His<sub>6</sub>-tagged proteins were eluted according to the manufacturer's protocol (Gold Biotechnology). The proteins were dialyzed for one hour and then overnight in dialysis buffer (50 mM NaH<sub>2</sub>PO<sub>4</sub> pH 7.4, and 300 mM NaCl) and concentrated using 3 kDa molecular weight spin filters (EMD Millipore) prior to aminoacylation assays.

Immediately after Co<sup>2+</sup>-affinity purification and dialysis, the concentrated GatCAB was injected onto a SEC column packed with Sephacryl S-300 high-resolution size exclusion chromatographic resin (GE Healthcare Bio-Sciences, Uppsala, Sweden). The proteins were eluted with SEC buffer (50 mM NaH<sub>2</sub>PO<sub>4</sub> pH 7.4, and 300 mM NaCl) and

fractions (5 mL) were collected and analyzed by SDS-PAGE. The fractions containing pure GatCAB were combined and concentrated.

The empty *M. smegmatis* mc<sup>2</sup>-155 was grown in the above-mentioned culture medium (without hygromycin B) and incubated at 37 °C, 200 rpm. The pellet was collected and treated to the same purification protocol as GatCAB.

#### **2.4.3 Overexpression and purification of *M. smegmatis* ND-AspRS and ND-GluRS**

*M. smegmatis* ND-AspRS and ND-GluRS (vectors provided by Dr. Babak Javid), were each overexpressed in *E. coli* BI21(DE3)-RIL in Luria-Bertani medium (LB, 1 L) supplemented with kanamycin (50 µg/mL), chloramphenicol (100 µg/mL), and glucose (0.5%). The cultures were inoculated with a saturated overnight culture grown from a single colony the same medium. The cultures were incubated at 37 °C, 200 rpm and protein overexpression was induced at OD<sub>600</sub> = 0.8-1 with IPTG (1 mM). The cells were collected by centrifugation at 4,000 rpm for 10 min at 4 °C after 1-hour induction period. The proteins were purified by Co<sup>2+</sup>-affinity as discussed above.

#### **2.4.4 *In vivo* expression and purification of tRNAs**

*M. smegmatis* tRNA<sup>Asn</sup> and tRNA<sup>Gln</sup> (*M. smegmatis* vectors provided by Dr. Babak Javid) were overexpressed, purified, and quantified as previously described (52, 73).

#### **2.4.5 Aminoacylation assays with purified GatCAB**

Aminoacylation assays were conducted in buffer containing 20 mM HEPES-OH, pH 7.5, 4 mM MgCl<sub>2</sub>, 2 mM ATP, 100 µM amino acid, and 50 µCi/mL <sup>3</sup>H-labeled amino acid. Assays were carried out using 10 µM *M. smegmatis* tRNA<sup>Asn</sup> or tRNA<sup>Gln</sup> as noted. The Co<sup>2+</sup>-affinity purified GatCAB was added to a final concentration of 1 µg/mL and 0.8 µg/mL of GatCAB was used after the two-column purification. All assays were conducted

in triplicate from different protein purifications. The same assays were carried out with empty cell line purifications: in this case, the protein sample was concentrated to the same volume as GatCAB and an equivalent volume was used.

#### **2.4.6 Aminoacylation assays with purified recombinant *M. smegmatis* ND-AspRS and ND-GluRS from *E. coli***

The extended (90 min) aminoacylation assays were conducted in buffer containing 20 mM HEPES-OH, pH 7.5, 4 mM MgCl<sub>2</sub>, 2 mM ATP, 200 μM amino acid, and 25 μCi/mL <sup>3</sup>H-labeled amino acid. Assays were carried out using 10 μM *M. smegmatis* tRNA<sup>Asn</sup> or tRNA<sup>Gln</sup> as noted. Purified recombinant *M. smegmatis* ND-AspRS and ND-GluRS were added to a final concentration of 1 μM.

#### **2.4.7 Mass spectrometric analysis of co-purified protein bands from *M. smegmatis* GatCAB purification**

The eluted GatCAB sample from Co<sup>2+</sup>-affinity purification was separated on a 12% SDS-PAGE gel and visualized with Sypro Ruby stain (Molecular Probes, Eugene, OR). The gel bands were excised, subjected to in-gel trypsin digestion, and analyzed by LC-MS/MS at the WSU Proteomics Facility as previously described (112).

#### **2.4.8 Transamidosome assembly analysis by electrophoretic mobility shift assays**

Transamidosome formation between ND-AspRS (0.2 μM), ND-GluRS (0.2 μM), and GatCAB (0.2, 0.4 and 0.8 μM) was examined by native gel electrophoresis. The protein samples were mixed as indicated and incubated at 4 °C for 30 min. The complexes were separated on an 8% native PAGE in Tris-glycine buffer (25 mM Tris, 200 mM glycine, pH 8.8). The gel bands were visualized by Western blot using *anti*-His<sub>6</sub> antibodies

(BIO-RAD, Hercules, CA). Both ND-AspRS and ND-GluRS contained C-terminal His<sub>6</sub>-tags. GatCAB contained a C-terminus His<sub>6</sub>-tag on the GatB subunit.

## CHAPTER 3

### BACTERIAL ASPARTYL-TRNA SYNTHETASE HAS GLUTAMYL-TRNA SYNTHETASE ACTIVITY

The majority of this chapter is in press for publication in a special issue of *Genes*. Rathnayake, U. M.; and Hendrickson, T. L. Bacterial Aspartyl-tRNA Synthetase Has Glutamyl-tRNA Synthetase Activity. *Genes* **2019**, *10*, 262. DOI: 10.3390/genes10040262  
Copyright © 2019, MDPI, reprinted with permission.

#### 3.1 Introduction

The fidelity of protein translation depends on the accurate pairing of cognate tRNAs to their cognate amino acids. The ligation of the amino acid to its tRNA is catalyzed by a highly specific group of enzymes known as the aminoacyl-tRNA synthetases (aaRS) (2, 11, 15). Under normal conditions, these enzymes maintain high accuracy and specificity in selecting their cognate amino acid and tRNA substrates. In fact, decades of research have been dedicated to demonstrating that the aaRSs are exquisitely specific for their cognate substrates and are key players in defining the accuracy of the proteome (15, 113-115). An increasing body of work, however, is emerging that demonstrates that some aaRSs can alter their activity or relax their selectivity in response to stress, even promoting errors in translation (4, 84, 116-119).

Aspartyl-tRNA synthetase (AspRS) is an exception to the rule of one aaRS per amino acid/tRNA pair. It can be found in two general forms: discriminating and non-discriminating, based on divergent tRNA specificities. Discriminating AspRS, the canonical enzyme, is found in eukaryotes and some bacteria (*e.g. Escherichia coli* or *Ec*) and archaea, and catalyzes the aspartylation of tRNA<sup>Asp</sup> to produce Asp-tRNA<sup>Asp</sup> (**Figure 3.1A**) (16). The non-discriminating form, ND-AspRS, is found in many

bacteria and archaea and some organelles; this enzyme cannot differentiate between  $\text{tRNA}^{\text{Asp}}$  and  $\text{tRNA}^{\text{Asn}}$  and aminoacylates both with aspartate to generate  $\text{Asp-tRNA}^{\text{Asp}}$  and the misacylated  $\text{Asp-tRNA}^{\text{Asn}}$ , respectively (**Figure 3.1B**) (31, 33, 35, 43).  $\text{Asp-tRNA}^{\text{Asn}}$  is then converted to  $\text{Asn-tRNA}^{\text{Asn}}$  by a glutamine-dependent amidotransferase (AdT) (35-37, 43).

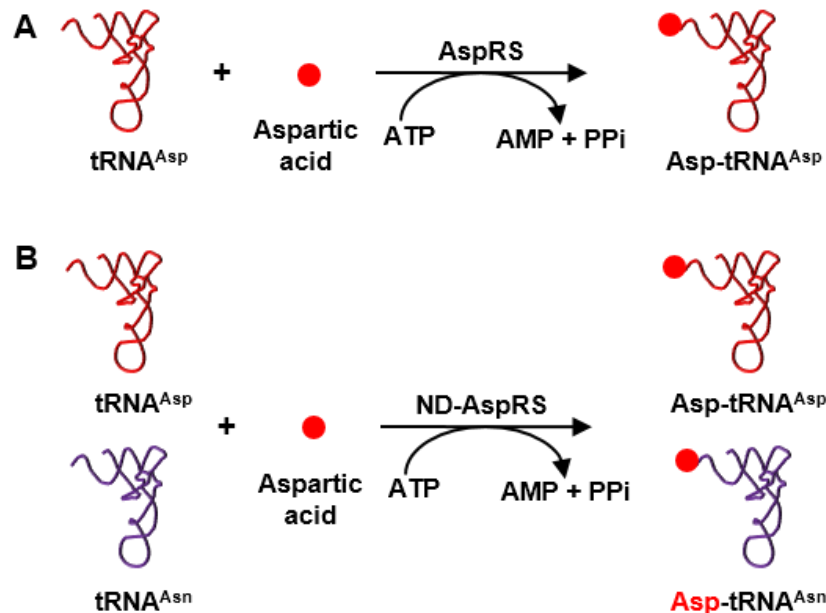


**Figure 3.1. Canonical roles of AspRS and ND-AspRS.** (A) AspRS aminoacylates  $\text{tRNA}^{\text{Asp}}$  with aspartic acid to produce  $\text{Asp-tRNA}^{\text{Asp}}$ . (B) ND-AspRS catalyzes the aspartylation of both  $\text{tRNA}^{\text{Asp}}$  and  $\text{tRNA}^{\text{Asn}}$  to produce  $\text{Asp-tRNA}^{\text{Asp}}$  and the misacylated  $\text{Asp-tRNA}^{\text{Asn}}$ .

The requirement for a discriminating AspRS versus an ND-AspRS differs from organism to organism; however, ND-AspRS is always accompanied by AdT (35-38). ND-AspRS and AdT are typically found in organisms that lack asparaginyl-tRNA synthetase (AsnRS) and/or asparagine synthetase (AsnS). **Table 1.4**, in chapter 1, lists examples of such organisms and the gene distribution patterns of relevant genes. For example, *Pseudomonas aeruginosa* (*P. aeruginosa*) and *Helicobacter pylori* (*H. pylori* or *Hp*) lack both AsnRS and AsnS and consequently require ND-AspRS and AdT to produce both

Asn-tRNA<sup>Asn</sup> and asparagine (49, 59). *Mycobacterium tuberculosis* lacks AsnRS but has AsnS, so it only uses indirect tRNA aminoacylation to produce Asn-tRNA<sup>Asn</sup> (50). In contrast, *Staphylococcal aureus* (*S. aureus* or *Sa*) has a functioning AsnRS but lacks AsnS; thus, indirect aminoacylation is still required as the sole biosynthetic route to asparagine (51). Some bacteria like *Thermus thermophilus* and *Deinococcus radiodurans* encode for more than one copy of AspRS (45, 54). In these cases, the longer, bacterial-type AspRS is discriminating and catalyzes the synthesis of Asp-tRNA<sup>Asp</sup>. The second AspRS (AspRS2) is non-discriminating and produces Asp-tRNA<sup>Asn</sup> along with Asp-tRNA<sup>Asp</sup>.

The relaxed specificity of archaeal and bacterial ND-AspRSs has been characterized to some extent. The anticodon-binding domain of the archaeal-type and bacterial-type AspRS are responsible for recognition of the anticodon bases of tRNA<sup>Asp</sup> (AspRS and ND-AspRS) and tRNA<sup>Asn</sup> (ND-AspRS only). Many mutagenesis studies have been conducted on this region of various AspRSs and ND-AspRSs from bacteria and archaea to better understand how these enzymes recognize tRNA<sup>Asp</sup> and tRNA<sup>Asn</sup>. **Table 3.1** summarizes the AspRS and ND-AspRS characterizations from different archaea and bacteria reported so far. **Figure 3.2** shows a sequence alignment of the anticodon-binding domains of several bacteria and archaea and the crystal structure of *E. coli* AspRS with tRNA<sup>Asp</sup>, highlighting the residues used in mutagenesis studies.

**Table 3.1. Summary of mutagenesis studies of AspRSs and ND-AspRSs anticodon-binding domains**

Organism	Domain	D/ND <sup>1</sup>	Mutations <sup>3</sup>	Phenotype	Ref.
<i>Thermococcus kodakaraensis</i>	archaea	D	<ul style="list-style-type: none"> <li>• W26H</li> <li>• K85P</li> <li>• W26H/K85P</li> </ul>	<ul style="list-style-type: none"> <li>• Converts D-AspRS to ND-AspRS</li> <li>• Increases specificity towards tRNA<sup>Asn</sup></li> </ul>	(120)
<i>Deinococcus radiodurans</i>	bacteria	ND <sup>2</sup>	<ul style="list-style-type: none"> <li>• H28Q</li> <li>• P77K</li> <li>• H28Q/P77K</li> </ul>	<ul style="list-style-type: none"> <li>• Converts ND-AspRS to D-AspRS</li> <li>• Reduces specificity towards tRNA<sup>Asn</sup></li> </ul>	(121)
<i>Pseudomonas aeruginosa</i>	bacteria	ND	<ul style="list-style-type: none"> <li>• H31L</li> <li>• G83K</li> <li>• H31L/G83K</li> </ul>	<ul style="list-style-type: none"> <li>• Converts ND-AspRS to D-AspRS</li> <li>• Reduces specificity towards tRNA<sup>Asn</sup></li> </ul>	(122)
<i>Helicobacter pylori</i>	Bacteria	ND	<ul style="list-style-type: none"> <li>• L81N</li> <li>• L86M</li> <li>• L81N/L86M</li> </ul>	<ul style="list-style-type: none"> <li>• Converts ND-AspRS to D-AspRS</li> <li>• Reduces specificity towards tRNA<sup>Asn</sup></li> </ul>	(49)

<sup>1</sup> D is for discriminating AspRS and ND is for a nondiscriminating AspRS

<sup>2</sup> Archaeal-type ND-AspRS

<sup>3</sup> These mutations are highlighted in Figure 3.2A



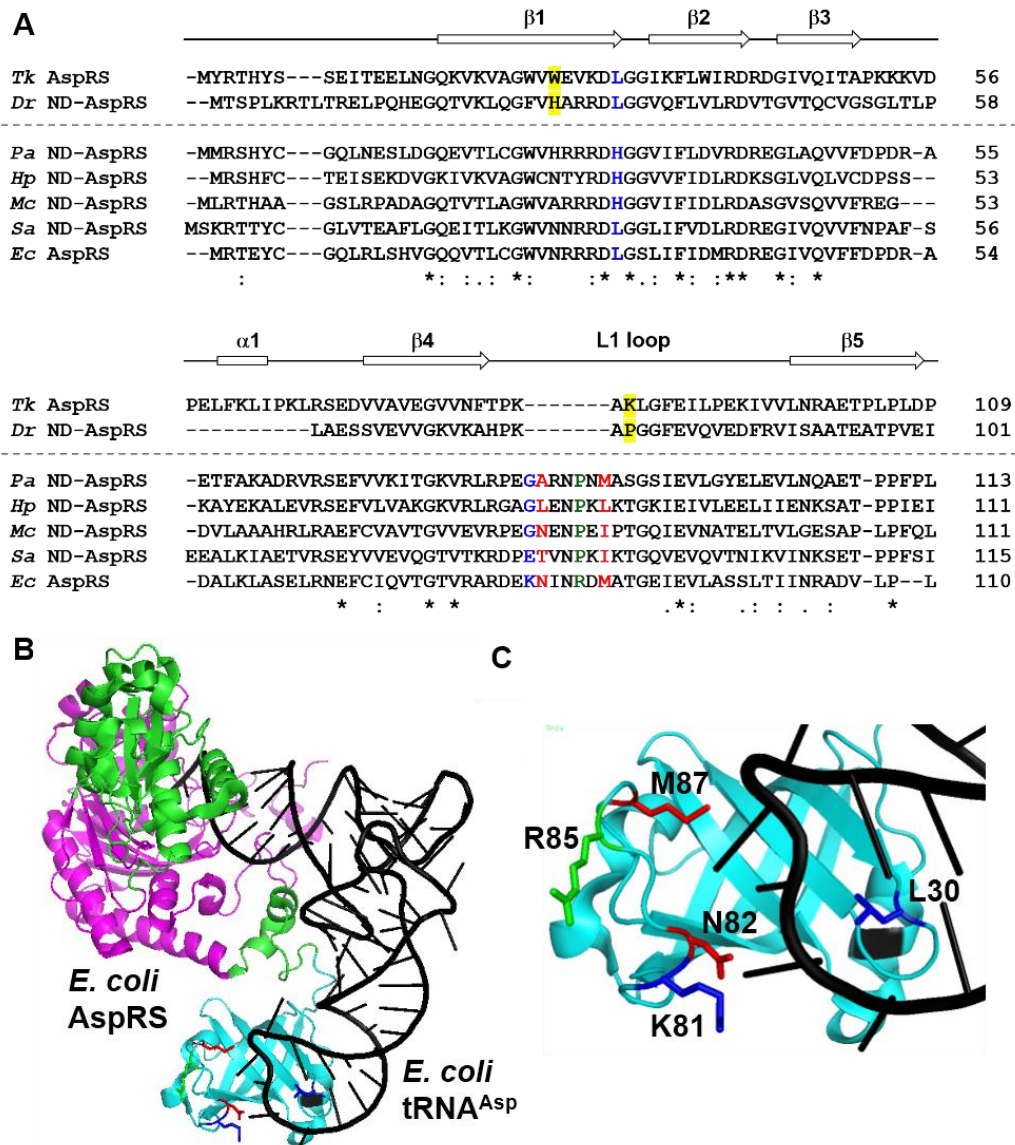


**Figure 3.2. Anticodon-binding domains of the archaeal-type and bacterial-type AspRSs.** (A) Sequence alignment of anticodon-binding domains of different AspRSs. The secondary structure of *H. pylori* ND-AspRS is indicated above the alignment. The dashed, grey line indicates the separation between archaeal-type and bacterial-type AspRSs. *Tk*: *T. kodakaraensis*; *Dr*: *D. radiodurans*; *Pa*: *P. aeruginosa*; *Hp*: *H. pylori*; *Ms*: *M. smegmatis*; *Sa*: *S. aureus*; and *Ec*: *E. coli*. Mutated residues in the *P. aeruginosa* study are in blue (122) and those of the *H. pylori* study are in purple (49). The proline residue in the L1-loop is marked in green. The mutated residues in archaeal-type AspRS are highlighted in yellow (120-121). (B) The crystal structure of *E. coli* AspRS with tRNA<sup>Asp</sup> (PDB entry 1C0A). tRNA<sup>Asp</sup> is in black, the anticodon binding domain is in cyan, and the catalytic domain is in magenta (123). (C) Close up of the anticodon-binding domain of *E. coli* AspRS. The residues investigated by mutagenesis are represented in the same color as in (A).

While ND-AspRS clearly demonstrates relaxed tRNA substrate specificity, it remains fine-tuned as it only aspartylates tRNA<sup>Asp</sup> and tRNA<sup>Asn</sup>, only in organisms that have AdT, and it presumably discriminates against other tRNAs as potential substrates. In this way, the fidelity of the genetic code is maintained. Evidence of further relaxation in substrate specificity for either a discriminating AspRS or an ND-AspRS has not been reported. In this chapter, we demonstrate that these enzymes are capable of specifically producing Glu-tRNA<sup>Glu</sup> while maintaining their canonical roles: the production of Asp-tRNA<sup>Asp</sup> (AspRS and ND-AspRS) and Asp-tRNA<sup>Asn</sup> (ND-AspRS only). To the best of our knowledge, this is the first example of an aaRS capable of producing a non-cognate, but correctly aminoacylated, tRNA.

## 3.2 Results

### 3.2.1 *H. pylori* ND-AspRS appears to aminoacylate *H. pylori* tRNA<sup>Gln</sup> with aspartate and glutamate

ND-AspRS has relaxed tRNA specificity and aspartylates both tRNA<sup>Asp</sup> and tRNA<sup>Asn</sup> to produce Asp-tRNA<sup>Asp</sup> and Asp-tRNA<sup>Asn</sup>, respectively (35, 43). We have previously demonstrated that the *Hp* ND-AspRS has this dual tRNA specificity, as expected (49). Given the nature of the genetic code and decades of work characterizing the aaRSs, ND-AspRS should not demonstrate broader substrate specificity for non-cognate tRNAs or amino acids. We examined *Hp* ND-AspRS and GluRS2, a tRNA<sup>Gln</sup>-specific GluRS (41-42), for possible cross-reactivity with overexpressed tRNA<sup>Asn</sup> and tRNA<sup>Gln</sup> with both aspartate and glutamate (**Figure 3.3**). We performed these assays with longer time points to look at plateau levels of aminoacylation and to detect any low levels of aminoacylation. As expected, ND-AspRS produced Asp-tRNA<sup>Asn</sup> and did not produce

Glu-tRNA<sup>Asn</sup> (**Figure 3.3, panels A, and B, respectively**). Unexpectedly, this enzyme showed aminoacylation activity in both assays with tRNA<sup>Gln</sup> (**Figure 3.3, panels C and D**), suggesting that it was producing the non-cognate product *Hp* Asp-tRNA<sup>Gln</sup> and Glu-tRNA<sup>Gln</sup>. However, because these tRNAs were overexpressed *in vivo*, a practice necessary to introduce required post-transcriptional modifications like queuosine (124) and 2-thiouridine (125), the tRNAs used in these experiments were contaminated with total *Ec* tRNA. Thus, the possibility also exists that *Hp* ND-AspRS is aminoacylating one or more *Ec* tRNAs instead. For comparison, GluRS2 showed only its expected activity, producing Glu-tRNA<sup>Gln</sup> (**Figure 3.3, panel D**), but not Asp-tRNA<sup>Asn</sup>, Glu-tRNA<sup>Asn</sup>, or Asp-tRNA<sup>Gln</sup> (**Figure 3.3, panels A-C**). We conducted these same, longer aminoacylation assays using the *Ms* ND-AspRS and ND-GluRS (**Figure 3.4**): we observed the same behavior with glutamate, indicating that this phenomenon is found in bacteria beyond *H. pylori*.

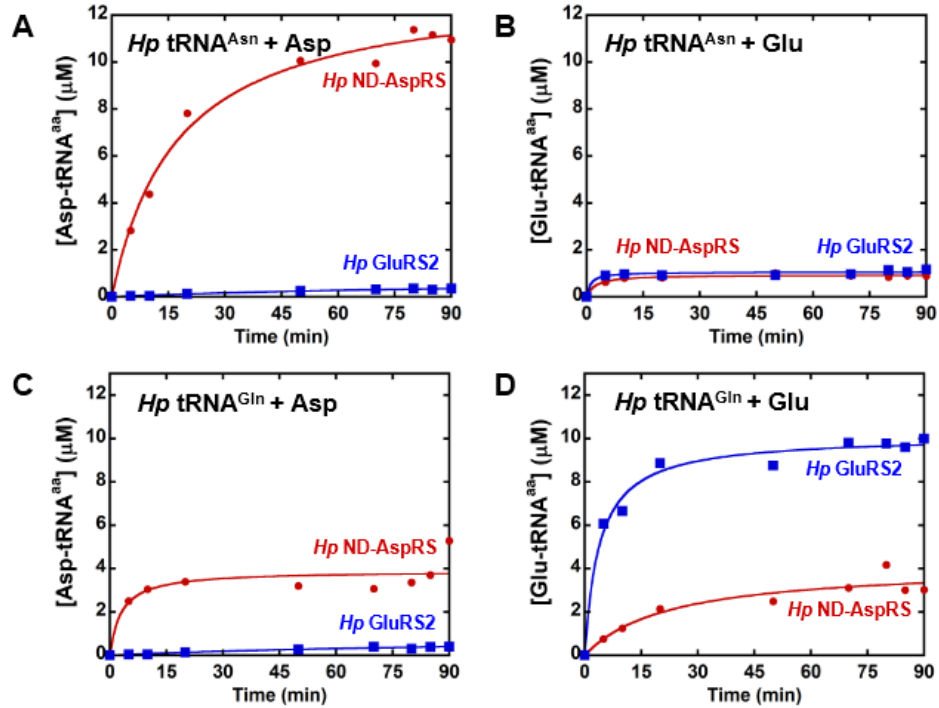


**Figure 3.3. Extended *H. pylori* tRNA<sup>Asn</sup> or tRNA<sup>Gln</sup> aminoacylation assays with *H. pylori* ND-AspRS and GluRS2 with aspartate versus glutamate.** *Hp* ND-AspRS (●, 1  $\mu\text{M}$ ) and GluRS2 (■, 1  $\mu\text{M}$ ) were tested in cross-aminoacylation assays using *Hp* tRNA<sup>Asn</sup> and tRNA<sup>Gln</sup> with aspartate and glutamate. The indicated tRNA isoacceptor concentration in each assay was 10  $\mu\text{M}$ ; but each was contaminated with total *Ec* tRNA. **(A)** *Hp* tRNA<sup>Asn</sup> aminoacylated with aspartate, **(B)** *Hp* tRNA<sup>Asn</sup> aminoacylated with glutamate, **(C)** *Hp* tRNA<sup>Gln</sup> aminoacylated with aspartate, and **(D)** *Hp* tRNA<sup>Gln</sup> aminoacylated with glutamate.

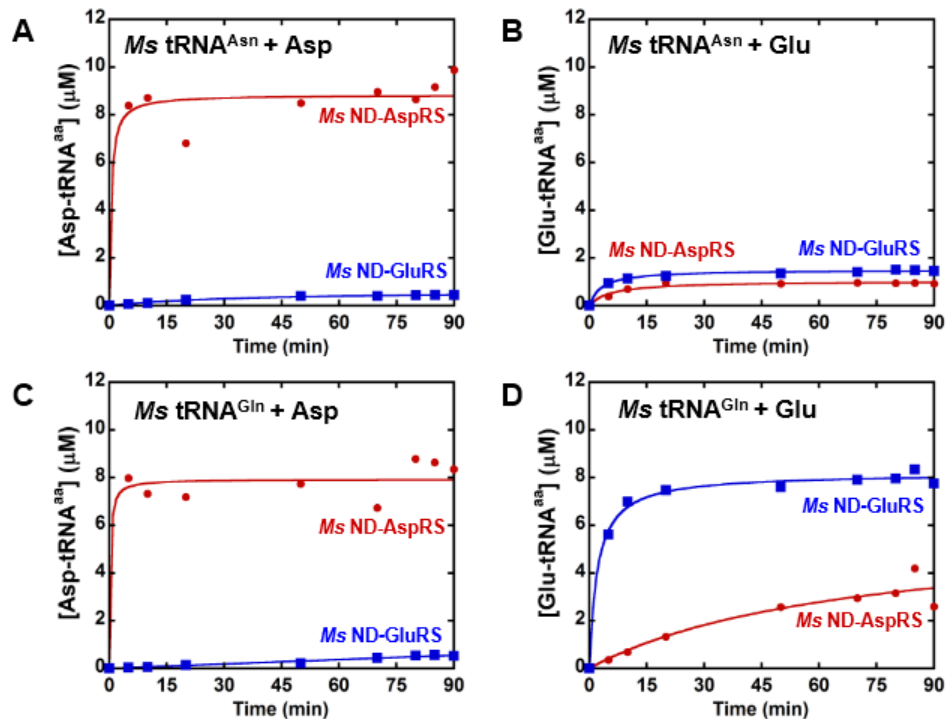


**Figure 3.4. Extended *M. smegmatis* tRNA<sup>Asn</sup> or tRNA<sup>Gln</sup> aminoacylation assays with *M. smegmatis* ND-AspRS and ND-GluRS with aspartate versus glutamate.** *Ms* ND-AspRS (●, 1 μM) and ND-GluRS (■, 1 μM) were tested in cross-aminoacylation assays using *Ms* tRNA<sup>Asn</sup> and tRNA<sup>Gln</sup> with aspartate and glutamate. The indicated tRNA isoacceptor concentration in each assay was 10 μM; but each was contaminated with total *Ec* tRNA. **(A)** *Ms* tRNA<sup>Asn</sup> aminoacylated with aspartate, **(B)** *Ms* tRNA<sup>Asn</sup> aminoacylated with glutamate, **(C)** *Ms* tRNA<sup>Gln</sup> aminoacylated with aspartate, and **(D)** *Ms* tRNA<sup>Gln</sup> aminoacylated with glutamate.

We repeated the assays shown in Figure 3.3 with shorter time points and lower enzyme concentrations to look at initial rates (**Figure 3.5**). Under these more standard conditions, the ability of ND-AspRS to ligate glutamate onto either *Hp* tRNA<sup>Gln</sup> or a contaminating *Ec* tRNA was masked (**Figure 3.5D**), offering an explanation for why this activity has remained undiscovered. Robust aspartylation by *Hp* ND-AspRS, presumably of contaminating *Ec* tRNA<sup>Asp</sup> and/or tRNA<sup>Asn</sup>, was observed, as anticipated (**Figure 3.5C**).

Our use of extended time point assays (**Figure 3.3**) revealed an unexpected activity for ND-AspRS that was invisible under initial rate conditions (**Figure 3.5**). To our knowledge, this is the first evidence of an ND-AspRS utilizing glutamate instead of

aspartate as its amino acid substrate. This activity makes some sense, however, given the close structural similarities between aspartate and glutamate. Nevertheless, the results presented in **Figures 3.3, 3.4, and 3.5**, still contained ambiguity with respect to the identity of the relevant tRNA substrate since each tRNA was overexpressed and purified with contaminating *Ec* tRNAs.

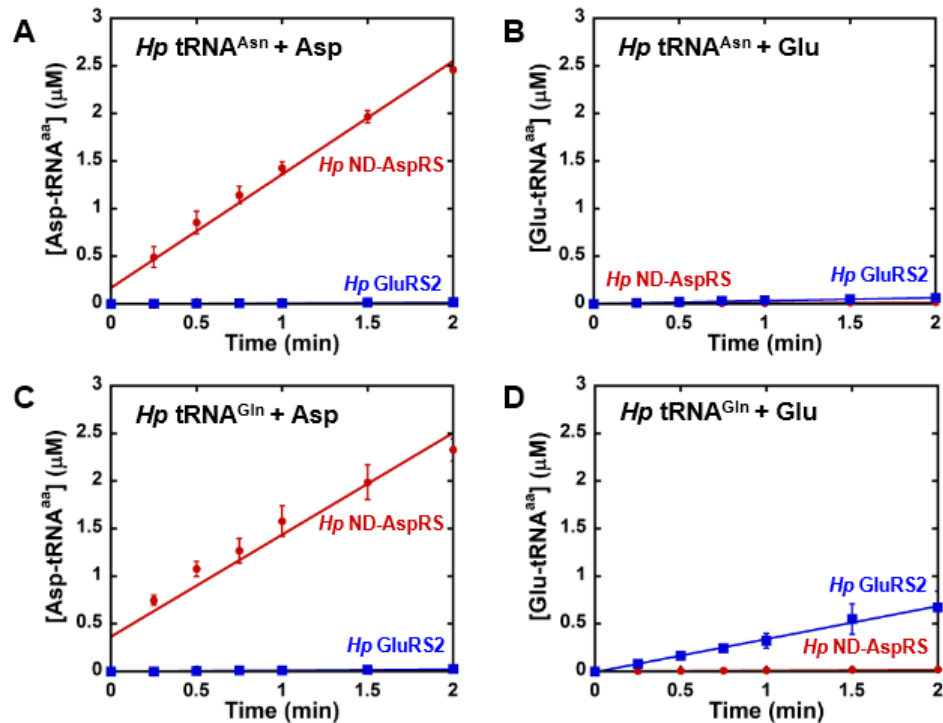


**Figure 3.5.** *H. pylori* ND-AspRS shows unexpected aminoacylation activity with overexpressed *H. pylori* tRNA<sup>Gln</sup> suggesting cross-reactivity with *E. coli* tRNA. *H. pylori* ND-AspRS (●, 200 nM) and GluRS2 (■, 200 nM) were tested in cross-aminoacylation assays using *H. pylori* tRNA<sup>Asn</sup> and tRNA<sup>Gln</sup> with aspartate and glutamate. The indicated tRNA isoacceptor concentration in each assay was 10  $\mu\text{M}$ ; however, each tRNA was contaminated with total *Ec* tRNA. **(A)** *H. pylori* tRNA<sup>Asn</sup> aminoacylated with aspartate, **(B)** *H. pylori* tRNA<sup>Asn</sup> aminoacylated with glutamate, **(C)** *H. pylori* tRNA<sup>Gln</sup> aminoacylated with aspartate, and **(D)** *H. pylori* tRNA<sup>Gln</sup> aminoacylated with glutamate. Error bars represent standard deviation from biological replicates in triplicate.

### 3.2.2 *H. pylori* ND-AspRS aminoacylates *E. coli* tRNA<sup>Glu</sup> with glutamate to produce Glu-tRNA<sup>Glu</sup>

To more precisely examine the unexpected aminoacylation reaction(s) catalyzed by *Hp* ND-AspRS, we turned to acid gel electrophoresis and Northern blotting techniques (126). We continued to use *Hp* GluRS2 as a control because of its high specificity for Glu-tRNA<sup>Gln</sup> production (41-42). The advantages of this approach are two-fold. First, the acidic pH of these gels enables the separation of aminoacylated-tRNAs from their deacylated counterparts, due to the extra charge provided by the protonated amino terminus of the amino acid (126). Second, oligonucleotides can be designed for Northern blot visualization that are specific for a desired tRNA isoacceptor. Thus, this approach allows us to unequivocally identify the tRNA(s) being aminoacylated in a given experiment, clearly resolving the ambiguity of the results presented above. Since *Hp* ND-AspRS uses glutamate as a substrate (**Figure 3.3**), we hypothesized that it may be adding glutamate onto *Hp* tRNA<sup>Gln</sup> or *Ec* tRNA<sup>Glu</sup>. Consequently, we used this methodology to examine *Hp* ND-AspRS-catalyzed aminoacylation of *Hp* tRNA<sup>Gln</sup> and *Ec* tRNA<sup>Glu</sup> with aspartate versus glutamate as its amino acid substrates. Northern blots were conducted with overexpressed *Hp* tRNA<sup>Gln</sup> contaminated with total *Ec* tRNA as a source of *Ec* tRNA<sup>Glu</sup>. In both cases, oligonucleotides were designed to visualize only the tRNA of interest: *Hp* tRNA<sup>Gln</sup> and *Ec* tRNA<sup>Glu</sup>.

*Hp* ND-AspRS does not aminoacylate *Hp* tRNA<sup>Gln</sup> with either aspartate or glutamate (**Figure 3.6, blot 1, lanes 2 and 3**), suggesting that the activities observed above (**Figure 3.3C and D**) are the result of aminoacylation of one or more *Ec* tRNAs. (Compare to the production of Glu-tRNA<sup>Gln</sup> by *Hp* GluRS2 in **Figure 3.6, blot 1, lane 4**.)

In contrast, *Hp* ND-AspRS aminoacylates *Ec* tRNA<sup>Glu</sup> with glutamate to produce Glu-tRNA<sup>Glu</sup> (**Figure 3.6, blot 2, lane 3**), offering direct evidence that this ND-AspRS has non-canonical aminoacylation activity that goes beyond its ability to aspartylate tRNA<sup>Asp</sup> and tRNA<sup>Asn</sup>. We considered the possibility that *E. coli* glutamyl-tRNA synthetase (*Ec* GluRS) had inadvertently co-purified with *Hp* ND-AspRS, however, no evidence of this contamination was observed by SDS-PAGE (**Figure 3.7**). Remarkably, *Hp* ND-AspRS remains accurate, by pairing glutamate with tRNA<sup>Glu</sup> to produce correctly acylated Glu-tRNA<sup>Glu</sup> but not the misacylated Asp-tRNA<sup>Glu</sup> (**Figure 3.6, blot 2, lanes 3 and 2 respectively**). In other words, this enzyme is exhibiting activity consistent with a canonical GluRS, in that it is ligating glutamate specifically to tRNA<sup>Glu</sup>.

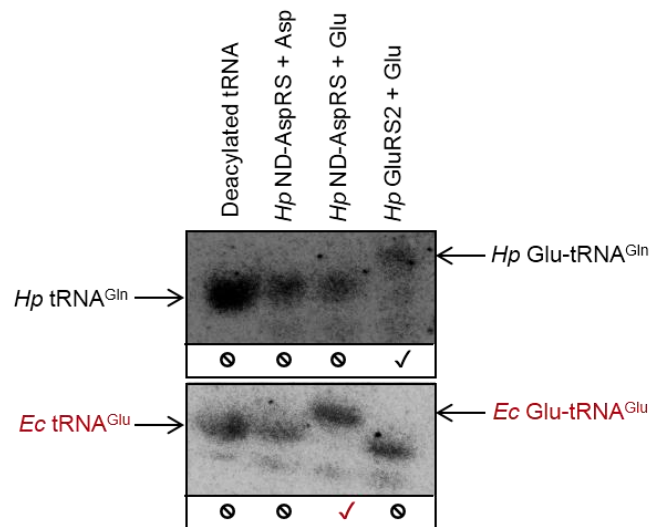


**Figure 3.6.** *H. pylori* ND-AspRS aminoacylates *E. coli* tRNA<sup>Glu</sup> with glutamate producing Glu-tRNA<sup>Glu</sup>. *Hp* tRNA<sup>Gln</sup>, contaminated with total *Ec* tRNA, was aminoacylated with either *Hp* ND-AspRS or GluRS2 with aspartate versus glutamate. Aminoacylated versus deacylated tRNAs were separated in an acid gel. Specific tRNAs and aminoacylated tRNAs were imaged using <sup>32</sup>P-labeled oligonucleotides in the Northern blots. The top panel was visualized with a *Hp* tRNA<sup>Gln</sup>-specific primer and the bottom panel used an *Ec* tRNA<sup>Glu</sup>-specific primer. Expected tRNA aminoacylation activity is indicated with a black check mark (✓); unexpected aminoacylation activity is indicated in red (✓); the absence of aminoacylation activity with a given tRNA is indicated with a no symbol (○).



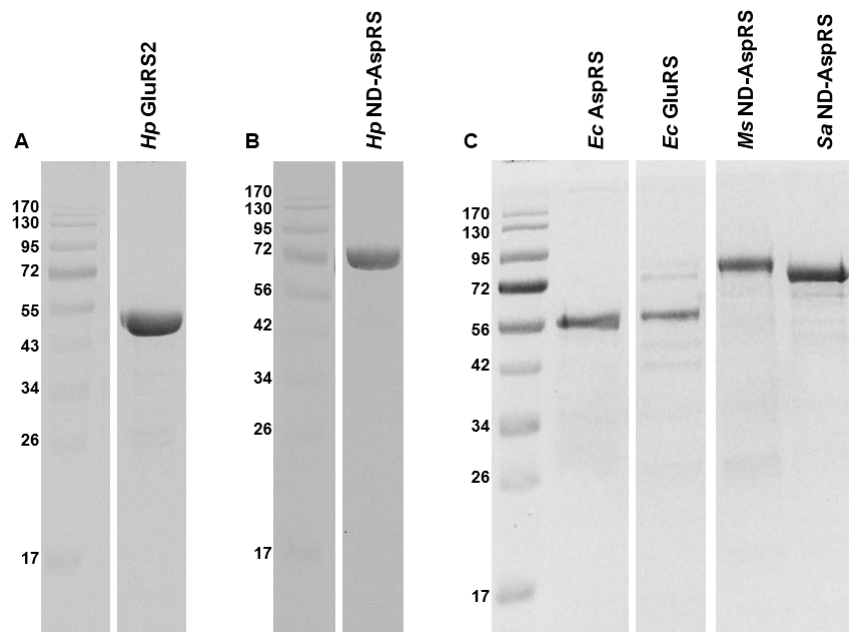


**Figure 3.7. SDS-PAGE of purified aaRSs.** Each His<sub>6</sub>-tagged protein was purified to near homogeneity by cobalt affinity followed by DEAE column purification. The proteins were loaded onto an SDS-PAGE gel after this two-step purification. For clarity, intermittent lanes were removed, as indicated by the white break between different lanes. Each panel (A, B, and C) shows the results from a single gel. **(A)** SDS-PAGE analysis of *Hp* GluRS2. **(B)** SDS-PAGE analysis of *Hp* ND-AspRS. **(C)** SDS-PAGE analysis of *Ec* AspRS, GluRS, and ND-AspRS from *Ms* and *Sa*.

Next, we compared the initial rates and extents of glutamylation of total *Ec* tRNA by *Hp* GluRS2, an enzyme that naturally uses glutamate as its substrate (41-42), and *Hp* ND-AspRS, which unexpectedly also uses glutamate (**Figure 3.8 and 3.9**). Here, to ensure that we could visualize this novel activity, we increased the concentration of each enzyme when looking at aminoacylation of a non-cognate tRNA. We also verified that *Ms* ND-AspRS has this ability to glutamylated total *Ec* tRNA (**Figure 3.10**). In these experiments, the ability of ND-AspRS to produce Glu-tRNA<sup>Glu</sup> is clearly apparent.

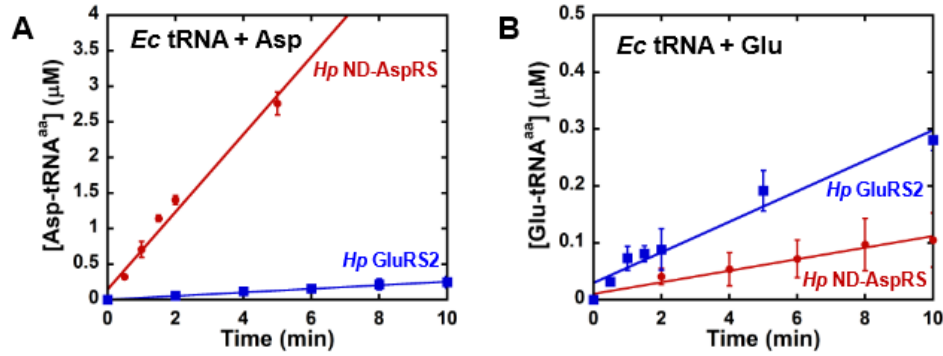


**Figure 3.8.** *H. pylori* ND-AspRS attaches glutamate to an *E. coli* tRNA. *Hp* ND-AspRS was tested for its activity to aminoacylate *Ec* tRNA (50-100 μM) with aspartate and glutamate. *Hp* GluRS2 was also assayed for comparison. **(A)** Aminoacylation of *Ec* tRNA with aspartate by *Hp* ND-AspRS (●, 100 nM) versus GluRS2 (■, 500 nM). **(B)** Aminoacylation of *Ec* tRNA with glutamate by *Hp* ND-AspRS (●, 500 nM) versus GluRS2 (■, 100 nM). Error bars represent standard deviation from biological replicates in triplicate.

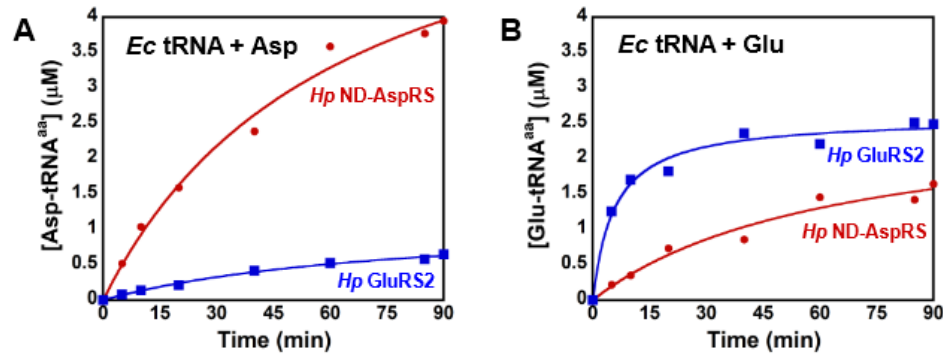


**Figure 3.9.** Extended total *E. coli* tRNA aminoacylation assays with *H. pylori* ND-AspRS and GluRS2 with aspartate versus glutamate. *Hp* ND-AspRS (●, 1 μM) was tested for its activity with *Ec* tRNA (50-100 μM) and aspartate versus glutamate. *Hp* GluRS2 (■, 1 μM) was also assayed for comparison. **(A)** Aminoacylation of *Ec* tRNA with aspartate. **(B)** Aminoacylation of *Ec* tRNA with glutamate.

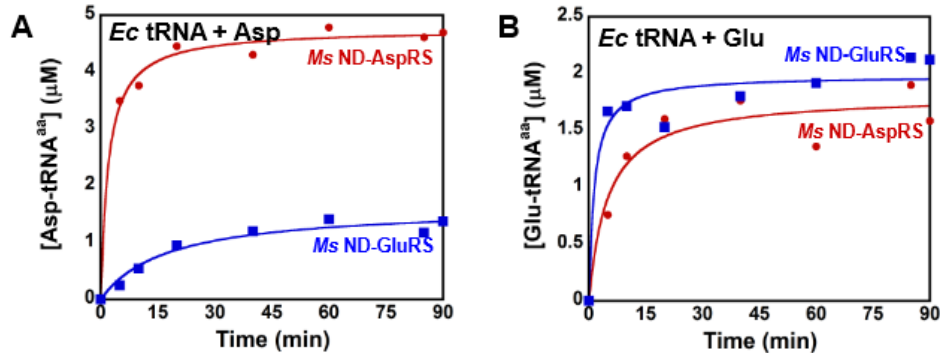


**Figure 3.10. Extended total *E. coli* tRNA aminoacylation assays with *M. smegmatis* ND-AspRS and ND-GluRS with aspartate versus glutamate.** *Ms* ND-AspRS (●, 1 μM) was tested for its activity with *Ec* tRNA (50-100 μM) and aspartate versus glutamate. *Ms* ND-GluRS (■, 1 μM) was also assayed for comparison. **(A)** Aminoacylation of *Ec* tRNA with aspartate. **(B)** Aminoacylation of *Ec* tRNA with glutamate.

### 3.2.3 Glu-tRNA<sup>Glu</sup> production is common among bacterial non-discriminating and discriminating AspRSs

All experiments described so far with *Hp* and *Ms* ND-AspRS demonstrate that these enzymes can attach glutamate to *Ec* tRNA and *Hp* ND-AspRS specifically produces *Ec* Glu-tRNA<sup>Glu</sup>. Given that these are inter-species pairings in both cases, we decided that it was important to examine the *Ec* discriminating AspRS for this activity with homologous *Ec* tRNA. We also included the ND-AspRS from *S. aureus* to gain additional perspective into the ubiquity of this unexpected activity. Acid gels and Northern blot analyses using oligonucleotide probes that are specific for four different *Ec* tRNAs (tRNA<sup>Glu</sup>, tRNA<sup>Gln</sup>, tRNA<sup>Asp</sup>, and tRNA<sup>Asn</sup>) were conducted with all four enzymes: the discriminating AspRS from *E. coli* and the ND-AspRSs from *H. pylori*, *M. smegmatis*, and *S. aureus* (**Figure 3.11**). In many of the Northern blots shown below, the deacylated and the aminoacylated tRNAs appear as two bands, presumably due to differences in post-transcriptional modifications of the tRNAs, as previously reported (42).

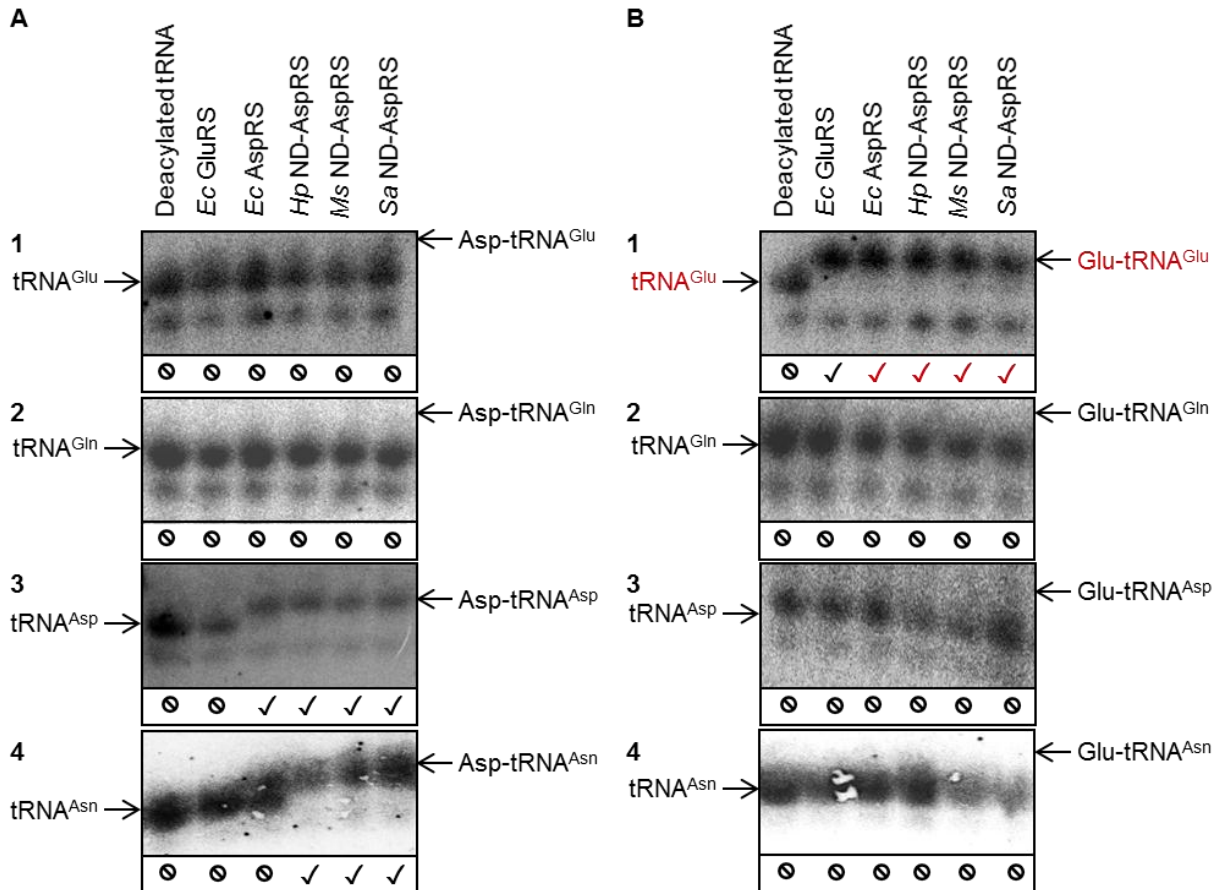


**Figure 3.11. Some bacterial AspRS's aminoacylate *E. coli* tRNA<sup>Glu</sup> with glutamate producing Glu-tRNA<sup>Glu</sup>.** Northern blot analyses of total *Ec* tRNA aminoacylated with (A) aspartate and (B) glutamate by *Ec* GluRS, *Ec* AspRS, *Hp* ND-AspRS, *Ms* ND-AspRS, and *Sa* ND-AspRS. <sup>32</sup>P-labeled oligonucleotides specific for *Ec* tRNA<sup>Glu</sup>, tRNA<sup>Gln</sup>, tRNA<sup>Asp</sup> and tRNA<sup>Asn</sup> were used for each blot as indicated. Expected tRNA aminoacylation activities are indicated with a black check mark (✓); unexpected activities are indicated in red (✓); the absence of aminoacylation activity with a given tRNA is indicated with a no symbol (⊙).

**Figure 3.11** shows the Northern blot results obtained from total *Ec* tRNA aminoacylated with aspartate (A) and glutamate (B) by different bacterial aaRSs: *Ec* GluRS was used as a control. The results of panel A reveal that each AspRS attaches aspartate to tRNA<sup>Asp</sup> and the three ND-AspRSs also attach aspartate to tRNA<sup>Asn</sup>, as expected (**Figure 3.11A, blots 3 and 4**). Furthermore, none of the enzymes tested were

capable of attaching significant amounts of aspartate to either non-cognate tRNA substrates tRNA<sup>Glu</sup> or tRNA<sup>Gln</sup> (**Figure 3.11A, blots 1 and 2**).

The most interesting and critical results are revealed in **blot 1** in **Figure 5B** and are highlighted with red checkmarks. This blot was probed with a <sup>32</sup>P-labeled oligonucleotide specific for *Ec* tRNA<sup>Glu</sup>; Glu-tRNA<sup>Glu</sup> formation by *Ec* GluRS was used as a positive control. A clear shift is observed between deacylated tRNA<sup>Glu</sup> and Glu-tRNA<sup>Glu</sup> produced by *Ec* GluRS (**Figure 3.11B, blot 1, lanes 1 and 2**). What is remarkable is that all four AspRSs showed this same shift, clearly indicative of ubiquitous Glu-tRNA<sup>Glu</sup> production. The remaining blots in **Figure 3.11B** demonstrate that this glutamylation activity is specific for tRNA<sup>Glu</sup> as none of the enzymes tested were capable of adding Glu onto *Ec* tRNA<sup>Gln</sup>, tRNA<sup>Asp</sup>, or tRNA<sup>Asn</sup>. These data demonstrate that *Ec* AspRS and the three ND-AspRSs tested all aminoacylate tRNA<sup>Glu</sup> with glutamate to produce Glu-tRNA<sup>Glu</sup>. These reactions represent a new, non-canonical activity for AspRS that can be viewed as that of a discriminating GluRS.

### 3.3 Discussion

In this work, we demonstrate that bacterial discriminating and non-discriminating AspRSs have quantifiable GluRS activity as they are capable of specifically generating Glu-tRNA<sup>Glu</sup>. Using total *Ec* tRNA, this activity was observed with four different AspRSs: the *Ec* discriminating AspRS and three non-discriminating AspRSs from *H. pylori*, *M. smegmatis*, and *S. aureus*. All four enzymes have canonical AspRS activity and produce Asp-tRNA<sup>Asp</sup> (**Figure 3.11A, blot 3**). The three ND-AspRSs also produce misacylated Asp-tRNA<sup>Asn</sup> (**Figure 3.11A, blot 4**); this intermediate would be converted to Asn-tRNA<sup>Asn</sup>

*in vivo* by AdT. All four enzymes were also capable of specifically producing Glu-tRNA<sup>Glu</sup> (**Figure 3.11B, blot 1**) without adding glutamate to other related tRNAs.

We considered the possibility of the co-purification of contaminating *Ec* GluRS as an alternative explanation for this activity. However, each AspRS was purified in two steps: cobalt affinity and DEAE chromatography. *Ec* GluRS elutes from our DEAE column at a lower KH<sub>2</sub>PO<sub>4</sub> concentration (~50-100 mM) than the tested AspRSs (~200-300 mM), such that any GluRS that survived the affinity purification step would have been removed by DEAE chromatography. Furthermore, no evidence of GluRS contamination was visible by SDS-PAGE gel (**Figure 3.7**). Thus, this two-step purification strategy eliminates the possibility of contaminated *Ec* GluRS in the AspRS samples confirming that this activity is due to AspRS alone.

This GluRS-like activity of AspRSs is remarkable and unexpected because it is accurate and yet outside the normal purview of an AspRS. It truly is GluRS activity as each AspRS specifically attaches glutamate only to tRNA<sup>Glu</sup> producing Glu-tRNA<sup>Glu</sup>. The fact that *Ec* AspRS demonstrates this activity is particularly important because of the homologous nature of this result: *Ec* AspRS produces *Ec* Glu-tRNA<sup>Glu</sup>. All other results herein arose from heterologous pairings of an AspRS with *Ec* tRNA. Our results with *Ec* AspRS demonstrate that this activity is not simply a result of cross-species recognition of a non-cognate tRNA. It is also remarkable that no evidence of misacylated Asp-tRNA<sup>Glu</sup>, Glu-tRNA<sup>Asp</sup>, or Glu-tRNA<sup>Asn</sup> was observed, given the ability of these AspRSs to produce Glu-tRNA<sup>Glu</sup>. This observation is important because it demonstrates that this GluRS activity does not threaten the fidelity of the genetic code. Nevertheless, it poses an unexpected problem with molecular recognition: How does AspRS know to specifically

attach Asp to tRNA<sup>Asp</sup> (and tRNA<sup>Asn</sup>) and Glu to tRNA<sup>Glu</sup> without cross misacylation of these tRNAs? Our results suggest that communication between the amino acid and tRNA binding sites must occur to achieve this specificity. Further research is needed to understand this apparent tRNA-induced conformational change.

AaRSs almost always recognize discrete molecular features in their tRNA substrates, termed identity elements. These determinants can be positive and favor recognition or negative and disfavor interactions. **Figure 3.12** shows the identity elements of *E. coli* tRNA<sup>Asp</sup> and tRNA<sup>Glu</sup>. For *Ec* tRNA<sup>Asp</sup>, the GUC anticodon, the G73 discriminator base, the G2:C71 base pair in the acceptor stem, C38 in the anticodon loop, and G10 in the D arm serve as the positive identity elements for *Ec* AspRS (25, 127-128). In contrast, *Ec* GluRS recognizes the G1:C72 and U2:A71 base pairs in the acceptor stem, A37 in the anticodon loop, U11:A24 base pair in D arm, and the U13:G22-A46 tertiary base pair in *Ec* tRNA<sup>Glu</sup>. Further, the lack of a nucleotide at position 47 and the modified uridine (s<sup>2</sup>U) in the UUC anticodon of tRNA<sup>Glu</sup> are also known identity determinants (25, 27, 125, 129-130). *Ec* tRNA<sup>Glu</sup> does contain several tRNA<sup>Asp</sup> identity elements: the G73 discriminator base, G10 in the D arm, and C38 in the anticodon loop. But are these shared elements enough for recognition of *Ec* tRNA<sup>Glu</sup> by *Ec* AspRS? Or is an alternative, expanded identity set recognized in such a way as to favor glutamylation of *Ec* tRNA<sup>Glu</sup>. To answer these questions, the identity elements in *Ec* tRNA<sup>Glu</sup> that allow recognition by *Ec* AspRS would have to be specifically evaluated.

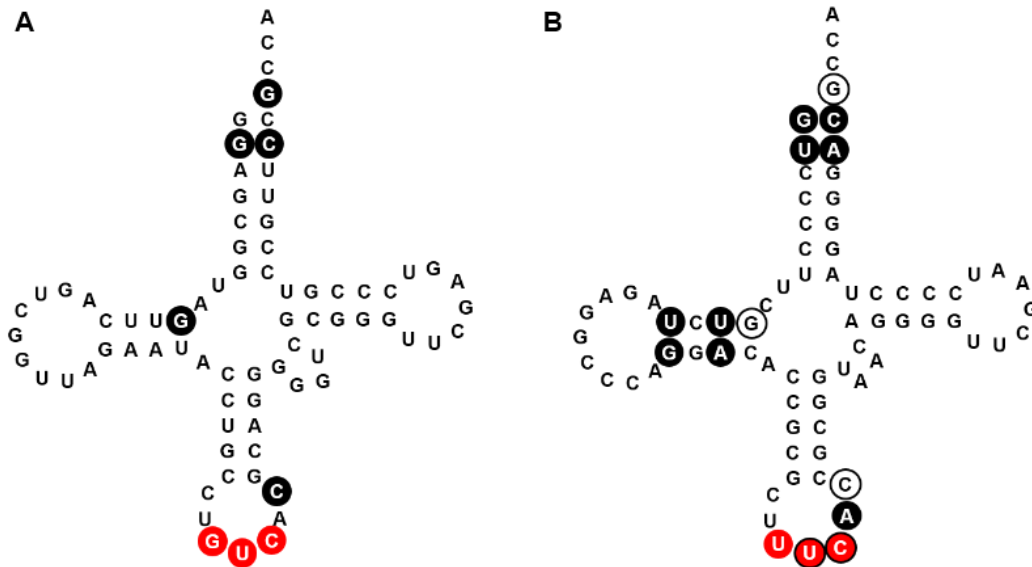


**Figure 3.12. Sequence and secondary structure of *E. coli* tRNAs. (A) *Ec* tRNA<sup>Asp</sup> and (B) *Ec* tRNA<sup>Glu</sup>. The major identity elements are highlighted by filled circles in red (anticodon) and in black (other regions). The tRNA<sup>Asp</sup> identity elements that are found in tRNA<sup>Glu</sup> are circled in black.**

In conclusion, we have demonstrated that bacterial AspRSs have modest, background GluRS activity and are capable of producing Glu-tRNA<sup>Glu</sup>, at least *in vitro*. The relevance of this reaction *in vivo* is very difficult to demonstrate as it is unlikely that this activity is robust enough to enable deletion of the native *Ec* GluRS, especially in the presence of the cognate tRNA<sup>Asp</sup> substrate. It is possible that this activity exists as a backup in case the cognate GluRS becomes damaged, for example. It is also possible that it is a remnant of early AspRS evolution. The early genetic code was likely sloppy with ancestral aaRSs capable of aminoacylating multiple tRNAs with different amino acids (114). Evidence also suggests that Class I and II enzymes emerged in pairs (12, 131), with early AspRSs and GluRSs perhaps as a co-evolving pair that recognized and acylated the same early tRNA or tRNA-like substrates. These enzymes would have recognized opposite faces of the tRNA, facilitating this co-evolution and protecting the tRNA from hydrolysis (12). Given that the background GluRS activity exhibited by AspRS



doesn't put the genetic code in jeopardy, it wouldn't have been selected against as the genetic code evolved to be more selective and specific. The results presented here also suggest the possibility that other aaRSs retain similar background activities, a hypothesis that awaits further testing.

### **3.4 Materials and Methods**

#### **3.4.1 Materials**

Potassium dihydrogen phosphate ( $\text{KH}_2\text{PO}_4$ ), sodium dihydrogen phosphate ( $\text{NaH}_2\text{PO}_4$ ), L-aspartic acid (catalog #A93100, batch #12002LC), L-glutamic acid (catalog #G1251, lot #SLBK8671V), magnesium chloride, and oligonucleotides were purchased from Sigma-Aldrich (St. Louis, MO). The radiolabeled reagents aspartic acid, L-[2,3- $^3\text{H}$ ] (catalog #ART 0211, lot #180606), glutamic acid, L-[2,3,4- $^3\text{H}$ ] (catalog #ART 0132, lot #180710) and adenosine triphosphate (ATP) [ $\gamma$ - $^{32}\text{P}$ ] were purchased from American Radiolabeled Chemicals (St. Louis, MO). Ampicillin, chloramphenicol, kanamycin, 4-(2-hydroxyethyl)-1-piperazineethanesulfonic acid (HEPES), ethylenediaminetetraacetic acid (EDTA), isopropyl- $\beta$ -D-thiogalactopyranoside (IPTG), phenylmethanesulfonyl fluoride (PMSF), and tris(hydroxymethyl) aminomethane (Tris) were from GoldBio Biotechnology, Inc. (St. Louis, MO). Potassium chloride (KCl), sodium chloride (NaCl), and ammonium acetate ( $\text{NH}_4\text{OAc}$ ) were purchased from Fisher Scientific (Hampton, NH).

#### **3.4.2 Overexpression and purification of aaRSs**

*Hp* ND-AspRS (49), the *Hp* tRNA<sup>Gln</sup>-specific glutamyl-tRNA synthetase (GluRS2) (42), *Ms* ND-AspRS, *Ms* ND-GluRS (*Ms* vectors provided by Dr. Babak Javid), and *Ec* AspRS and *Ec* GluRS (*Ec* vectors provided by Dr. Takuya Ueda (132)) were each overexpressed in *E. coli* BL21(DE3)-RIL in Luria-Bertani medium (LB, 1 L) inoculated with

a saturated overnight culture grown from a single colony. The cultures were incubated at 37 °C, 200 rpm. IPTG (1 mM) was used to induce overexpression in each case. For *Hp* ND-AspRS and GluRS2 overexpression, the medium was supplemented with ampicillin (100 µg/mL), chloramphenicol (100 µg/mL), and glucose (0.5%). IPTG was added when the OD<sub>600</sub> reached 0.8-1.0. Cells were collected after a 1-hour induction period. For *Ms* ND-AspRS and ND-GluRS, the only difference was that kanamycin (25 µg/mL) was added instead of ampicillin. The two discriminating *E. coli* enzymes were grown in the same medium as the two *H. pylori* enzymes. IPTG induction was initiated when the OD<sub>600</sub> reached between 0.4 and 0.6 and continued for 4 hours. Cells were harvested by centrifugation and frozen at -80 °C until ready for use.

The *Sa* ND-AspRS (vector provided by Dr. Kelly Sheppard) was overexpressed and purified as previously described (51). In all other cases, cell pellets were suspended in lysis buffer (50 mM NaH<sub>2</sub>PO<sub>4</sub> pH 7.4, 300 mM NaCl, 10 mM imidazole) and the cells were lysed with lysozyme (2 mg/mL) and sonication. Saturated PMSF (15 µL/mL) was added every 20 min to reduce proteolysis. Typically, a cell extract was added to a polyrep column that contained high-density cobalt agarose beads (~2 mL, Gold Biotechnology, Inc.) pre-washed with lysis buffer. The lysate was incubated with the resin by rotating at 4 °C for 1 hour. The His<sub>6</sub>-tagged aaRSs were eluted according to the manufacturer's protocol (Gold Biotechnology).

The eluents were dialyzed against dialysis buffer (20 mM KH<sub>2</sub>PO<sub>4</sub> pH 7.2, 0.5 mM Na<sub>2</sub>EDTA, 5 mM β-mercaptoethanol) at 4 °C for 1-2 hour and then against fresh dialysis buffer overnight. The aaRSs were adsorbed onto a HiTrap™ DEAE FF column (GE Healthcare Life Sciences). The proteins were eluted with a stepwise gradient of 20-300

mM  $\text{KH}_2\text{PO}_4$ , pH 7.2, supplemented with 0.5 mM  $\text{Na}_2\text{EDTA}$ , 5 mM  $\beta$ -mercaptoethanol. The proteins were concentrated with 30 kDa molecular weight spin filters (EMD Millipore). After this two-column purification procedure, all enzymes were judged to be >99% pure by SDS-PAGE. Final protein concentrations were determined by UV-Vis spectroscopy at 280 nm, using extinction coefficients calculated using the ExPASy ProtParam tool (133). The aaRSs were immediately used in aminoacylation assays.

### 3.4.3 *In vivo* transcription and purification of tRNAs

*Hp* tRNA<sup>Asn</sup> (49), *Hp* tRNA<sup>Gln</sup> (42), *Ms* tRNA<sup>Asn</sup>, and *Ms* tRNA<sup>Gln</sup> (*Ms* vectors provided by Dr. Babak Javid) were overexpressed in *E. coli* MV1184 and purified as previously described (73). After deacylation, the tRNAs were electroeluted in a denaturing urea gel for further purification. The tRNA band was excised from the gel, crushed, and incubated overnight at 37 °C in crush and soak buffer (0.5 mM  $\text{NH}_4\text{OAc}$  pH 5.2, 1 mM  $\text{Na}_2\text{EDTA}$ ). The eluted tRNA sample was isopropanol precipitated. The resultant pellet was dissolved in water, folded and quantified by aminoacylation assay as previously described (73). These purifications yield tRNA that is enriched with the overexpressed tRNA isoacceptor but also contains total *Ec* tRNA. Separately, total *Ec* tRNA was isolated from a saturated *E. coli* MV1184 culture that had been grown at 37 °C in LB medium supplemented with glucose (0.5%) and purified as described (73). The concentration of total tRNA was calculated by UV-Vis spectroscopy at 260 nm assuming 1 OD = 1.6  $\mu\text{M}$ .

### 3.4.4 Initial rate aminoacylation assays

Each tRNA was pre-folded as previously described (73). Aminoacylation assays were conducted in buffer containing 100 mM Na-HEPES, pH 7.5, 30 mM KCl, 12 mM  $\text{MgCl}_2$ , 2 mM ATP, 0.1 mg/mL BSA, 20  $\mu\text{M}$  amino acid, 50  $\mu\text{Ci/mL}$   $^3\text{H}$ -labeled amino acid,

and 10  $\mu\text{M}$  *Hp* tRNA<sup>Asn</sup> or tRNA<sup>Gln</sup> as noted. Assays were conducted at 37 °C and were initiated with the addition of 200 nM *Hp* ND-AspRS or GluRS2. Aliquots were removed and quenched on Whatman filter pads containing trichloroacetic acid (TCA). The pads were washed 3 times for 15 min with chilled 5% TCA. Pads were dried and counted in 3 mL ECOLITE(+) scintillation fluid (MP Biomedicals). Aminoacylation assays with total *Ec* tRNA were carried out in the same buffer containing 50 to 100  $\mu\text{M}$  total tRNA. *Hp* ND-AspRS (100 nM or 500 nM) or *Hp* GluRS2 (100 nM or 500 nM) were used in these assays as noted. All experiments were conducted using biological replicates in triplicate.

### **3.4.5 Extended aminoacylation assays (90 min) by aaRSs**

All the aaRSs used in these assays were only purified by cobalt affinity purification. The aminoacylation assays were conducted in buffer containing 20 mM HEPES-OH, pH 7.5, 4 mM MgCl<sub>2</sub>, 2 mM ATP, 100  $\mu\text{M}$  amino acid, and 25  $\mu\text{Ci/mL}$  <sup>3</sup>H-labeled amino acid. All aaRSs were added to a final concentration of 1  $\mu\text{M}$ . Overexpressed tRNA isoacceptor (10  $\mu\text{M}$ ) or total *E. coli* tRNA (50 – 100  $\mu\text{M}$ ) were included as indicated.

### **3.4.6 Acid gel electrophoresis and Northern blot analysis**

Aminoacylation reactions were conducted as described above only without radiolabeled amino acid for 90 min at 37 °C with 500 nM aaRS. NaOAc (0.3 mM, pH 4.5) was added to each reaction and they were quenched with phenol/chloroform (1:1 v/v, pH 4.5). The tRNAs were ethanol precipitated and the resultant pellets were dissolved in buffer containing 10 mM NaOAc, pH 4.5, 1 mM Na<sub>2</sub>EDTA. Acid gel electrophoresis was used to separate deacylated tRNAs from their aminoacylated counterparts. The tRNA samples were quantified by UV-Vis spectroscopy at 260 nm and 0.05 OD<sub>260</sub> units were loaded per lane for overexpressed tRNAs. This amount was increased to 0.25 OD<sub>260</sub> units

for total *Ec* tRNA. Isoacceptor-specific oligonucleotides were used in Northern blots to visualize each tRNA (**Table 3.2**). The tRNA specific DNA probes were prepared as previously described (42). The acid gel and Northern blot analyses were performed as previously described (42, 126), with the exception that a non-specific DNA oligonucleotide (0.1  $\mu$ M) was added during the first three washing steps after probe hybridization.

**Table 3.2. The tRNA specific oligonucleotide sequences used in Northern blot analyses**

<b>tRNA</b>	<b>Sequence</b>
<i>H. pylori</i> tRNA <sup>Gln</sup>	CTCGGAATGCCAGGACCAA
<i>E. coli</i> tRNA <sup>Glu</sup>	CCCTGTTACCGCCGTGAAA
<i>E. coli</i> tRNA <sup>Gln(UUG)</sup>	CAGGGAATGCCGGTATCAAA
<i>E. coli</i> tRNA <sup>Asp</sup>	CCGCGACCCCCTGCGTGACA
<i>E. coli</i> tRNA <sup>Asn</sup>	CAGTGACATACGGATTAACA

## CHAPTER 4

### CLONING, OVEREXPRESSION, AND PURIFICATION OPTIMIZATION STRATEGIES FOR HP0100, A PROTEIN INVOLVED IN INDIRECT TRNA AMINOACYLATION

#### 4.1 Introduction

*H. pylori* and other organisms that do not have either AsnRS and/or GlnRS utilize an indirect tRNA aminoacylation pathway to produce Asn-tRNA<sup>Asn</sup> and/or Gln-tRNA<sup>Gln</sup> (11, 15, 31-32, 34, 37, 42). The first step for Asn-tRNA<sup>Asn</sup> synthesis involves misacylation of tRNA<sup>Asn</sup> with aspartate to produce Asp-tRNA<sup>Asn</sup> by ND-AspRS (35, 43). Subsequently, an amidotransferase called GatCAB converts Asp-tRNA<sup>Asn</sup> to Asn-tRNA<sup>Asn</sup> (34, 37, 44-45). An analogous, two-step processes exists to produce Gln-tRNA<sup>Gln</sup>. In this case, ND-GluRS or GluRS2 in *H. pylori* misacylates tRNA<sup>Gln</sup> to produce Glu-tRNA<sup>Gln</sup> (40-42), which is then converted to Gln-tRNA<sup>Gln</sup> by GatCAB (34, 36, 38). (This pathway is discussed in detail in chapter 1, section 1.3.) Mechanism/s for the quick delivery of misacylated-tRNAs, either from ND-AspRS or ND-GluRS/GluRS2 to GatCAB must exist to ensure the fidelity of protein synthesis. For example, *T. thermophilus* assembles a stable ribonucleoprotein complex called the Asn-transamidosome from tRNA<sup>Asn</sup>, GatCAB, and ND-AspRS. This complex protects the aminoacyl ester linkage in Asp-tRNA<sup>Asn</sup>, sequesters Asp-tRNA<sup>Asn</sup> from the ribosome until it is converted to Asn-tRNA<sup>Asn</sup> by AdT, and ensures efficient production of Asn-tRNA<sup>Asn</sup> (77, 82).

Efforts to characterize an *H. pylori* Asn-transamidosome, composed of tRNA<sup>Asn</sup>, ND-AspRS, and GatCAB were unsuccessful (80, 83). However, data-mining of a published Y2H interaction profile of the *H. pylori* proteome led our lab to discover a protein called Hp0100, which shows interactions with both proteins (ND-AspRS and GatCAB) involved in Asn-tRNA<sup>Asn</sup> biosynthesis (79, 86).

Dr. Gayathri Silva demonstrated that Hp0100 is an essential component of a tRNA-independent Asn-transamidosome in *H. pylori* (79, 87). In the proposed Asn-transamidosome, first, Hp0100 brings ND-AspRS and GatCAB together to form a stable apo-transamidosome. This complex then binds tRNA<sup>Asn</sup> to form a holo-transamidosome and ND-AspRS aspartylate tRNA<sup>Asn</sup> to form Asp-tRNA<sup>Asn</sup>. Next, GatCAB transamidates the misacylated Asp-tRNA to Asn-tRNA<sup>Asn</sup> and the correctly aminoacylated product is released, regenerating the apo-transamidosome (**Chapter 1, Figure 1.8**) (79). Further, Dr. Silva demonstrated that Hp0100 accelerates the GatCAB catalyzed transamidation of Asp-tRNA<sup>Asn</sup> into Asn-tRNA<sup>Asn</sup> ~35-fold (2) and Glu-tRNA<sup>Gln</sup> into Gln-tRNA<sup>Gln</sup> ~ 3-fold (87) (**Chapter 1, Figure 1.9**).

A conserved domain analysis of Hp0100 identified two putative ATPase domains; an AANH domain and a P-loop motif (88). Hp0100 hydrolyzes ATP to ADP and Pi, and mutational studies demonstrated that these two active sites each respond to a different misacylated tRNAs. The AANH domain enhances its activity in the presence of Glu-tRNA<sup>Gln</sup> and the P-loop is stimulated with Asp-tRNA<sup>Asn</sup> (**Chapter 1, Figure 1.10**) (87).

Further, sequence analysis of Hp0100 revealed a possible metal binding motif with a CXXC signature sequence in the P-loop ATPase domain. The predicted model structure also displayed several other cysteines that are clustered together with this possible metal binding cysteines (**Chapter 1, Figure 1.11**) (87). Preliminary metal binding studies by Dr. Gayathri Silva showed that Hp0100 preferentially binds divalent metal ions such as Fe(II), Zn(II) and Ni(II).

The Hp0100 plasmid construct (pTC034), that was used by Dr. Gayathri Silva, encodes an N-terminal six-histidine tag. Several challenges arose when working with



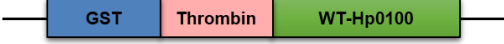




Hp0100 from this plasmid. First, given that His<sub>6</sub>-tags can bind metal ions, we were concerned that results obtained with His<sub>6</sub>-Hp0100 would be difficult to interpret, particularly with respect to any efforts to characterize its metal-binding sites. Second, purification of His<sub>6</sub>-Hp0100 results in the co-purification of *E. coli* AspRS (87). Third, this construct did not always lead to successful purifications of His<sub>6</sub>-Hp0100, due to solubility challenges with this protein. To address all of these issues, we set out to evaluate better ways to overexpress Hp0100 to homogeneity. Many different strategies were assessed, none of which proved to be robustly effective. Representative examples of these purification attempts are discussed here.

## 4.2 Results

**Table 4.1** summarizes the different plasmids of Hp0100 that were constructed and examined here. Efforts to purify Hp0100 using each of these different plasmids will be separately discussed.



Table 4.1. Plasmids encoding different variations of Hp0100

Plasmid	Parent plasmid	Description	Illustration
pUD002	pGS024	Removal of the His <sub>6</sub> tag	
pUD003	pUD002	Site-directed mutagenesis to convert S84A mutant back to wild type	
pUD007	pGEX-4T3	Appendage of an N-terminal glutathione S-transferase (GST) tag followed by a thrombin cleavage site	
pUD009	pTC034	Insertion of a tobacco etch virus (TEV) protease cleavage sequence between the His <sub>6</sub> tag and the <i>hp0100</i> gene	
pUD010	pQE-80L	Codon-optimized <i>hp0100</i> gene with an N-terminal TEV site (GenScript) was cloned into the pQE-80L vector	
pUD011	2S-T	Cloned wild type <i>hp0100</i> gene into the 2S-T vector (Addgene) to add a cleavable N-terminal Sumo tag	
pUD012	2S-T	Cloned codon-optimized <i>hp0100</i> gene into the 2S-T vector (Addgene) to add a cleavable N-terminal Sumo tag	

#### 4.2.1 Cloning, overexpression and purification of untagged Hp0100

To remove the N-terminal His<sub>6</sub>-tag from wild type (WT) and mutant Hp0100 containing plasmids, the plasmids were digested with *EcoRI* and *BamHI* restriction endonucleases, as these sites two flanks codons of the His<sub>6</sub>-tag. After digestion, primers lacking the His<sub>6</sub>-coding sequence (UD005 and UD006) were dropped in between the *EcoRI* and *BamHI* sites. The resulting plasmid encodes the untagged Hp0100. This approach was first successful using pGS024, a plasmid from Dr. Silva, that encodes the S84A Hp0100 mutant. The mutant *hp0100* gene in the resulting plasmid, pUD002, was reverted to WT by site-directed mutagenesis to obtain plasmid pUD003.

Using pUD003, we set out to optimize the overexpression and purification of WT Hp0100 without a tag. Growth and overexpression conditions were varied in DH5 $\alpha$  and BL21(DE3)-RIL cell lines by examining expression at different growth temperatures, induction times, and IPTG concentrations. Most of the tested conditions resulted in minimal soluble overexpression of Hp0100 protein compared to uninduced controls (results not shown). However, overexpression in DH5 $\alpha$  at 19 °C with 1 mM IPTG induction at OD<sub>600</sub> for 16-18 hours resulted in considerable solubilized protein and therefore was used in the optimization of purification protocols.

With the removal of the His<sub>6</sub>-tag from the plasmid, a new purification protocol had to be developed. **Figure 4.1** shows a representative example of these efforts to purify untagged WT Hp0100 protein. Hp0100 was partially purified by ammonium sulfate precipitation (**Figure 4.1A**). Cation exchange chromatography produced moderately pure Hp0100 (**Figure 4.1B**) however yields were low and not robustly reproducible. Based on

these results, we chose to examine the applicability of other affinity tags on the purification of Hp0100.

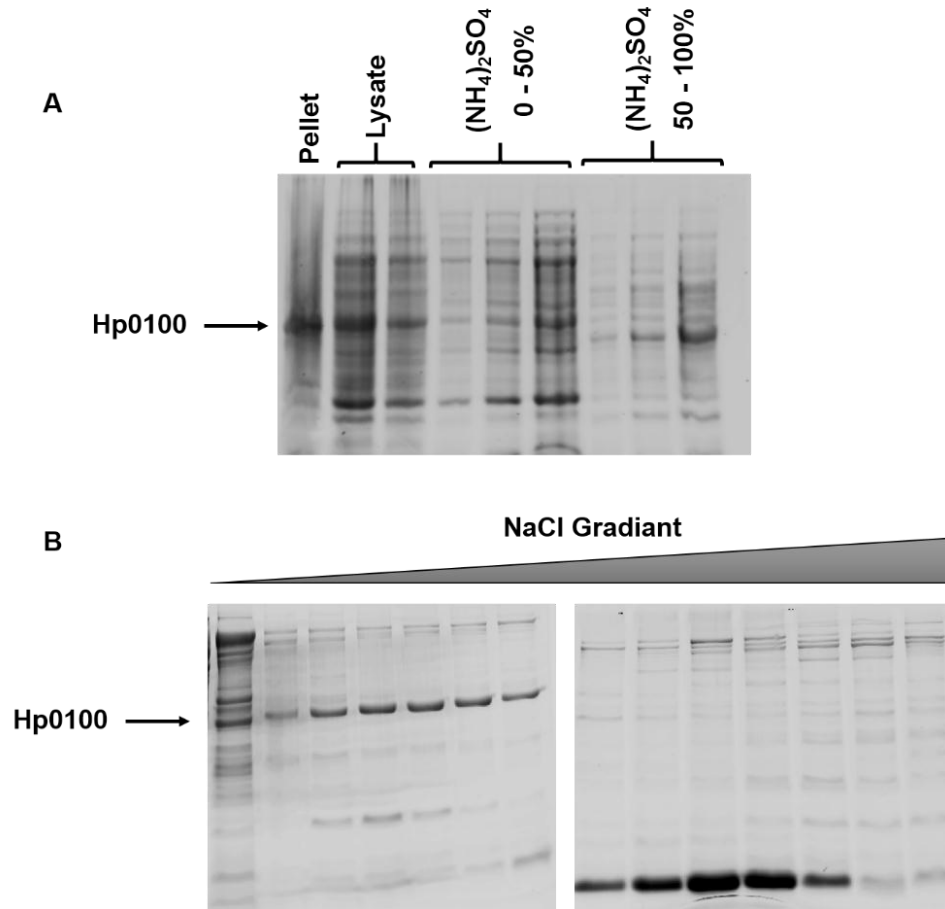


**Figure 4.1. Purification optimization of untagged Hp0100 protein.** (A) SDS-PAGE analysis of ammonium sulfate precipitation. The protein is soluble in lysis buffer and precipitated with 50% ammonium sulfate. Each lane represents different loading volumes. (B) SDS-PAGE analysis of cation exchange chromatographic elution fractions. Untagged Hp0100 elutes with 300-350 mM NaCl concentration.

#### 4.2.2 Cloning, and overexpression of GST-Thrombin-Hp0100

The WT *hp0100* gene from pUD003 was cloned into the pGEX-4T3 expression vector using *Bam*HI and *Xma*I restriction site, resulting in an N-terminal GST tag followed by a thrombin cleavage sequence (pUD007). This plasmid construct allows for protein purification by glutathione affinity followed by cleavage of the GST tag using thrombin.

Hp0100 was overexpressed from pUD007 in *E. coli* BL21(DE3)-RIL. Protein overexpression was carried out at two different temperatures, 19 °C and 37 °C, with different IPTG concentrations and expression times. GST-thrombin-Hp0100 could be overexpressed under these conditions however the protein was insoluble and was only observed in the pellet fraction (**Figure 4.2**).

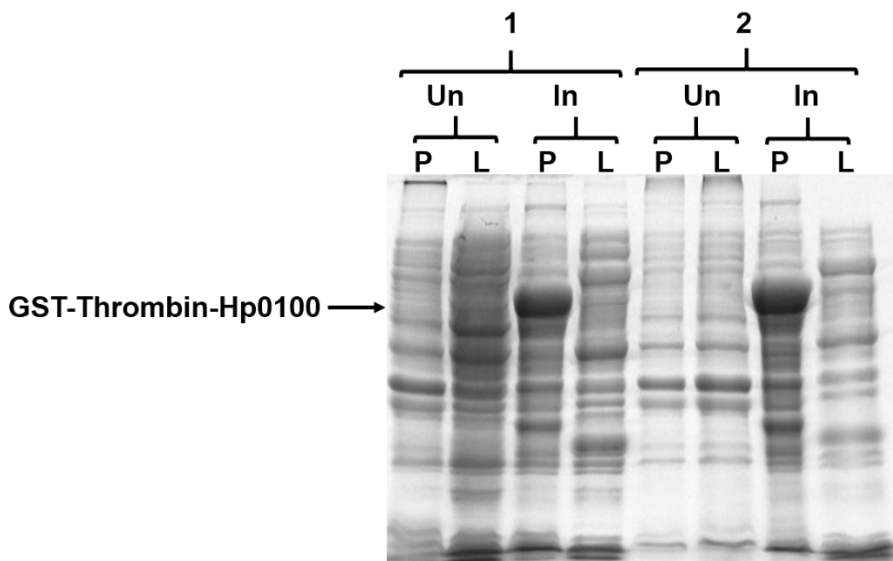


**Figure 4.2. SDS-PAGE analysis of the overexpression of GST-thrombin-Hp0100 in *E. coli* BL21(DE3)-RIL.** Overnight induction with 1 mM IPTG at 0.4-0.6 OD<sub>600</sub> at 19 °C (**1**) and 4-hour induction with 1 mM IPTG at 0.4-0.6 OD<sub>600</sub> at 37 °C (**2**). Un: uninduced; In: Induced; P: pellet; L: lysate.

#### 4.2.3 Cloning, overexpression and purification of His<sub>6</sub>-TEV-Hp0100

A TEV protease cleavage site was inserted into pTC034 between the His<sub>6</sub> codons and the Hp0100 open reading frame to facilitate removal of the His<sub>6</sub>-tag after affinity purification. To this end, the plasmid was digested with *Bam*HI and DNA oligonucleotides containing the TEV protease recognition sequence (UD015 and UD016) were inserted into the digested plasmid (pUD009). We also purchased a codon-optimized *hp0100* gene with a 5'-TEV protease cleavage sequence for expression from GenScript. This codon

optimized *hp0100* gene sub-cloned into the pQE-80L expression vector using *Bam*HI and *Sa*II sites to incorporate an N-terminal polyhistidine tag (pUD010).

Overexpression conditions for the WT and codon-optimized His<sub>6</sub>-TEV-Hp0100 constructs were tested under different conditions. Under a variety of different conditions, both clones resulted in visible overexpression and the majority of the protein was in the soluble fractions as desired. **Figure 4.3** shows representative results with the codon-optimized gene.

We chose to purify codon-optimized His<sub>6</sub>-TEV-Hp0100 from a DH5 $\alpha$  culture grown at 19 °C with 1 mM IPTG induction for 16 hours. The strategy was to purify this protein by Ni<sup>+2</sup>-affinity (**Figure 4.4A**) and cation exchange chromatography (**Figure 4.4B**), followed by cleavage of the N-terminal His<sub>6</sub>-tag using TEV protease (**Figure 4.4C**). Unfortunately, Hp0100 was only modestly purified by Ni<sup>+2</sup>-affinity purification. Although the cation exchange chromatography resulted in further purification (**Figure 4.4B**), the major issue with this purification was failure in the TEV protease cleavage reaction (**Figure 4.4C**). Different lysis methods and TEV protease cleavage conditions were tested, but none proved to be successful.

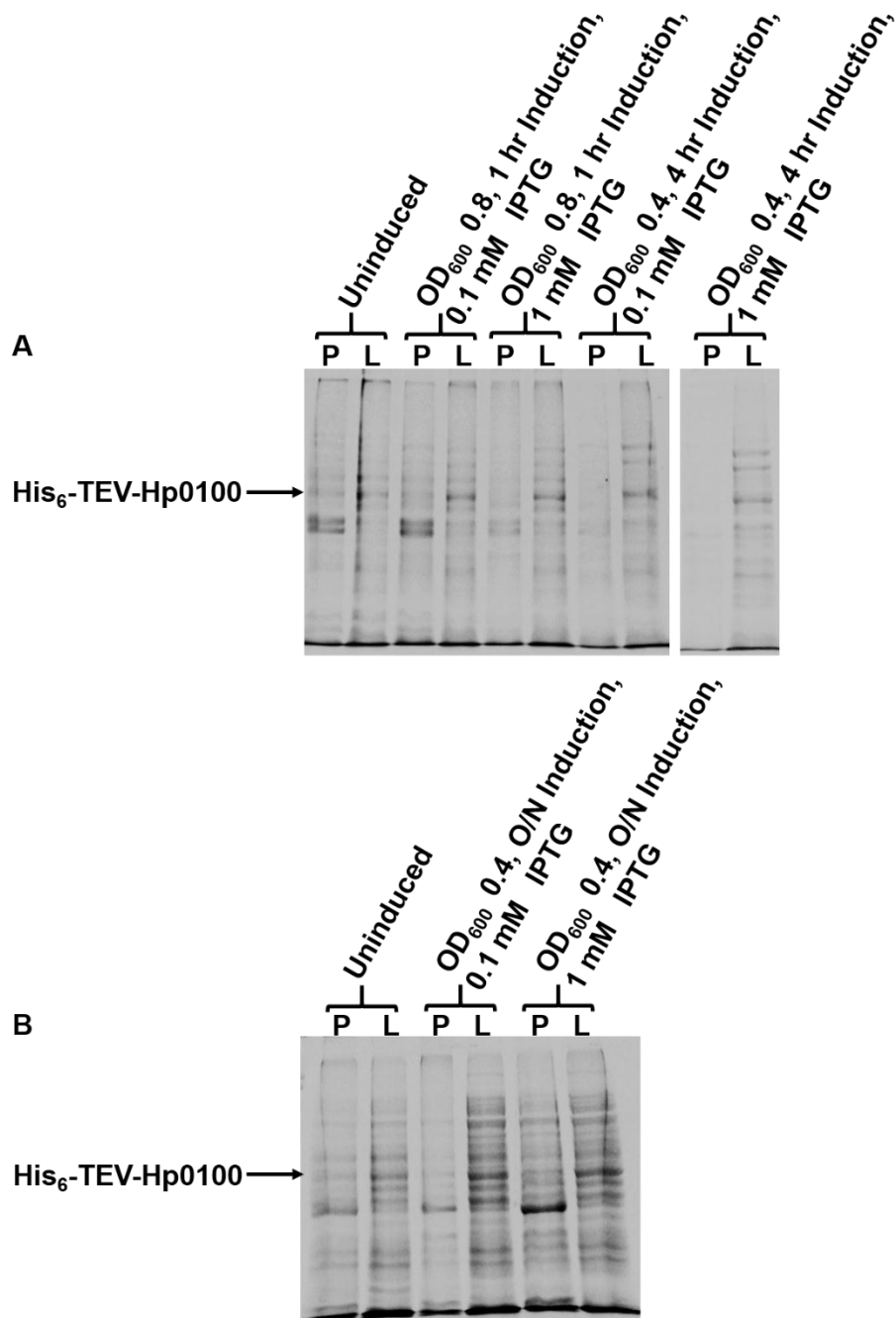


**Figure 4.3. SDS-PAGE analysis of the overexpression of His<sub>6</sub>-TEV-codon optimized Hp0100 (pUD010) in *E. coli* DH5 $\alpha$ . (A) Overexpression analysis at 37 °C. (B) Overexpression analysis at 19 °C. Each lane was loaded with 10  $\mu$ g of total protein. P: pellet. L: lysate.**

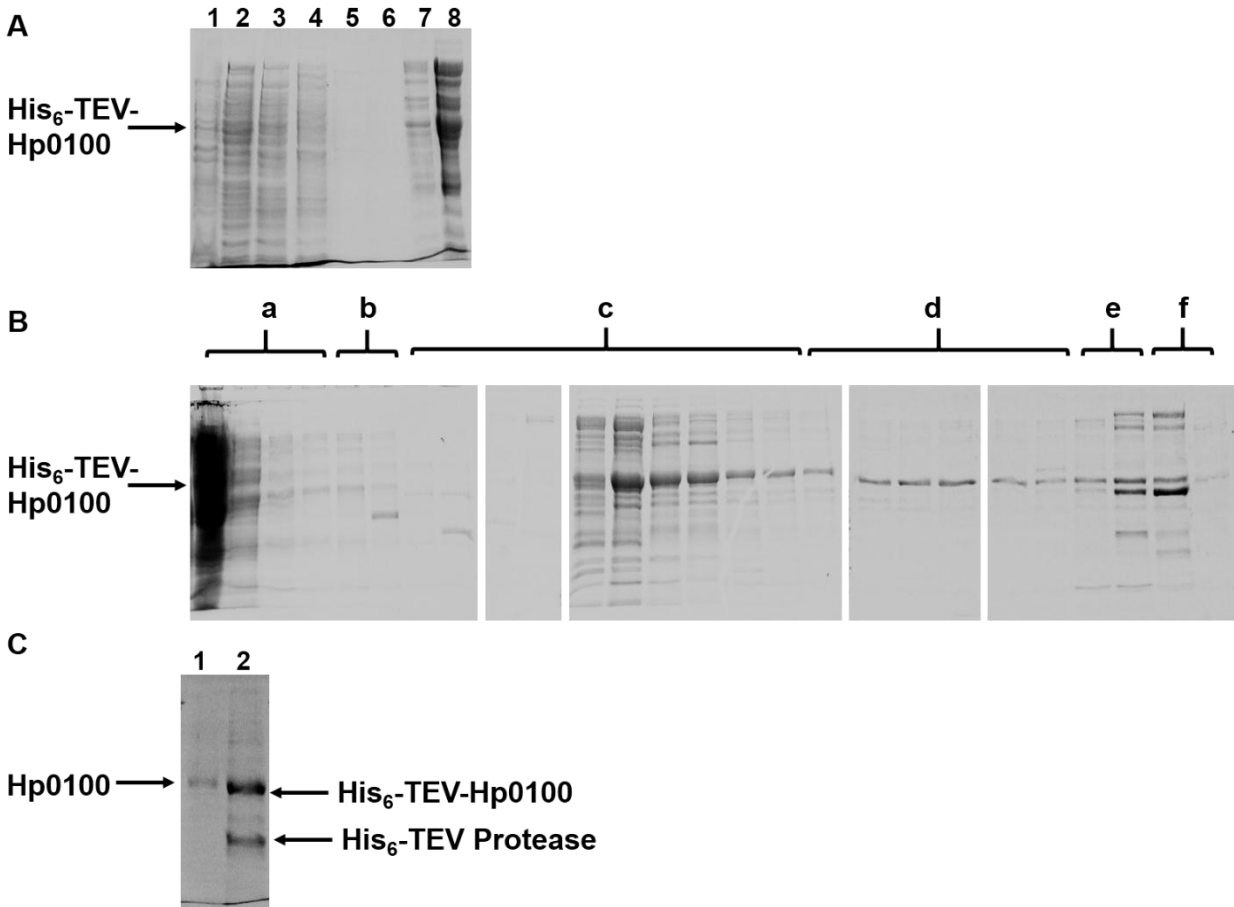


**Figure 4.4. SDS-PAGE analysis of His<sub>6</sub>-TEV-Hp0100 (pUD010) purification.** (A) Ni<sup>2+</sup>-HiTrap Chelating Hi Performance affinity chromatography purification of Hp0100. Pellet (lane 1), lysate (lane 2), flow through (lane 3), 0 mM imidazole wash (lane 4), 2.5 mM imidazole wash (lane 5 and 6), 250 mM imidazole elution (lane 7), and concentrated elution (lane 8). (B) Cation exchange chromatographic purification of Hp0100 from A. 0 mM NaCl (a), 100 mM NaCl (b), 200 mM NaCl (c), 300 mM NaCl (d), 400 mM NaCl (e), and 500 mM NaCl (f). (C) TEV protease cleavage analysis. TEV protease cleaved Hp0100 sample (lane 1) and the elution after TEV protease (lane 2).

#### 4.2.4 Cloning, overexpression and purification of His<sub>6</sub>-SUMO-TEV-Hp0100

We also cloned the WT and codon optimized *hp0100* genes into a vector with a small Ubiquitin-like Modifier (SUMO) tag. The pET-His<sub>6</sub>-SUMO-TEV-LIC cloning vector (2S-T) appends a TEV protease cleavable N-terminal His<sub>6</sub>-SUMO tag to the cloned gene. We tested different overexpression conditions, and some are shown in **Figure 4.5**. None of the tested conditions yielded appreciable amounts of soluble protein.

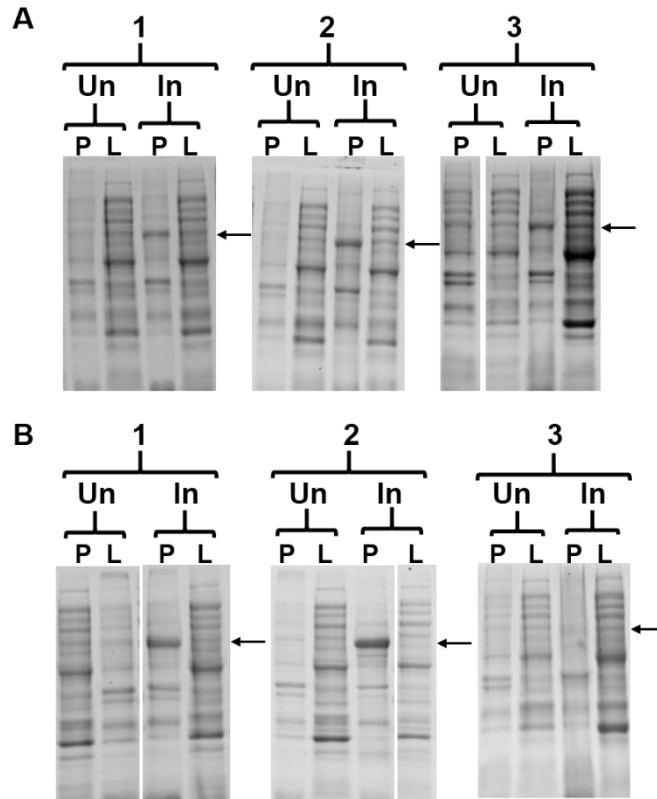


**Figure 4.5. SDS-PAGE analysis of overexpression of SUMO tagged Hp0100 in *E. coli* BL21(DE3)-RIL cell line. (A)** Analysis of His<sub>6</sub>-SUMO-TEV-WT Hp0100 overexpression from pUD011. **(B)** Analysis of His<sub>6</sub>-SUMO-TEV-codon optimized Hp0100 overexpression from pUD012. (1) One-hour induction with 1 mM IPTG at 0.8-1 OD<sub>600</sub> at 37 °C; (2) 4-hour induction with 1 mM IPTG at 0.4-0.6 OD<sub>600</sub> at 37 °C; and, (3) overnight induction with 1 mM IPTG at 0.4-1 OD<sub>600</sub> at 19 °C. Each lane contains 20 µg total protein. The arrow indicates the size of the His<sub>6</sub>-SUMO-TEV-Hp0100 protein. Un: uninduced; In: Induced; P: pellet; and, L: lysate

### 4.3 Discussion

Since we hypothesized that the misacylated tRNA-dependent ATPase activity of Hp0100 depends on the binding of metals to Hp0100 protein, we set out to clone, overexpress, and purify Hp0100 without a His<sub>6</sub>, metal-binding tag. We cloned the *H. pylori* *hp0100* gene (WT and codon-optimized to express in *E. coli*) into multiple expression vectors introducing untagged or cleavable N-terminal tags.



The untagged WT *hp0100* in the pQE-80L expression vector was tested for protein overexpression under various conditions: different cell lines, growth temperatures, inducer concentrations, induction times, etc. Growth at a lower temperature and longer induction time resulted in considerable overexpression of protein compared to uninduced culture control. To overcome the problem with the solubility, the cell pellets were resuspended in higher salt (1 M NaCl) containing buffers. Different purification methods were tested to obtain pure Hp0100 protein. Ammonium sulfate precipitation followed by cation exchange chromatography resulted in more pure protein compared to all other methods examined. But the yield and the activity assays with this Hp0100 were not reliably reproducible.

One of the major problems in expressing Hp0100 is its insolubility. Lowering overexpression temperature, inducer concentration, and various induction times didn't improve solubility. Further, the use of different lysis buffers with high salt, use of detergents such as Triton X-100, and incorporation of chaotropic agents such as urea also don't increase the solubility of the protein.

To overcome the issues with protein insolubility, we introduced a SUMO tag to the N-terminal of the Hp0100 protein. The SUMO tag has proven to be useful for enhancing the solubility as well as the expression of proteins in *E. coli* expression systems (134-135). Unfortunately, in our case, we did not see an improvement in the overexpression or solubility of Hp0100 with the tested conditions.

The clone with an N-terminal TEV protease cleavable His<sub>6</sub>-tag Hp0100 overexpressed well compared to other tested clones and also resulted in soluble protein. The purification of this protein construct was also straightforward. Lysis was carried out

in phosphate buffer with high salt and the protein was purified by Ni<sup>2+</sup> affinity followed by cation exchange chromatography. Finally, the pure protein was subjected to TEV protease cleavage to remove the appended His<sub>6</sub>-tag. Although we were able to get pure Hp0100 using this construct, the TEV cleavage was unsuccessful. Since sonication sometimes results in protein aggregation (136) and osmotic lysis was proven to work with problematic TEV protease (137) cleavages, we also tried using osmotic lysis and TEV protease cleavage with this protein construct. But, this method did not enhance TEV protease cleavage.

In conclusion, in this chapter, we have described our unsuccessful efforts to purify Hp0100 using a variety of expression vectors with different N-terminal purification tags. With each clone, we encountered challenges during protein expression, solubilization, or purification. Parallel efforts have led to the successful cloning and purification of *S. aureus* Sa2591 (138), a truncated ortholog of Hp0100 that only contains 2/3 of its N-terminal primary sequence. This success suggests that the solubility and overexpression issues described herein may be due to the extra domain in the C-terminal of full length Hp0100 protein. Further experiments need to be done to confirm this assumption.

## **4.4 Materials and Methods**

### **4.4.1 Materials**

Sodium dihydrogen phosphate (NaH<sub>2</sub>PO<sub>4</sub>), magnesium chloride, cOmplete mini protease inhibitor tablets, and DNA oligos were purchased from Sigma-Aldrich (St. Louis, MO). Ampicillin, chloramphenicol, ethylenediaminetetraacetic acid (EDTA), isopropyl β-D-thiogalactopyranoside (IPTG), 4-(2-hydroxyethyl)-1-piperazineethanesulfonic acid (HEPES), lysozyme, and phenylmethanesulfonyl fluoride (PMSF) were from Gold

Biotechnology, Inc., (St. Louis, MO. Sodium chloride (NaCl). Restriction enzymes, T4 DNA ligase, and Calf Intestinal Alkaline Phosphatase (CIP) were purchased from New England Biolabs (NEB, Ipswich, MA). E.Z.N.A.® Plasmid Mini kit II was from Omega Bio-Tek (Norcross, GA).

#### 4.4.2 Cloning of untagged WT and mutant Hp0100

Plasmids containing WT and different mutant *hp0100* genes (pTC034, pGS018, pGS022, pGS023, and pGS024) were digested with *EcoRI* and *BamHI* restriction enzymes to remove the His<sub>6</sub>-tag coding sequence. Then, primers containing the intervening DNA sequence without the His<sub>6</sub>-coding sequence (CACCATCACCATCACCAT) were inserted into the *EcoRI* and *BamHI* digested plasmids to create untagged Hp0100 encoding plasmids. The sequences of the primers used were as follows; these primers contain complementary overhangs to the *EcoRI* and *BamHI* digested plasmids:

##### Forward primer UD005:

5'-AATTCATTAAGAGGAGAAATTA ACTATGAGAGGATCGG-3'

##### Reverse primer UD006:

5'-GATCCCGATCCTCTCATAGTTAATTTCTCCTCTTTAATG-3'

The primers (UD005 and UD006) were mixed in equal molar ratios and the primer mixture was added to double digested plasmids in different primer:plasmid ratios. A T4 DNA ligase reaction was performed according to the manufacturer's protocol (NEB). The ligation reactions were transformed into *E. coli* DH5 $\alpha$  calcium chloride competent cells and were plated on Luria Bertani (LB) plates supplemented with ampicillin (100  $\mu$ g/mL) and glucose (0.5%). Plasmids were isolated from individual colonies and the entire gene

was sequenced at the Applied Genomics Technology Center (AGTC), Wayne State University. The plasmid pGS024 (His<sub>6</sub>-Hp0100(S84A)) resulted in untagged Hp0100(S84A) mutant plasmid after the cloning process. This new plasmid was named pUD002.

pUD002 was subjected to site-directed mutagenesis to create a plasmid encoding WT untagged Hp0100 (pUD003). PCR mutagenesis was carried out according to the instructions provided by Stratagene (La Jolla, CA) using the primers listed below. Site directed-mutagenesis indicated in red letters.

**Forward mutagenesis primer UD010:**

5'-GGAATTGTTAGGGGAAAAAAGCGAACGCTGTTTTGAGTGCTTTG-3'

**Reverse mutagenesis primer UD011:**

5'-CAAAGCACTCAAACAGCGTTCGCTTTTTTCCCCTAACAATTCC-3'

#### **4.4.2 Overexpression and purification of untagged WT Hp0100**

Untagged WT Hp0100 (pUD003) was overexpressed in *E. coli* DH5 $\alpha$  by inoculating LB medium (1L) supplemented with glucose (0.5%) and ampicillin (100  $\mu$ g/mL) with a saturated overnight culture (10 mL) grown in the same medium. The culture was grown at 19 °C, 200 rpm until the OD<sub>600</sub> reached between 0.4 and 1. Protein overexpression was induced with IPTG (1 mM) and another round of ampicillin (100  $\mu$ g/mL) was added. After 16-18 hours of protein induction, the cells were harvested by centrifugation at 4000 rpm for 10 min at 4°C.

The cell pellet was suspended in lysis buffer (50 mM NaH<sub>2</sub>PO<sub>4</sub> pH 7.4, 1 M NaCl) and cells were lysed using lysozyme (2 mg/mL). A cOmplete protease inhibitor cocktail tablet was added to reduce proteolysis and incubated on ice for 30 min. The cell

suspension was sonicated 10 times using a Misonix Microson™ Ultrasonic cell Disruptor set at power level 4 for 10 s with 50 s rest cycles on ice between each pulse. The cell debris was removed by centrifugation at 14,000 rpm for 30 min at 4 °C. Ammonium sulfate was added to the clear cell lysate to 50% saturation and the mixture was rotated at 4 °C for 30 min. The protein was recovered by centrifugation at 14,000 rpm for 30 min at 4 °C and dissolved in dialysis buffer (20 mM HEPES, pH 7.4, 200 mM NaCl). The protein sample was dialyzed in 2 L of the same buffer for 2 hours and again against 2 L overnight. The filtered sample (~ 2 mL) was loaded onto a UNO S ion-exchange column (12 mL column volume, BIO-RAD, Hercules, CA). The protein was eluted with an increasing gradient of NaCl. Protein fractions were concentrated using an Amicon 30 kDa MWCO tube (EMD Millipore, Burlington, MA) and the purity of Hp0100 was analyzed by SDS-PAGE.

#### **4.4.3 Cloning and overexpression of GST-Hp0100**

The WT *hp0100* gene from pUD003 was subcloned into the pGEX-4T3 expression vector using *Bam*HI and *Xma*I restriction sites. This cloning results in *hp0100* with 5'-GST tag with an intervening thrombin cleavage site. pUD003 and pGEX-4T3 plasmids were digested with *Bam*HI and *Xma*I restriction endonuclease according to manufactures protocol. The insert and vector were gel purified. Calf Intestinal Alkaline Phosphatase (CIP) was used to remove the 5' and 3' phosphates from the digested vector. T4 DNA ligase reactions were performed using different vector:insert ratios (1:1, 1:2, 1: 5, and 1:10). The ligation reactions were transformed into *E. coli* DH5 $\alpha$  chemically competent cells and plated on LB plates supplemented with ampicillin (100  $\mu$ g/mL) and glucose

(0.5%). Plasmids were purified from single colonies and the correct sequence was confirmed by sequencing. The resultant plasmid was named pUD007.

The pUD007 plasmid was transformed into *E. coli* BI21(DE3)-RIL chemically competent cells and plated on plates with ampicillin (100 µg/mL), chloramphenicol (100 µg/mL), and glucose (5%). LB cultures (50 mL) supplemented with ampicillin (100 µg/mL), chloramphenicol (100 µg/mL), and glucose (5%) were inoculated with a saturated overnight culture grown from a single colony. The cultures were incubated at 37 °C until the OD at 600 nm reached ~0.4-0.6. Protein overexpression was induced with 1 mM IPTG at 19 °C overnight and at 37 °C for 4 hours. Cells were pelleted and lysed in lysis buffer (50 mM NaH<sub>2</sub>PO<sub>4</sub> pH 7.4, 300 mM NaCl) with lysozyme (2 mg/mL) and sonication. PMSF was added every 15-20 min to reduce proteolysis. The lysate and cell debris were analyzed by SDS-PAGE.

#### **4.4.4 Cloning, overexpression and purification of His<sub>6</sub>-TEV-Hp0100**

A TEV protease recognition sequence was inserted in between the His<sub>6</sub>-tag and the start codon of *hp0100* gene (pTC034). The insertion of the TEV protease site allows removal of the polyhistidine tag after purification. The plasmid pTC034 (His<sub>6</sub>-WT Hp0100 in pQE-80L) was digested with *Bam*HI. The digested plasmid was treated with CIP to remove the 5' and 3' phosphates. DNA oligos containing the TEV protease recognition sequence and complementary overhangs to the *Bam*HI were as follows:

##### **Forward primer UD015:**

5'-GATCCGAAAACCTGTACTTCCAAGGCGGTACCG-3'

##### **Reverse primer UD016:**

5'-GATCCGGTACCGCCTTGGGAAGTACAGGTTTTTCG-3'

These primers (UD015 and UD016) were mixed together in equimolar ratios. The mixture was heated up to 75 °C and slowly cooled to room temperature to anneal the primers. The primer mixture was added to the *Bam*HI-digested pTC034 DNA in different molar ratios. T4 DNA ligase reactions were performed according to the manufacturer's instructions (NEB). The reactions were transformed into *E. coli* DH5 $\alpha$  calcium chloride chemically competent cells and plated onto LB plates supplemented with ampicillin (100  $\mu$ g/mL) and glucose (0.5%). The correct DNA sequence was confirmed by sequencing (pUD009).

The *hp0100* gene with codon optimized for expression in *E. coli* with a 5'-TEV protease cleavage sequence and was chemically synthesized and inserted into the pUC57 vector by GenScript (GenScript Biotech Corp., Piscataway, NJ). The codon-optimized *TEV-hp0100* gene was subsequently cloned into the pQE-80L expression vector using *Bam*HI and *Sal*I restriction sites (pUD010). The correct sequence was confirmed by sequencing.

His<sub>6</sub>-TEV-optimized Hp0100 was overexpressed from pUD010 in *E. coli* DH5 $\alpha$ . Overexpression examined under different conditions. Culture of LB media (50 mL) supplemented with glucose (0.5%) and ampicillin (100  $\mu$ g/mL) was inoculated with a saturated overnight culture grown in the same medium. The cultures were grown at two different temperatures, 37 °C and 19 °C. The cultures grown at 37 °C was induced with IPTG (0.1 mM versus 1 mM) when their OD<sub>600</sub> reached 0.4-0.6 and protein induction was carried out for 4 hours. Another set of cultures that were grown at 37 °C and induced with IPTG (0.1 mM and 1 mM) when their OD<sub>600</sub> reached 0.8-1 and protein induction was carried out for one hour. For the cultures incubated at 19 °C, protein expression was

induced when their  $OD_{600}$  reached between 0.4 and 1 by adding IPTG (0.1 mM and 1 mM) for 16-18 hours. For these cultures, another round of ampicillin (100  $\mu\text{g}/\text{mL}$ ) was added after 24 hours. Cells were pelleted and lysed in lysis buffer (50 mM  $\text{NaH}_2\text{PO}_4$ , pH 7.4, 300 mM NaCl) with lysozyme (2 mg/mL) and sonication. PMSF was added every 15-20 min to reduce proteolysis. The lysate and cell debris were analyzed by SDS-PAGE. The protein expression at 19 °C with 1 mM IPTG for 16-18 hours was used as the optimized overexpression condition.

The cell pellet was resuspended in lysis buffer (50 mM  $\text{NaH}_2\text{PO}_4$  pH 7.4, 1 M NaCl) and the cells were lysed using lysozyme (2 mg/mL). A protease inhibitor cocktail tablet was added to reduce proteolysis and the suspension was incubated on ice for 30 min prior to sonication. After sonication, cell debris was removed by centrifugation at 14,000 rpm for 30 min and the clear lysate was filtered through 0.8  $\mu\text{m}$  and 0.2  $\mu\text{m}$  syringe filters (Pall Corporation, Port Washington, NY). The protein sample was injected onto a HiTrap  $\text{Ni}^{+2}$  Chelating Hi-Performance (HP) affinity chromatography column (GE Healthcare Life Sciences, Pittsburg, PA). The column was washed with wash buffer (50 mM  $\text{NaH}_2\text{PO}_4$  pH 7.4, 300 M NaCl, and 2.5 mM imidazole) and Hp0100 was eluted with elution buffer (50 mM  $\text{NaH}_2\text{PO}_4$  pH 7.4, 300 M NaCl, and 250 mM imidazole). The elution was dialyzed in dialysis buffer (2 L, 20 mM HEPES, pH 7.4) at 4 °C for 2 hours and against another round of dialysis buffer at 4 °C overnight. The protein sample was concentrated (~2 mL) and injected onto a UNO S ion-exchange column (12 mL column volume, BIO-RAD, Hercules, CA). The protein was eluted with a stepwise gradient of NaCl.

TEV protease cleavage was performed on the combined and concentrated His<sub>6</sub>-TEV-Hp0100 fractions after cation exchange chromatography. His<sub>6</sub>-TEV protease was



added to the purified His<sub>6</sub>-TEV-Hp0100 protein in a ratio of 1 mg of TEV protease to ~5 mg of Hp0100. The reaction was diluted using dialysis buffer A (~15 mL, 50 mM NaH<sub>2</sub>PO<sub>4</sub> pH 7.4, 300 M NaCl, 0.5 mM Na<sub>2</sub>EDTA, 10 mM β-mercaptoethanol) and dialyzed in dialysis buffer (2 L) at 4 °C overnight to remove the polyhistidine tag. The dialysis buffer was exchanged to dialysis buffer B (2 L, 50 mM NaH<sub>2</sub>PO<sub>4</sub> pH 7.4, 300 mM NaCl, 0.1 mM EDTA) and dialyzed at 4 °C for 1-2 hours. The His<sub>6</sub>-tagged TEV protease and the uncleaved His-tagged Hp0100 were removed by passing the reaction through HiTrap Ni<sup>+2</sup> chelating HP affinity column. The flow-through contained the untagged Hp0100.

#### 4.4.5 Cloning and overexpression of His<sub>6</sub>-SUMO-TEV-Hp0100

The WT and codon-optimized hp0100 genes were cloned into the pET His<sub>6</sub> SUMO TEV LIC cloning vector (2S-T, Addgene, Watertown, MA) to incorporate a cleavable N-terminal SUMO tag onto the *hp0100* gene using the ligation independent cloning (LIC) protocol from QB3 Macro lab, California Institute for Quantitative Biosciences (pUD011 and pUD012). The primers used in LIC is listed in table 4.2.

**Table 4.2. Oligonucleotide sequence used in LIC.**

Primer	Sequence	Plasmid
UD018	TACTTCCAATCCAATGCAATGCTCATTCATATTTGCTGCTC	pUD011
UD019	TTATCCACTTCCAATGTTATTATTACAGCAAATAAAACACC TTTTCTTC	
UD020	TACTTCCAATCCAATGCAATGCTGATCCACATTTGCTG	pUD012
UD021	TTATCCACTTCCAATGTTATTATTACAGCAGATAGAACACT TTTTCTTCC	

The His<sub>6</sub>-SUMO-TEV-WT Hp0100 (pUD0010) and His<sub>6</sub>-SUMO-TEV-codon optimized Hp0100 (pUD012) plasmids were overexpressed in *E. coli* BL21(DE3)-RIL by inoculating a culture of LB medium (50 mL) supplemented with ampicillin (100 µg/mL), chloramphenicol (100 µg/mL), and glucose (0.5%) with a saturated overnight culture grown in the same medium. The cultures were grown at two different temperatures: 37 °C and 19 °C. The cultures incubated at 37 °C were induced with IPTG (1 mM) at various OD<sub>600</sub> (0.4-0.6 and 0.8-1) for 4 hours and 1 hour, respectively. The cultures that were grown at 19 °C were induced at OD<sub>600</sub> 0.4-1 with IPTG (1 mM) overnight. The cells were lysed and analyzed by SDS-PAGE.

## CHAPTER 5

### PRELIMINARY CHARACTERIZATION OF SA2591, A TRUNCATED ORTHOLOG OF HP0100, A PROTEIN INVOLVED IN INDIRECT TRNA AMINOACYLATION

#### 5.1 Introduction

As discussed earlier in this dissertation, Hp0100 is an essential component of the *H. pylori* Asn-transamidosome (79). Apart from making a tRNA-independent transamidosome, Hp0100 accelerates the GatCAB-catalyzed transamidation of Asp-tRNA<sup>Asn</sup> to Asn-tRNA<sup>Asn</sup> by ~35 fold (79) and of Glu-tRNA<sup>Gln</sup> to Gln-tRNA<sup>Gln</sup> by ~3 fold (87). Further, Hp0100 has two putative ATPase domains; namely, an AANH domain and a P-loop motif. These two domains are activated by the two misacylated tRNAs produced during indirect tRNA aminoacylation: The AANH domain is activated by Glu-tRNA<sup>Gln</sup>, and the P-loop is activated by Asp-tRNA<sup>Asn</sup> (87). Previous work in our lab also suggests that Hp0100 has a metal binding motif with a CXXC consensus sequence (87, 138), although the functional role of this metal-binding site is unknown. These results highlight the importance of Hp0100 in the indirect biosynthesis of Asn-tRNA<sup>Asn</sup> and Gln-tRNA<sup>Gln</sup> in *H. pylori*.

Even though full-length orthologs of Hp0100 are found only in  $\epsilon$ -proteobacteria, truncated orthologs have been found in many other bacteria. These truncated versions contain roughly 2/3 of the primary N-terminal sequence of Hp0100. Importantly, these truncated variations were found in 7 of 18 of the drug-resistant strains listed as the “biggest threats” by the Center for Disease Control (CDC), USA (139). A partial sequence alignment of Hp0100 with the truncated orthologs found in methicillin-resistant *S. aureus* (MRSA, a firmicute; Sa2591) and *Neisseria gonorrhoeae* (*N. gonorrhoeae*, a  $\beta$ -proteobacteria causes the sexually-transmitted disease gonorrhea; NG0682) is shown in

**Figure 5.1.** These truncated orthologs contain the AANH and P-loop ATPase active site motifs (**Figure 5.1A and B**) critical to Hp0100 function. Furthermore, both bacteria use indirect tRNA aminoacylation. *N. gonorrhoeae* has a functional GlnRS but lacks AsnRS (140), so indirect tRNA aminoacylation is only used in the production of Asn-tRNA<sup>Asn</sup>. In contrast, *S. aureus* has AsnRS but lacks both GlnRS and AsnS, the enzyme that biosynthesizes asparagine (48). Therefore, the indirect tRNA aminoacylation pathway is utilized in producing Gln-tRNA<sup>Gln</sup> and in tRNA-dependent asparagine synthesis.

As shown in **Figure 5.1**, Sa2591 contains about 2/3 of the N-terminal sequence of Hp0100 and shares about 29% of sequence identity. This truncated ortholog contains both ATPase domains and the same CXXC motif found in Hp0100 (**Figure 5.1B, blue box**). Additionally, model structures of Hp0100 and Sa2591 (generated using the Robetta (89) and I-TASSER (141) respectively) show structural similarities between these two proteins (**Figure 5.2**).

Since *S. aureus* uses indirect tRNA aminoacylation to produce both Asn-tRNA<sup>Asn</sup> and Gln-tRNA<sup>Gln</sup> and Hp0100 and Sa2591 have sequence and structural similarities, we hypothesized that Sa2591 may function in a similar way to Hp0100.

In the early characterization of Hp0100, Dr. Gayathri Silva observed that purification of His<sub>6</sub>-Hp0100 from *E. coli* resulted in co-purification of *E. coli* AspRS (87). Similarly, Dr. Whitney N. Wood demonstrated that *E. coli* AspRS co-purifies with His<sub>6</sub>-Sa2591 (**Figure 5.3A**), offering the first experimental evidence that Sa2591 is a functional ortholog of Hp0100 (138).



**B**

**AANH-Like Domain**

Hp0100	1	MLIHICCSVD	NLYFLKKAKE	AFAGEKIVGF
Sa2591	38	ILLHSCCAPC	STYTLEFL-T	QYADIAI--Y
Ng0682	26	VLLHSCCAPC	SGEVMEAMLA	SGIGYTI--Y
		:*:*. **:	. ::	: * :

Hp0100	31	FYNPNIHPYS	EYLLRLEDVK	RTCEMLGIEL
Sa2591	65	FANSNIHPKN	EYLRRAKVQE	QFVEDFNKRT
Ng0682	54	FYNPNIHPHK	EYMLRKEENM	RFAEKFGIPE
		* * **** . **:	* :	: * :

**P-loop domain**

Hp0100	76	KGKELLGEKS	E--RCFECFD	LRLE
Sa2591	114	KDKELADEKE	GGLRCTACFE	MRLD
Ng0682	99	KAKGMEFEPE	RGIRCTMCFD	MRFE
		* * : * .	** **:	:*::

**Figure 5.1. Sequence similarities between Hp0100 and two putative truncated orthologs Sa2591 and Ng0682. (A)** A cartoon schematic comparing the position of the AANH and P-loop domains in Hp0100 and the truncated orthologs from *S. aureus* (Sa2591) and *N. gonorrhoeae* (Ng0682). **(B)** An alignment of the AANH domain and P-loop sequences from all three proteins. Motif-specific residues are colored in red. Rigorously conserved residues are labeled with an asterisk, colons mark highly conserved, and periods mark loosely conserved positions. The conserved CXXC motif in P-loop is boxed in blue.

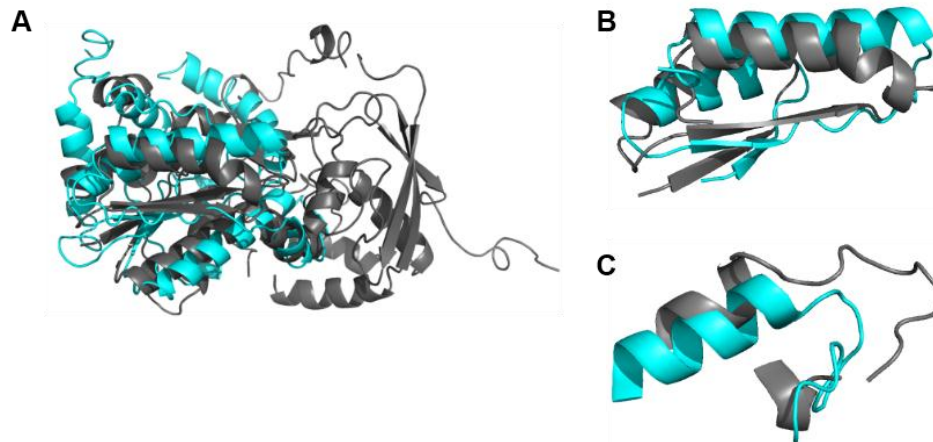


**Figure 5.2. Structural similarities between Hp0100.** (A) An overlay of the model structures of Hp0100 (grey) and Sa2591 (cyan). (B) A close-up of the two AANH domains. (C) A close-up of the two P-loop motifs.

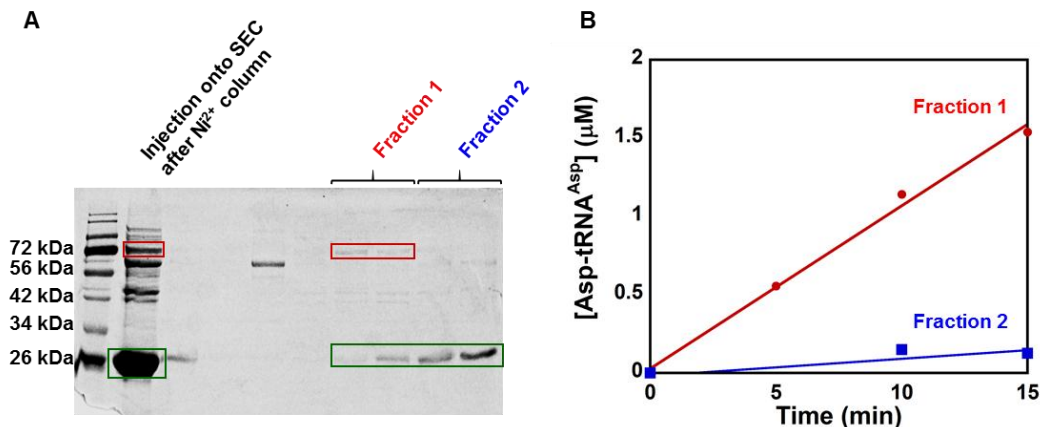


**Figure 5.3. *E. coli* AspRS co-purifies with Sa2591.** (A) SDS-PAGE gel showing co-purified *E. coli* AspRS with Sa2591. Lanes represent different fractions from an SEC purification. Sa2591 is noted in the green box and *E. coli* AspRS is shown in the red box. (B) Aminoacylation assays to confirm *E. coli* AspRS activity. Fractions 1 and 2 from panel A were assayed for AspRS activity. Fraction 1 produces Asp-tRNA<sup>Asp</sup> over time, confirming the identity of AspRS. Fraction 2 was assayed for comparison. Figure provided by Dr. Whitney Wood (138).

Also, like Hp0100, Sa2591 hydrolyzes ATP to ADP and Pi and this activity is enhanced in the presence of misacylated Asp-tRNA<sup>Asn</sup> (Figure 5.4) (138). Dr. Whitney Wood used a spectrophotometric enzyme-coupled assay to detect ADP production over time in the presence of Sa2591. In this assay, NADH oxidation to NAD<sup>+</sup> is directly correlated to the hydrolysis of ATP to ADP. Since NADH absorbs light at 340 nm and

NAD<sup>+</sup> does not, any decrease in absorbance at 340 nm indicates ATP hydrolysis (**Figure 5.4**). Most importantly, Dr. Wood observed that the ATPase activity of Sa2591 is only weakly stimulated by *in vitro* transcribed, misacylated Asp-tRNA<sup>Asn</sup>, compared to post-transcriptionally modified (overexpressed *in vivo*) misacylated Asp-tRNA<sup>Asn</sup> (**Figure 5.4B and D, respectively**). Moreover, Sa2591's ATPase activity is not affected by the presence of correctly aminoacylated Asp-tRNA<sup>Asp</sup> (**Figure 5.4A and C**). These results suggest the importance of post-transcriptional modifications to the ATPase activity of Sa2591 (138).

So far, we have demonstrated that Sa2591 might be a functional ortholog of Hp0100 with respect to its ATPase activity. In this chapter, we focus on further characterization of Sa2591, particularly regarding its effect on the GatCAB-catalyzed transamidation of Asp-tRNA<sup>Asn</sup> to Asn-tRNA<sup>Asn</sup>. The advantage of continuing this work with Sa2591, instead of Hp0100, is that it is much more readily and reliably purified in active form (see Chapter 4).

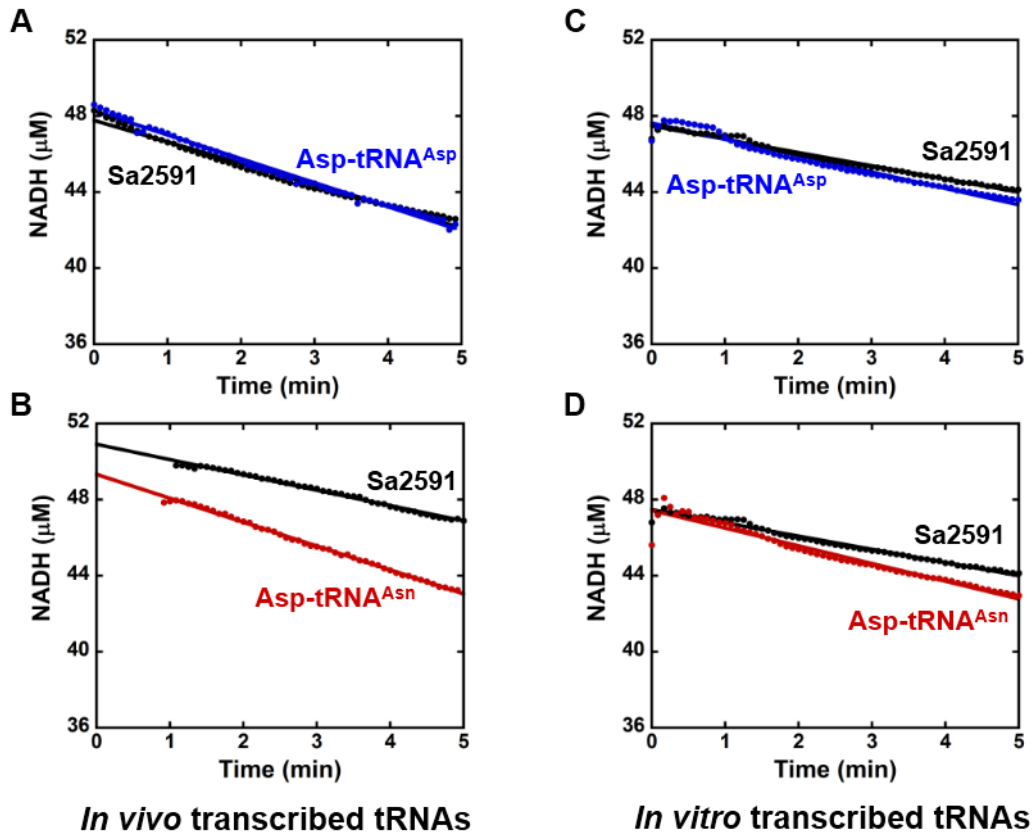


**Figure 5.4. Sa2591 is an ATPase that is activated by misacylated tRNAs.** (A) Sa2591 ATPase assays with *in vivo* transcribed correctly acylated tRNAs. ATPase activity is not stimulated by transcribed, misacylated Asp-tRNA<sup>Asn</sup>. (B) Sa2591 ATPase assays with *in vivo* transcribed misacylated tRNAs. ATP hydrolysis is stimulated by fully modified, misacylated Asp-tRNA<sup>Asn</sup>. (C) Sa2591 ATPase assays with *in vitro* transcribed correctly aminoacylated tRNAs. (D) Sa2591 ATPase assays with *in vitro* transcribed misacylated tRNAs. ATP hydrolysis is weakly stimulated by misacylated *in vitro* transcribed Asp-tRNA<sup>Asn</sup> compared to *in vivo* transcribed Asp-tRNA<sup>Asn</sup>. Figure provided by Dr. Whitney Wood (138).

## 5.2 Results

### 5.2.1 Sa2591 does not affect the GatCAB-catalyzed transamidation of *in vitro* transcribed *S. aureus* Asp-tRNA<sup>Asn</sup> to Asn-tRNA<sup>Asn</sup>

To further investigate Sa2591 as a functional ortholog of Hp0100, we assayed the impact of this enzyme on GatCAB-catalyzed transamidation of Asp-tRNA<sup>Asn</sup> to Asn-tRNA<sup>Asn</sup>. To this end, we utilized a P1 nuclease transamidation assay (Figure 5.5). In this



assay, the 3' end of tRNA<sup>Asn</sup> was first labeled with  $\alpha$ -<sup>32</sup>P-AMP. Then, this <sup>32</sup>P-labeled tRNA<sup>Asn</sup> sample was aminoacylated with aspartate by ND-AspRS. Next, GatCAB-catalyzed transamidation reactions were carried out in the presence and absence of Sa2591. After digestion with P1 nuclease, the <sup>32</sup>P radiolabel allows the conversion of aspartate to asparagine to be monitored via TLC separation of Asp-AMP and Asn-AMP and phosphorimaging.

Yields of *S. aureus* tRNA<sup>Asn</sup> were low when overexpressed in *E. coli* MV1184. For this reason, we prepared *in vitro* transcribed tRNA<sup>Asn</sup> for use in transamidation assays. This tRNA was readily aminoacylated by *S. aureus* ND-AspRS to produce Asp-tRNA<sup>Asn</sup> and converted to Asn-tRNA<sup>Asn</sup> by GatCAB. However, unlike Hp0100, Sa2591 did not show any effect on this transamidation activity (**Figure 5.6**). These results also suggest that Sa2591 may distinguish between transcribed and post-transcriptionally modified tRNAs, a hypothesis that requires further analysis.

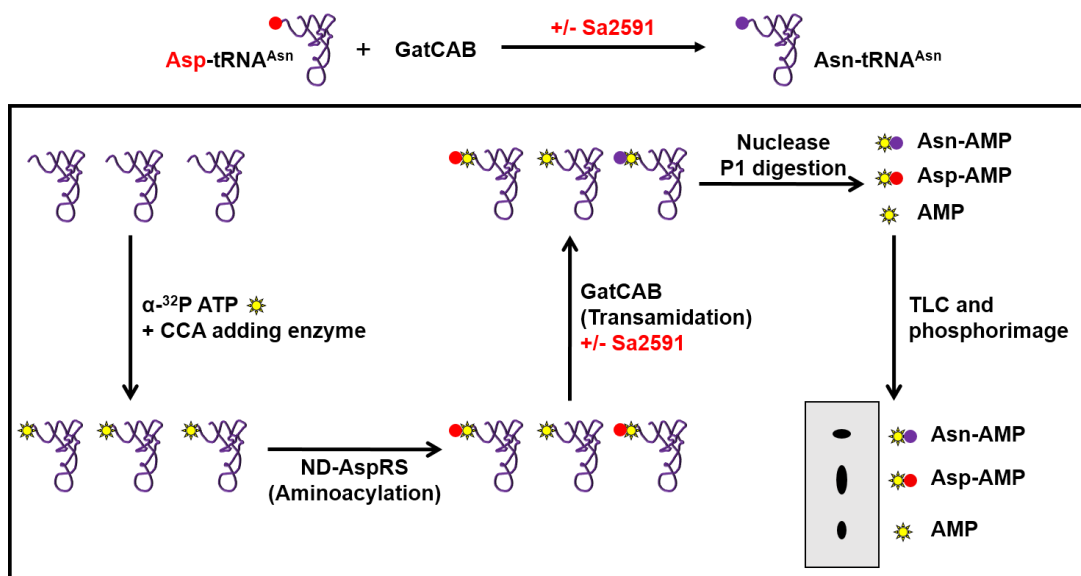


**Figure 5.5. Schematic representation of P1 nuclease transamidation assay.** Asp-tRNA<sup>Asn</sup> is labeled with α-<sup>32</sup>P-AMP using the CCA-adding enzyme and then aminoacylated by ND-AspRS. Following incubation with GatCAB in the presence and absence of Sa2591, the tRNA is digested with P1 nuclease, and Asp-AMP and Asn-AMP are separated by TLC. The radiolabel is quantified by phosphorimager. Figure modified from one provided by Dr. Gayathri Silva.

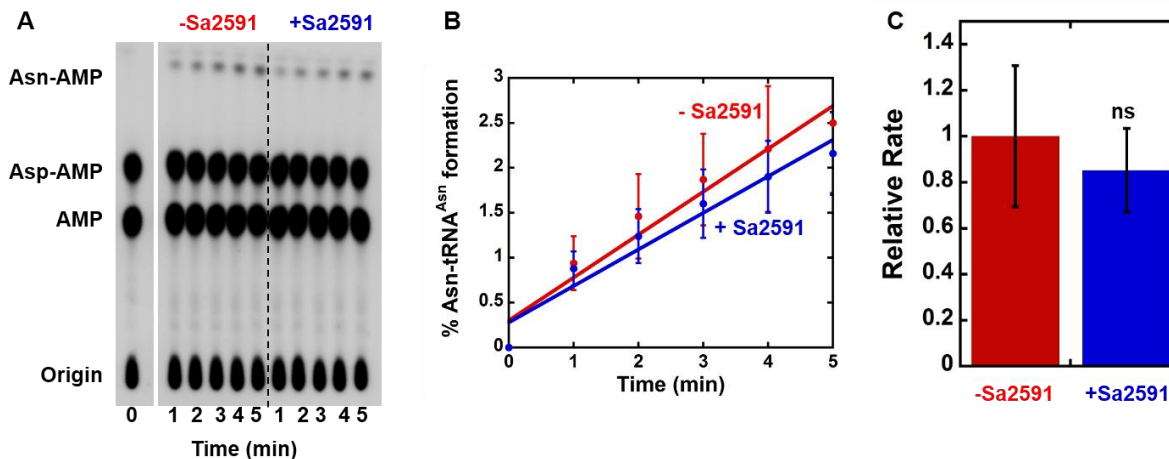


**Figure 5.6. Sa2591 does not affect Asn-tRNA<sup>Asn</sup> production by GatCAB.** (A) A representative phosphorimage of the results of a GatCAB (10 nM) transamidation reaction converting Asp-tRNA<sup>Asn</sup> (5 μM, indicated by Asp-AMP) into Asn-tRNA<sup>Asn</sup> (indicated by Asn-AMP) in the absence and presence of Sa2591 (500 nM). (B) Initial rates of Asn-tRNA<sup>Asn</sup> production, quantified from triplicate TLC plates as in A. (C) Bar graph representation of relative rates for the transamidation activity of GatCAB in the presence and absence of Sa2591. Error bars represent the standard error of the mean from triplicate measurements.

### 5.2.2 *S. aureus* GatCAB does not transamidate *H. pylori* Asp-tRNA<sup>Asn</sup>

To evaluate our hypothesis that post-transcriptional modifications are important for Sa2591 activity, we next investigated the effect of Sa2591 on GatCAB with modified tRNAs. Unfortunately, as noted above, *S. aureus* tRNA<sup>Asn</sup> is not produced in significant yields when overexpressed in *E. coli*. Consequently, we performed the same transamidation assays as above using modified *H. pylori* tRNA<sup>Asn</sup>. Dr. Whitney Wood had observed ATPase activity enhancement when Sa2591 was incubated with *H. pylori* tRNA<sup>Asn</sup> (138), leading us to anticipate that this heterologous combination of *H. pylori* tRNA<sup>Asn</sup>, Sa2591, and *S. aureus* GatCAB would be effective. Unfortunately, *H. pylori* Asp-tRNA<sup>Asn</sup> is not a robust substrate for *S. aureus* GatCAB, at least according to the preliminary results shown in **Figure 5.7**. Hence, the effect of Sa2591 on the transamidation activity of GatCAB remains undetermined.

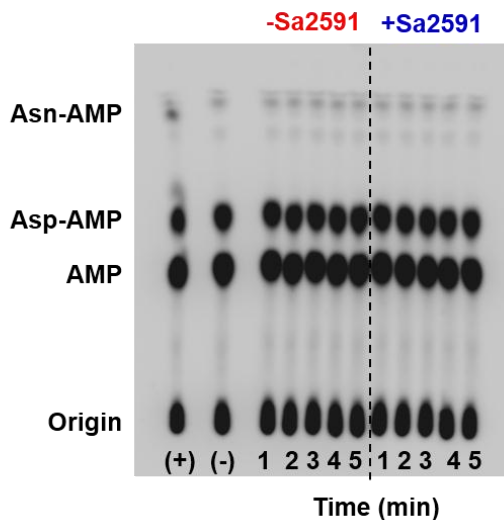


**Figure 5.7.** *H. pylori* Asp-tRNA<sup>Asn</sup> is a poor substrate for *S. aureus* GatCAB. A representative phosphorimage of an *S. aureus* GatCAB (10 nM) transamidation reaction with *H. pylori* Asp-tRNA<sup>Asn</sup> (5 μM) in the absence and presence of Sa2591 (500 mM). (+) indicates an Asn-tRNA<sup>Asn</sup> positive control and (-) represents Asp-tRNA<sup>Asn</sup> as a negative control.

### 5.3 Discussion

Many bacteria that lack AsnRS (and/or AsnS) and/or GlnRS utilize an indirect biosynthesis pathway to produce Asn-tRNA<sup>Asn</sup> (and/or asparagine) and Gln-tRNA<sup>Gln</sup> (34). These two tRNAs are first misacylated to form Glu-tRNA<sup>Gln</sup> and Asp-tRNA<sup>Asn</sup>, reactions that are catalyzed by ND-GluRS (100) (or GluRS2 in *H. pylori* (41-42)) and an ND-AspRS (43, 49), respectively. Then, these misacylated tRNAs are converted to Gln-tRNA<sup>Gln</sup> and Asn-tRNA<sup>Asn</sup> by an amidotransferase called GatCAB (15, 36, 44). The assembly of a stable ribonucleoprotein complex from tRNA<sup>Asn</sup>, GatCAB, and ND-AspRS, called the Asn-transamidosome, prevents premature release of Asp-tRNA<sup>Asn</sup> prior to repair by GatCAB and ensures the fidelity of protein synthesis (77-78, 82).

In contrast to the tRNA-dependent, Asn-transamidosome complexes from *T. thermophilus* and *P. aeruginosa*, *H. pylori* Asn-transamidosome formation depends on another protein partner called, Hp0100, instead of tRNA<sup>Asn</sup> (79). Hp0100 is an ATPase with two distinct ATPase sites which are activated by two different misacylated-tRNAs. Hp0100 also enhances the GatCAB-catalyzed transamidation of Asp-tRNA<sup>Asn</sup> to Asn-tRNA<sup>Asn</sup> and Glu-tRNA<sup>Gln</sup> to Gln-tRNA<sup>Gln</sup> (79, 87).

We have discovered several truncated orthologs of Hp0100 that contains 2/3 of the primary N-terminal sequence of Hp0100 from other bacteria. Here, we turned our focus onto the characterization of the truncated ortholog from *S. aureus*, called Sa2591. Because of their sequence and predicted model structural similarities (**Figure 5.1 and 5.2 respectively**), we hypothesized that Sa2591 would be functionally similar to Hp0100.

Dr. Whitney Wood showed that Sa2591 co-purifies with *E. coli* AspRS (**Figure 5.3**) (138), suggesting possible Asn-transamidosome formation in *S. aureus*. Further, Dr.

Wood confirmed that Sa2591 is an ATPase and catalyzes the hydrolysis of ATP to ADP (138). The Sa2591 ATPase activity is enhanced in the presence of misacylated tRNAs (**Figure 5.4**) specifically when these tRNAs are produced *in vivo* such that they contain post-transcriptional tRNA modifications (**Figure 5.4B and D**) (138).

As shown in **Figure 5.6**, Sa2591 does not show any influence on the GatCAB-catalyzed transamidation of Asp-tRNA<sup>Asn</sup> into Asn-tRNA<sup>Asn</sup>, distinguishing this protein from Hp0100. However, this divergence may be due to a lack of one or more post-transcriptional modifications in tRNA<sup>Asn</sup>. Future research is needed with modified *S. aureus* tRNAs to address this hypothesis.

Recently, Hp0100 and Sa2591, members of the DUF208 family of proteins of unknown function, were identified for their probable role in queuosine biosynthesis (99). Queuosine is a post-transcriptionally modified nucleotide found in the first position of the anticodon of four different tRNAs: tRNA<sup>Asp</sup>, tRNA<sup>Asn</sup>, tRNA<sup>His</sup>, and tRNA<sup>Tyr</sup> (94). The last step of queuosine biosynthesis pathway is the reduction of epoxyqueuosine to queuosine; this reaction was known to be characterized by a cobalamin-dependent enzyme called QueG (**Chapter 1, Figure 1.12**) (98, 142). However, in bacteria that lack QueG, the DUF208 family proteins act as epoxyqueuosine reductase and catalyze the last step in queuosine biosynthesis (99).

Pulling our preliminary results characterizing Sa2591, our published and unpublished results with Hp0100, and the reclassification of these enzymes as queuosine reductase (QueH), we believe that Sa2591 has different activities under different growth conditions. Under favorable growth conditions, Sa2591 would be involved in forming a stable Asn-transamidosome structure as we've demonstrated with Hp0100 (79).

However, under unknown stress conditions, Sa2591 may dissociate from the transamidosome to act as a queuosine reductase. Such a dissociation event would also allow for misincorporation of aspartate into proteins at asparagine codons as is the case in *M. tuberculosis* and *M. smegmatis* (50, 76). It is known that the levels of modified nucleotides in tRNAs, especially at anticodon wobble positions, increases during stress-induced conditions (143). Interestingly, Sa2591 mRNA transcripts are upregulated in *S. aureus* in acid-shocked cells, providing additional support to this hypothesis (144).

In conclusion, Sa2591 is a multi-functional protein as Hp0100. Due to this multi-functional nature of this protein it makes the data interpretation and characterization of this protein complicated. Further experiments needed to assess these activities of Sa2591 under favorable and stress-related growth environments.

## **5.4 Materials and Methods**

### **5.4.1 Materials**

Sodium dihydrogen phosphate ( $\text{NaH}_2\text{PO}_4$ ), L-aspartic acid, magnesium chloride, inorganic pyrophosphatase and diethyl pyrocarbonate (DEPC) were purchased from Sigma-Aldrich (St. Louis, MO). All radiolabeled reagents were purchased from American Radiolabeled Chemicals (St. Louis, MO). Ampicillin, chloramphenicol, kanamycin, ethylenediaminetetraacetic acid (EDTA), tris(hydroxymethyl) aminomethane (Tris), isopropyl  $\beta$ -D-thiogalactopyranoside (IPTG), dithiothreitol (DTT), bovine serum albumin (BSA), and phenylmethanesulfonyl fluoride (PMSF) were from Gold Biotechnology, Inc., (St. Louis, MO). Sodium chloride (NaCl), and ammonium acetate ( $\text{NH}_4\text{OAc}$ ) were purchased from Fisher Scientific (Hampton, NH). *Bst*NI was purchased from New England Biolabs (NEB, Ipswich, MA).

#### 5.4.2 Overexpression and purification of *S. aureus* Sa2591

*S. aureus* Sa2591 with an N-terminal TEV protease cleavable His<sub>6</sub>-tag (pWNW003) was overexpressed in DH5 $\alpha$ . LB medium (0.5 L) supplemented with ampicillin (100  $\mu$ g/mL) and glucose (0.5%) was inoculated with a saturated overnight culture grown from a single colony. The cultures were incubated at 37 °C, 200 rpm until the OD<sub>600</sub> of 0.4-0.6, and protein expression was induced with IPTG (1 mM). After induction, the cultures were grown at 19 °C for 14-16 hours and the cells were collected by centrifugation.

The cell pellet was suspended in lysis buffer (50 mM NaH<sub>2</sub>PO<sub>4</sub> pH 7.4, 1 M NaCl, 10 mM imidazole, 1 mM  $\beta$ -mercaptoethanol). The cells were lysed with lysozyme (2 mg/mL) and sonication. Aliquots of saturated PMSF (15  $\mu$ L/mL) were added every 15-20 min to reduce proteolysis. The cell debris was removed by centrifugation at 14,000 rpm for 30 min at 4 °C. The filtered lysate was loaded onto HiTrap Chelating High Performance (HP) affinity column (GE Healthcare Life Sciences, Pittsburg, PA), which was loaded with Ni<sup>2+</sup>. The His<sub>6</sub>-TEV-Sa2591 protein was purified essentially according to the manufacturer's protocol (GE Healthcare Life Sciences), with buffers containing  $\beta$ -mercaptoethanol (1 mM). The eluent was diluted with dialysis buffer A (~10 mL, 50 mM NaH<sub>2</sub>PO<sub>4</sub> pH 7.4, 300 mM NaCl, 0.5 mM Na<sub>2</sub>EDTA, 10 mM  $\beta$ -mercaptoethanol) and TEV protease was added in a ratio of 1 mg TEV to ~5 mg of tagged Sa2591. The cleavage reaction was dialyzed in dialysis buffer A (2 L) at 4 °C overnight and against dialysis buffer B (2 L, dialysis buffer A with 1 mM  $\beta$ -mercaptoethanol) for 1-2 hours. The cleaved His<sub>6</sub>-tag and His<sub>6</sub>-TEV protease were removed by passing through a Ni<sup>2+</sup>-coordinated HiTrap Chelating HP affinity column. The untagged Sa2591 was in the flow through and the

protein was concentrated using an Amicon 10 kDa MWCO (EMD Millipore, Burlington, MA). Final protein concentrations were determined by UV-Vis spectroscopy at 280 nm, using the extinction coefficient obtained from the ExPASy ProtParam tool (133). The protein was stored in glycerol (50%) at -20 °C and is stable for ~ 1 week after purification.

#### **5.4.3 Overexpression and purification of *S. aureus* ND-AspRS**

The *S. aureus* ND-AspRS (vector provided by Dr. Kelly Sheppard) was overexpressed in *E. coli* BL21(DE3)-RIL cell line and purified as previously described (51).

#### **5.4.4 Overexpression and purification of *S. aureus* GatCAB**

*S. aureus* GatCAB plasmid (vector provided by Dr. Isao Tanaka (60)) was overexpressed in *E. coli* BL21(DE3)-RIL. The culture was grown beginning with a single colony, in LB medium (1 L) supplemented with kanamycin (25 µg/mL), chloramphenicol (100 µg/mL), and glucose (0.5%) at 37 °C. Protein expression was induced with IPTG (1 mM) when the OD<sub>600</sub> reached 0.4-0.6. After 4 hours, cells were harvested by centrifugation at 4000 rpm for 10 min at 4 °C. The cells were resuspended in lysis buffer (50 mM NaH<sub>2</sub>PO<sub>4</sub> pH 7.4, 300 mM NaCl, 10 mM imidazole) containing saturated PMSF (15 µL/mL) and lysozyme (2 mg/mL). The cell suspension was incubated on ice for 30 min and sonicated 6-10 times using a Misonix Microson™ Ultrasonic Cell Disruptor set at level 4 for 10 seconds, with 50 second recovery intervals on ice between each pulse. After centrifugation at 14,000 rpm for 30 min at 4 °C, the lysate was added to a PolyPrep column that contained High-density cobalt agarose beads (~ 2 mL, Gold Biotechnology, Inc.) pre-washed with lysis buffer. The lysate was incubated on the resin for 1 hour at 4



°C while rotating. His<sub>6</sub>-GatCAB was purified according to the manufacturer's protocol (Gold Biotechnology).

#### **5.4.5 *In vitro* transcription and quantification of *S. aureus* tRNA<sup>Asn</sup>**

The *S. aureus* tRNA<sup>Asn</sup> plasmid was synthesized by GenScript (GenScript Biotech Corp. Piscataway, NJ). The gene was synthesized with a 5'-T7 RNA polymerase promoter sequence and a 3'-*Bst*M site and then sub-cloned into the pUC57 vector. Since the tRNA<sup>Asn</sup> sequence starts with uracil (U), a hammerhead ribozyme sequence was added between the T7 RNA polymerase promoter sequence and the start of the tRNA<sup>Asn</sup> DNA sequence. This vector design allows run-off transcription of the *Bst*M-digested plasmid DNA to produce tRNA<sup>Asn</sup> with a 5'-hammerhead ribozyme sequence (145-146). After transcription, the hammerhead ribozyme reaction cleaves the transcript to provide the unmodified tRNA<sup>Asn</sup> transcript with its native 5'-U base.

The tRNA<sup>Asn</sup> plasmid was transformed into DH5 $\alpha$  calcium chloride competent cells and the plasmid was isolated from a saturated overnight culture in LB medium supplemented with ampicillin (~50-200 mL, 100  $\mu$ g/mL) using the E.Z.N.A.® Plasmid Maxi kit (Omega Bio-Tek, Norcross, GA). The eluted DNA sample was concentrated by isopropanol precipitation.

All buffers used in this section were made with DEPC-treated water. *Bst*M digestion of the tRNA<sup>Asn</sup> plasmid DNA (1  $\mu$ g/ $\mu$ L) was carried out in NEB 3.1 buffer (1 $\times$ ) with *Bst*M (0.1 units// $\mu$ L). The digestion was performed at 60 °C overnight. The digested plasmid DNA was extracted with phenol/chloroform (1:1 v/v, pH 7-8) and isopropanol precipitated.

The transcription reactions were performed in buffer containing Tris-HCl (40 mM pH 8.1), spermidine (1 mM), DTT (5 mM), NTP (1 mM each), BSA (5  $\mu$ g/mL), inorganic pyrophosphatase (0.45 U) and 30 mM  $MgCl_2$  (146). Transcription was carried out using 1  $\mu$ g/ $\mu$ L of the *Bst*M-digested plasmid and 5  $\mu$ M T7 RNA polymerase at 30 °C for 2 hours. The hammerhead ribosome reaction was performed as previously described (145) over two hours. After phenol/chloroform (1:1 v/v, pH ~4.3) extraction and isopropanol precipitation, the tRNA was purified on a denaturing urea gel (8% acrylamide and 9 M urea). The tRNA<sup>Asn</sup> band was excised from the gel, crushed, and incubated in crush and soak buffer (0.5 mM  $NH_4OAc$  pH 5.2, 1 mM  $Na_2EDTA$ ) rotating at 37 °C overnight. The eluted tRNA<sup>Asn</sup> sample was isopropanol precipitated and the resultant pellet was dissolved in water.

The tRNA<sup>Asn</sup> sample was refolded in the presence of  $MgCl_2$  (2 mM) and quantified using *S. aureus* ND-AspRS as previously described (49).

#### 5.4.6 <sup>32</sup>P/nuclease P1 GatCAB transamidation assays

The 3'-end of the *S. aureus* tRNA<sup>Asn</sup> was labeled with  $\alpha$ -<sup>32</sup>P-AMP and aminoacylated as previously described (73). (The plasmid overexpressing the CCA-adding enzyme was provided by Dr. Rebecca Alexander, Wake Forest University).

P1 nuclease transamidation assays were performed as previously described (73). GatCAB (10 nM) with or without Sa2591 (500 nM) was pre-equilibrated with 40 mM HEPES-KOH (40 mM), pH 7.5,  $MgCl_2$  (8 mM) and KCl (25 mM) on ice for 15 min. <sup>32</sup>P-labeled Asp-tRNA<sup>Asn</sup> (5 mM) was added and the reaction was initiated with ATP (4 mM) and glutamine (2 mM) at 37 °C. The digested samples were spotted on a prewashed, dried PEI-cellulose TLC plates (Sigma-Aldrich, St. Louis, MO). The TLC was developed

in running buffer (25 mM  $\text{NH}_4\text{OAc}$ , 5% acetic acid). The plates were imaged overnight and quantified by phosphoimager.

## CHAPTER 6

### CONCLUSIONS AND FUTURE DIRECTIONS

#### 6.1 Introduction

This dissertation work focused on the functional characterization of accessory proteins and novel activities of enzymes involved in direct and indirect tRNA aminoacylation. Chapter 2 described the first characterization of the *M. smegmatis* Asn-transamidosome. Chapter 3 focused on the discovery of an unexpected enzymatic activity of bacterial AspRSs, namely the synthesis of Glu-tRNA<sup>Gln</sup> by these enzymes. Chapter 4 summarized efforts to more effectively overexpress and purify untagged or cleavable tagged Hp100 constructs. Chapter 5, the preliminary characterization of a truncated ortholog of Hp0100 called Sa2591 from *S. aureus* were discussed.

Since proteins play critical roles in structure, function, and regulation in cells, it is important to maintain high fidelity during protein synthesis. The first step in protein synthesis is the pairing up of the cognate tRNA to its cognate amino acid. This esterification reaction is catalyzed by a group of enzymes called the aaRSs (3, 11, 13, 147). Since organisms contain twenty different amino acids, there should be at least 20 aaRSs, one for each aa-tRNA isoacceptor pair. This scenario holds true in eukaryotes, and some microorganisms like *E. coli* (30). However, many prokaryotes do not have a full set of 20 aaRSs (11, 15, 32). In fact, many organisms lack AsnRS and/or GlnRS and use a two-step, indirect tRNA aminoacylation pathway to produce Asn-tRNA<sup>Asn</sup> and Gln-tRNA<sup>Gln</sup>, respectively (15, 34, 36, 43).

The work presented in this dissertation focused on three different pathogenic bacteria: *H. pylori*, *M. smegmatis*, and *S. aureus*. Among these three bacteria, *H. pylori*

and *M. smegmatis* both lack genes encode for AsnRS and GlnRS and therefore utilize indirect tRNA aminoacylation to produce Asn-tRNA<sup>Asn</sup> and Gln-tRNA<sup>Gln</sup> (42, 49-50). *S. aureus* does not contain a GlnRS, so it uses the indirect route to produce Gln-tRNA<sup>Gln</sup> (48). Further, *S. aureus* also lacks AsnS and hence cannot biosynthesize asparagine in the absence of tRNA. Therefore, in *S. aureus*, asparagine synthesis also occurs via this indirect tRNA aminoacylation pathway (51).

The first step in indirect aminoacylation of Asn-tRNA<sup>Asn</sup> is the aspartylation of tRNA<sup>Asn</sup> to produce the misacylated product Asp-tRNA<sup>Asn</sup> by ND-AspRS. Next, this misacylated Asp-tRNA<sup>Asn</sup> is transaminated to Asn-tRNA<sup>Asn</sup> by an amidotransferase called GatCAB. An analogous, two-step process exists to produce Gln-tRNA<sup>Gln</sup>. In this case, ND-GluRS (or GluRS2 in *H. pylori*) misacylates tRNA<sup>Gln</sup> to produce Glu-tRNA<sup>Gln</sup>, which is then converted to Gln-tRNA<sup>Gln</sup> by the same GatCAB. In these organisms, it is necessary to prevent the misacylated-tRNAs, Asp-tRNA<sup>Asn</sup> and Glu-tRNA<sup>Gln</sup>, from entering the ribosome, which would lead to translational errors by incorporating aspartate and glutamate into asparagine and glutamine codons respectively (49, 53, 148). Mechanism/s for the quick delivery of misacylated-tRNAs, either from ND-AspRS or ND-GluRS to GatCAB must exist to ensure the fidelity of protein synthesis.

One such mechanism is the formation of a ribonucleoprotein complex called transamidosome (77-82). For example, *T. thermophilus*, a thermophilic bacterium assembles a stable ribonucleoprotein complex composed of four tRNA<sup>Asn</sup>, two GatCAB, and two dimeric ND-AspRS. This complex is called the Asn-transamidosome and it protects the aminoacyl ester linkage in Asp-tRNA<sup>Asn</sup> and ensures efficient production of Asn-tRNA<sup>Asn</sup> (77, 82). There are only a few examples of Gln-transamidosome

characterized so far. The *T. maritima* Gln-transamidosome is composed of one tRNA<sup>Gln</sup>, one GatCAB, and one monomeric ND-GluRS (81). But compared to the Asn-transamidosomes, these Gln-transamidosomes are less stable and more dynamic in nature and may not be physiologically relevant.

Unlike the above mentioned thermophilic transamidosomes, the mesophilic *H. pylori* Asn-transamidosome requires a novel protein partner, Hp0100, instead of tRNA<sup>Asn</sup>, for stable assembly (79). Hp0100 is not only involved in making a stable transamidosome, but it also accelerates both GatCAB-catalyzed transamidation reactions. The addition of Hp0100 increases Asp-tRNA<sup>Asn</sup> transamidation by ~35-fold (79) and Glu-tRNA<sup>Gln</sup> transamidation by ~3-fold (87). Further, Hp0100 contains two ATPase domains: an adenosine nucleotide alpha hydrolase (AANH) domain and a P-loop motif. Hp0100 hydrolyzes ATP to ADP and Pi, and this ATP hydrolysis is enhanced in the presence of either Asp-tRNA<sup>Asn</sup> or Glu-tRNA<sup>Gln</sup>. Analysis of mutations in the two ATPase domains demonstrated that both are catalytically active and the AANH domain activity is specifically accelerated by Glu-tRNA<sup>Gln</sup> while the P-loop responds to Asp-tRNA<sup>Asn</sup> (87). Hp0100 also contains several, clustered, conserved cysteine residues, including a possible metal binding motif with CXXC signature sequence in the P-loop ATPase domain. **Figure 6.1** summarizes the findings on Hp0100 so far.

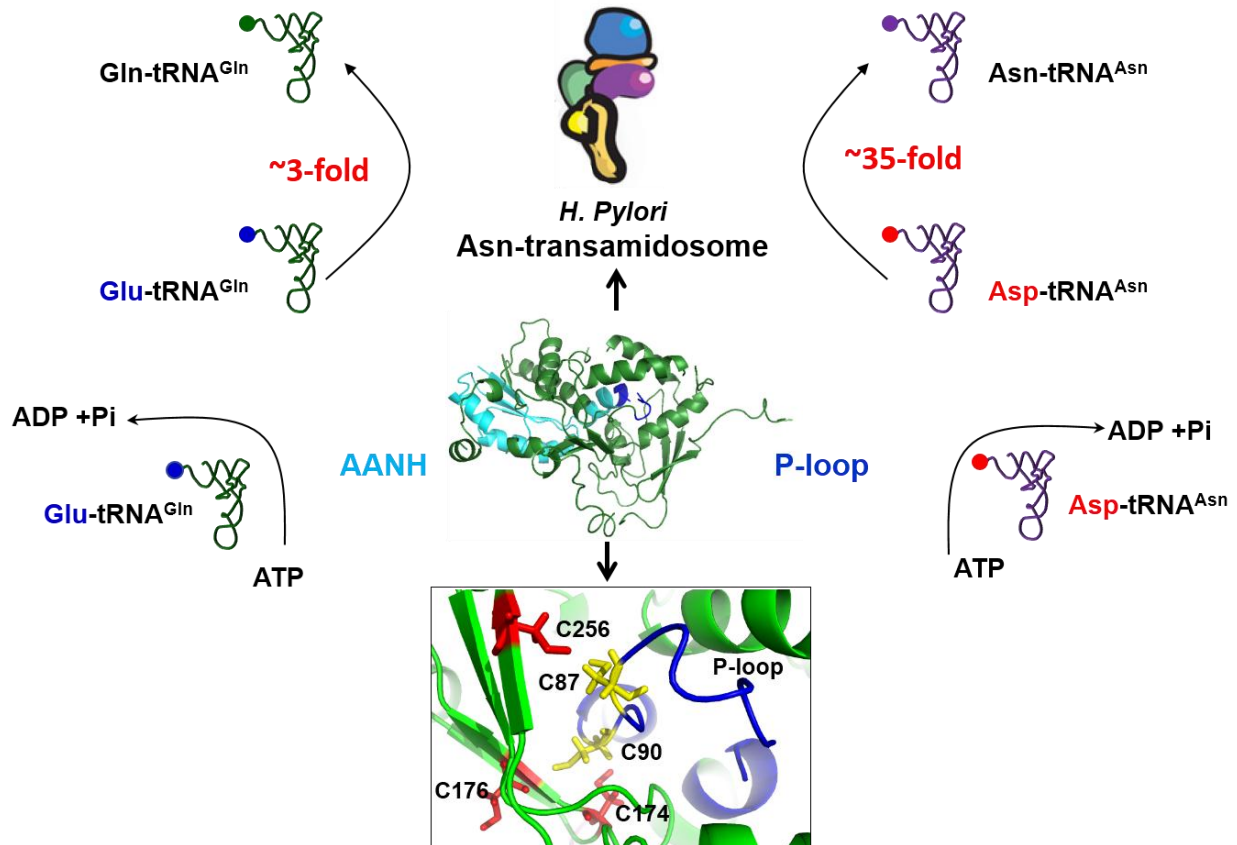


**Figure 6.1. Hp0100 is a multi-functional protein.** Hp0100 is a component of the *H. pylori* Asn-transamidosome. Hp0100 enhances the transamidation of both Asp-tRNA<sup>Asn</sup> and Glu-tRNA<sup>Gln</sup> to Asn-tRNA<sup>Asn</sup> and Gln-tRNA<sup>Gln</sup>, respectively. It has two ATPase domains: AANH and P-loop, which are specifically activated by the two misacylated tRNAs. Hp0100 also contains a metal binding motif with a CXXC consensus sequence.

## 6.2 The components of the indirect tRNA aminoacylation pathway of *M. smegmatis* assemble into an Asn-transamidosome

We have demonstrated that the overexpressed and purified *M. smegmatis* GatCAB from *M. smegmatis* mc<sup>2</sup>-155 co-purifies with endogenous ND-AspRS. Standard aminoacylation assays clearly showed that the co-purified ND-AspRS is active in the Asn-transamidosome complex form (**Figure 2.3 and 2.4**). To our knowledge, the co-purification of *M. smegmatis* GatCAB and ND-AspRS represents the first Asn-transamidosome isolation from *Mycobacteria*

*Mycobacteria* is the only bacterial clade that exhibits a clear connection between indirect tRNA aminoacylation and mistranslation leading to persistence (76). It would be useful to investigate the composition of the *M. smegmatis* transamidosome in more detail. Are there two separate Asn and Gln-transamidosomes or do these proteins all assemble into one larger ribonuclear protein complex? Is complex formation tRNA-dependent or does it require another protein partner in a manner similar to that of Hp0100 (79)? Will the composition of the transamidosome vary under mistranslation induces conditions? These questions are worth investigating in the future.

### **6.3 *M. smegmatis* GatCAB co-purified with other putative accessory proteins**

We have identified two putative accessory proteins that repeatedly co-purified with *M. smegmatis* GatCAB. The two proteins that were identified were a universal stress protein (USP, MSMEG3950) and superoxide dismutase (SOD) (**Figure 2.1**). Both are stress-related proteins (110-111). We hypothesize that these proteins may disrupt transamidosome formation in response to external stressors and result in mistranslation providing conditions beneficial for the organism's survival. It would be interesting to confirm the observed interactions between these proteins and the *M. smegmatis* transamidosome and to test the strength of these interactions under different stress-related growth conditions to see if a connection between stress, growth, and persistence can be identified.

### **6.4 Some bacterial AspRSs exhibits GluRS like activity**

We have discovered that some bacterial AspRSs and ND-AspRSs display considerable GluRS activity. These AspRSs are capable of aminoacylating tRNA<sup>Glu</sup> with glutamate to produce Glu-tRNA<sup>Glu</sup>. This activity is interesting as these enzymes do not



glutamylate their “natural” substrates tRNA<sup>Asp</sup> and tRNA<sup>Asn</sup> to produce Glu-tRNA<sup>Asp</sup> or Glu-tRNA<sup>Asn</sup> respectively (**Figure 3.11B**). Further, these AspRSs are incapable of putting aspartate onto tRNA<sup>Glu</sup> as well (**Figure 3.11A**). This unexpected GluRS-like activity is noteworthy because it is accurate and the product does not put the genetic code into jeopardy. We believe that this activity is a remnant of early AspRS evolution. Future research should focus on identifying the molecular recognition elements in tRNA<sup>Glu</sup> that allow for efficient glutamylation by ND-AspRS while discriminating against the misacylated species mentioned above. An important question is: How do these AspRS enzymes know to only put Glu onto tRNA<sup>Glu</sup>? This observation suggests an intriguing, subtle communication process.

### **6.5 Hp0100 and Sa2591 are involved in indirect tRNA aminoacylation and exhibit different activities under different growth conditions**

Although full-length orthologs of Hp0100 are found only in  $\epsilon$ -proteobacteria, truncated orthologs of Hp0100 have been found in many other bacteria in different clades. These truncated versions contain roughly 2/3 of the primary N-terminal sequence of Hp0100 and contain both ATPase domains (**Figure 5.1**).

Working with full-length His<sub>6</sub>-Hp0100 proved to be challenging for several reasons: potential complications with respect data interpretation with the His<sub>6</sub>-tagged Hp0100 due to the metal-binding nature of this tag and the metal-binding motif in Hp0100; challenges purifying His<sub>6</sub>-Hp0100 due to solubility issues; and the co-purification of *E. coli* AspRS with His<sub>6</sub>-Hp0100 (87). None of the strategies undertaken to better overexpress and purify Hp0100 were successful. Due to these difficulties in working with the full-length Hp0100,

we focused on characterizing the truncated ortholog of Hp0100, Sa2591 from *S. aureus*, which proved to be more reliably easy to handle and manipulate.

The preliminary characterizations of Sa2591 by Dr. Whitney Wood highlight the involvement of Sa2591 in possible Asn-transamidosome formation. She demonstrated that Sa2591 hydrolyzes ATP to ADP and Pi and that this ATPase activity is enhanced in the presence of misacylated tRNAs (138). However, as demonstrated in **Figure 5.6** in chapter 5, Sa2591 impact the transamidation activities of GatCAB, in contrast to the impact of Hp0100. Since these data were obtained with *in vitro* transcribed tRNAs, this loss of transamidation enhancement of GatCAB by Sa2591 may due to the lack of post-transcriptional modifications on the tRNAs. With the recent identification of Sa2591 and Hp0100 as epoxyqueuosine reductases (99), we think that these proteins may be screening tRNA<sup>Asn</sup> for the presence of queuosine. Thus, we hypothesize that these two proteins promote transamidation in fully-modified tRNAs, but are coopted for queuosine biosynthesis when needed.

Overall, we think that these accessory proteins Hp0100 and Sa2591 have different activities under different growth environments (**Figure 6.2**). Under healthy growth conditions, these proteins will promote stable Asn-transamidosome assembly, encourage biosynthesis of Asn-tRNA<sup>Asn</sup>, and ensure the insertion of asparagine into proteins at asparagine codons during protein translation. Under stressful growth conditions, Hp0100 and Sa2591 would dissociate from the Asn-transamidosome, resulting in an accumulation of misacylated Asp-tRNA<sup>Asn</sup> and insertion of aspartate into asparagine codons. This mistranslation may beneficial to the organisms for survival under stress related conditions. This hypothesis is supported by the discovery of misincorporation of aspartate

into asparagine codons in *Mycobacteria*, which facilitated adaptive rifampicin-specific phenotypic resistance (76). Moreover, after leaving the transamidosome free Hp0100 and Sa2591 could also upregulate queuosine biosynthesis. This theory is backed by the recent discoveries of increased levels of modified tRNAs under stress-induced conditions (143) and the increase in Sa2591 mRNA levels in *S. aureus* in response to pH changes (144). Further experiments need to be carried out to validate this hypothesis.

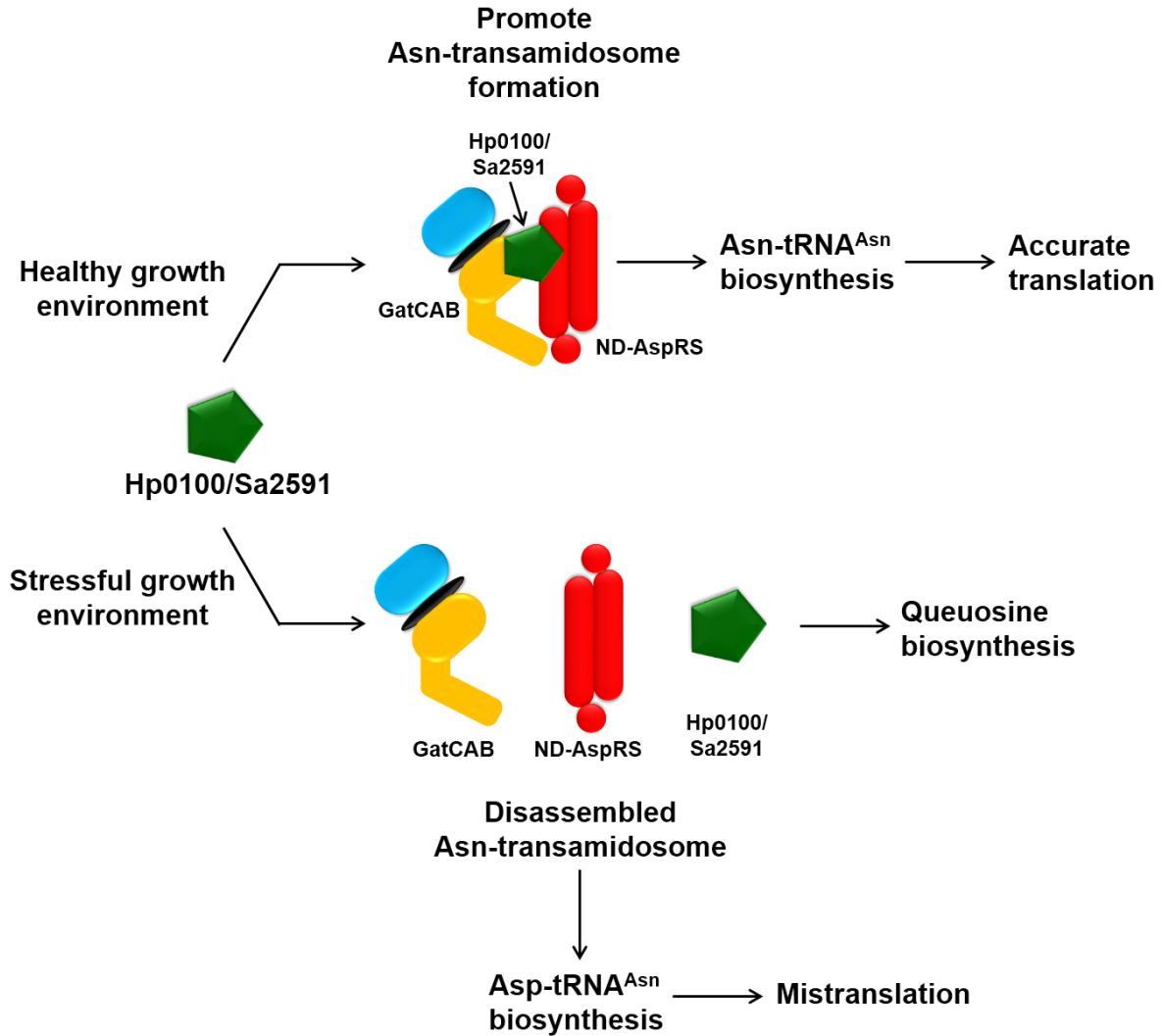


**Figure 6.2. Schematic representation of the role of Hp0100 and Sa2591 under different growth conditions.** Under healthy growth conditions, Hp0100 and Sa2591 would promote Asn-transamidosome assembly, which would lead to the biosynthesis of Asn-tRNA<sup>Asn</sup> and accurate translation. In a stressed environment, the Asn-transamidosome would dissociate, causing the production of Asp-tRNA<sup>Asn</sup> and mistranslation. Hp0100 and Sa2591 would then act as epoxyqueuosine reductase and increase the levels of tRNA modifications in cells.

## APPENDIX A

### EFFECT OF EXOGENOUS AMMONIA ON THE TRANSAMIDASE ACTIVITY OF WT AND D185 GATCAB VARIANTS

The work presented in this appendix is included here because it is unrelated to the rest of the work presented in this dissertation and is the result of a side project. Reproduced with permission from Zhao, L.; Rathnayake, U. M.; Dewage, S. W.; Wood, W. N.; Veltri, A. J.; Cisneros, G. A.; and Hendrickson, T. L. Characterization of tunnel mutants reveals a catalytic step in ammonia delivery by an aminoacyl-tRNA amidotransferase. *FEBS Lett.* **2016**, *590*, 3122-3132. Copyright © 2016, John Wiley and Sons, reprinted with permission.

#### A.1 Introduction

In *H. pylori* and other organisms that do not have AsnRS and/or GlnRS, the production of Asp-tRNA<sup>Asn</sup> and Gln-tRNA<sup>Gln</sup> occurs through an indirect tRNA aminoacylation pathway (34, 36-37, 43). In this pathway, the misacylated intermediates Asp-tRNA<sup>Asn</sup> and Glu-tRNA<sup>Gln</sup> are converted to Asn-tRNA<sup>Asn</sup> and Gln-tRNA<sup>Gln</sup> by a glutamine-dependent amidotransferase called GatCAB (34, 37, 44). GatCAB is composed of three subunits GatA, GatB, and GatC.

GatCAB catalyzes three discrete reactions (**Chapter 1, Figure 1.5**) (37, 71, 73). GatA hydrolyzes glutamine to produce glutamate and ammonia. The ammonia is then delivered to the active site of GatB through an unusually hydrophilic ammonia tunnel (~40 Å). GatB catalyzes the ATP-dependent phosphorylation of Asp-tRNA<sup>Asn</sup> and Glu-tRNA<sup>Gln</sup>, followed by the delivery of the ammonia from GatA to convert phosphoryl-Asp-tRNA<sup>Asn</sup> and phosphoryl-Glu-tRNA<sup>Gln</sup> into Asn-tRNA<sup>Asn</sup> and Gln-tRNA<sup>Gln</sup> respectively (37, 71, 73).

There are two proposed ammonia tunnels in *S. aureus* GatCAB, tunnel I (60) and tunnel II (70). While the proposed tunnel I is hydrophilic in nature, tunnel II is mostly lined with hydrophobic residues. Nakamura and coworkers proposed that ammonia delivery through the hydrophilic tunnel I occurs via a series of protonation and deprotonation steps (60). The D185 residue of *H. pylori* GatCAB is located at the top of this tunnel and may serve as the first catalytic residue in this proton relay process acting as an acid and a base. Dr. Liangjun Zhao carried out the characterization of this D185 residue in wild-type GatCAB and D185A, D185E, and D185N mutations (73). He monitored the participation of these residues in the three reactions catalyzed by GatCAB: glutamine hydrolysis, phosphorylation of Glu-tRNA<sup>Gln</sup>, and transamidation to produce Gln-tRNA<sup>Gln</sup> (73). My work focused on the characterization of the transamidation reaction of WT GatCAB and these D185 tunnel mutants with ammonium chloride as the ammonia donor (instead of glutamine).

## A.2 Results

According to the data from Dr. Liangjun Zhao, the D185A and D185N GatCAB mutants exhibit reduced glutamine hydrolysis and phosphorylation activities compared to WT GatCAB (73). In contrast, the transamidation activities of these two mutants were almost completely disrupted when glutamine was used as the source of ammonia (2% and 6% of WT, respectively, **Figure A.1**). It is highly unlikely that the partial reductions in initial rates for glutamine hydrolysis and phosphorylation account for the dramatic decrease in transamidase activity observed. In contrast, the D185E GatCAB mutant maintained robust transamidase activity (107% of the WT, **Figure A.1**), in addition to glutaminase and kinase activities. The fact that D185E GatCAB, but not D185N GatCAB

retains WT transamidation activity directly points to a requirement for an ionizable carboxylate/carboxylic acid side chain.

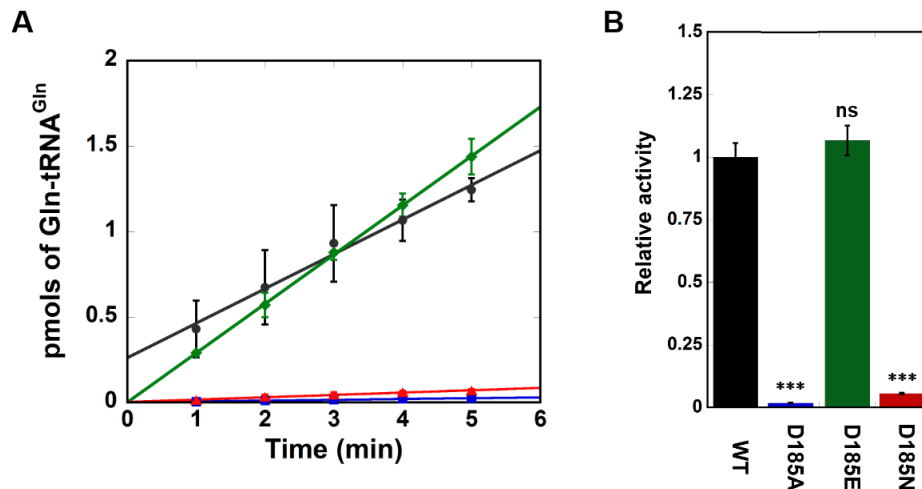


**Figure A.1. The use of glutamine as an ammonia source for WT and D185 GatCAB mutants. (A)** Initial rates of transamidation of WT and D185 mutants with glutamine. Results are shown for WT (●), D185A (■), D185E (◆), and D185N (▲). Assays were carried out with 1 nM GatCAB and 5 mM glutamine. **(B)** Bar graph representation of relative activities of the initial rates for the transamidation of Glu-tRNA<sup>Gln</sup> to Gln-tRNA<sup>Gln</sup> by WT GatCAB and D185 mutants. Error bars represent standard deviation from biological triplicates (\*\*\*)  $P < 0.001$ ). Figure provided by Dr. Liangjun Zhao and republished with permission (73).

Many glutamine-dependent amidotransferases, including GatCAB (44), can utilize exogenous ammonia as a substrate replacing glutamine hydrolysis. We compared rates of ammonia utilization between WT GatCAB and our D185 mutations with Glu-tRNA<sup>Gln</sup> as a substrate (**Figure A.2**). WT GatCAB utilizes ammonia as the ammonia donor at a rate that is 0.8% that observed with glutamine. As with our other assay results, the activity of the D185E GatCAB variant resembles the WT enzyme with an ammonia-dependent rate of transamidation that is 117% that of WT. Surprisingly, the D185A GatCAB variant also uses ammonia as a substrate (56% activity compared to WT), while the D185N mutation is much less active in the presence of ammonia (14% compared to WT). These results differentiate the activities of D185A GatCAB from D185N GatCAB. The initial rates and

transamidase activity with glutamine and exogenous ammonia of WT and GatCAB mutants are summarized in **Table A1**.

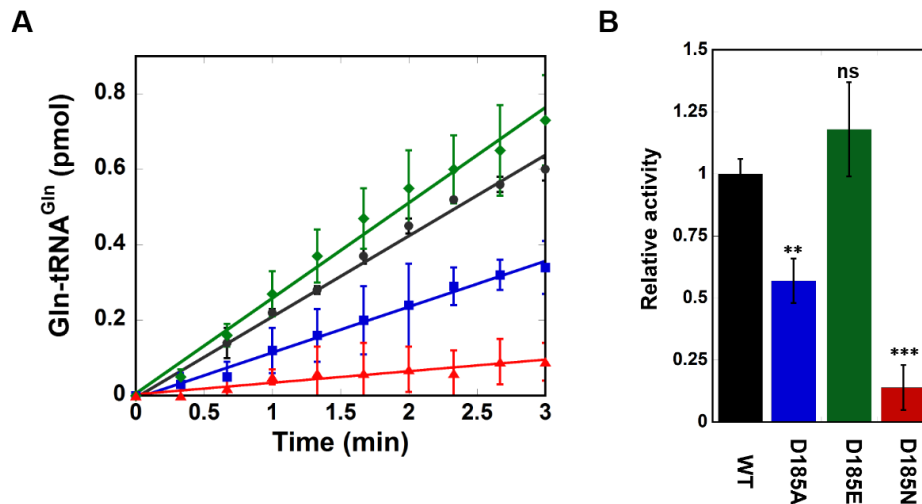


**Figure A.2. The use of ammonium chloride as an ammonia source for WT and D185 GatCAB mutants. (A)** Initial rates of transamidation of WT and D185 mutants with NH<sub>4</sub>Cl. Results are shown for WT (●), D185A (■), D185E (◆), and D185N (▲). Assays were carried out with 100 nM GatCAB and 20 mM NH<sub>4</sub>Cl. **(B)** Bar graph representation of relative activities of the initial rates for the transamidation of Glu-tRNA<sup>Gln</sup> to Gln-tRNA<sup>Gln</sup> by WT GatCAB and D185 mutants. Error bars represent standard deviation from biological triplicates (\*\*P < 0.01, \*\*\*P < 0.001). Figure republished with permission (73).

**Table A.1. Initial rates for transamidation of WT and D185 GatCAB variants with NH<sub>4</sub>Cl as ammonia donor.**

GatCAB	Transamidase with glutamine		Transamidase with NH <sub>4</sub> Cl	
	Initial rate (μM/min)	Enzyme activity* (s <sup>-1</sup> )	Initial rate (μM/min)	Enzyme activity* (s <sup>-1</sup> )
<b>WT</b>	0.270 ± 0.015	4.50 ± 0.25	0.214 ± 0.012	0.036 ± 0.002
<b>D185A</b>	0.005 ± 0.001	0.08 ± 0.02	0.122 ± 0.020	0.020 ± 0.003
<b>D185E</b>	0.288 ± 0.020	4.80 ± 0.34	0.253 ± 0.040	0.042 ± 0.007
<b>D185N</b>	0.015 ± 0.002	0.26 ± 0.03	0.031 ± 0.018	0.005 ± 0.003

\*Enzyme activity is defined as the initial rate divided by enzyme concentration (1 nM with glutamine and 100 nM with NH<sub>4</sub>Cl).



### A.3 Discussion

To characterize the importance of the D185 residue in the GatA subunit of GatCAB in ammonia transport, this residue was mutated to alanine, glutamate, and asparagine. The three enzyme reactions catalyzed by GatCAB: glutaminase, phosphorylation of tRNA and transamidase, were examined experimentally to compare the behavior of WT GatCAB to its D185A, D185N, and D185E variants.

The D185E GatCAB variant retained WT-like activity for all three reactions. The D185A and D185N GatCAB mutants had reductions in glutamine hydrolysis and phosphorylation compared to WT and their transamidation activities were almost completely disrupted when glutamine was used as the source of ammonia (73). It is highly unlikely that the partial reductions in initial rates for glutamine hydrolysis and phosphorylation account for the dramatic decrease in transamidase activity observed.

Unexpectedly, when we replaced glutamine with ammonium chloride as the source of ammonia and compared the activities of these D185 variants (**Figure A.2**), differences between the D185A and D185N mutations were unmasked. The D185N GatCAB was essentially insensitive to the source of ammonia; when either glutamine or ammonium chloride was used as the substrate for transamidation, observed transamidation rates were 6% and 14% that of WT, respectively. In contrast, D185A GatCAB utilized ammonia as a substrate with a rate that was 56% that of WT, in stark contrast to the 2% of WT activity that was observed when this mutant was assayed with glutamine as the ammonia source.

To explain this divergence between the D185A and D185N GatCAB variants with ammonium chloride as an exogenous ammonia source, we considered two scenarios:

these mutations could differentially hinder accessibility of ammonia to the GatCAB ammonia tunnel through GatA (scenario 1) or ammonia could passively diffuse into the GatB active site (scenario 2). The data herein strongly favor the first scenario, wherein ammonia access to the GatB active site is only (or predominantly) achieved via migration through the ammonia tunnel.

Scenario 2 considers the possibility that ammonia can passively diffuse into the GatB active site, without migration through that GatCAB ammonia tunnel. In this case, one would expect the initial transamidation rates of all four D185 GatCAB variants (including WT) to be nearly indistinguishable from each other with ammonium chloride as the sole source of ammonia for transamidation. Instead, significant differences were observed in these transamidation rates. The WT and D185E GatCAB variants both use ammonium chloride with initial rates just under 1% observed with glutamine (**Table A1**), and the D185N GatCAB has an ammonium chloride-dependent rate of transamidation that is only 2% that of the corresponding glutamine-dependent initial rate. In stark contrast, the impact of switching from glutamine to ammonium chloride is much less dramatic with the D185A GatCAB mutant: this mutant enzyme retains 25% of its glutamine-dependent, initial rate of transamidation when ammonium chloride is used instead. The broad range of the transamidase activity ratios comparing ammonium chloride to glutamine (from 0.1% to 25%) strongly argues against passive diffusion of ammonia into the GatB active site (scenario 2).

The significant loss of transamidase activity using exogenous ammonia donor (versus glutamine) suggests that the usable exogenous ammonia has to be transferred through the internal ammonia tunnel (scenario 1). The differences between the D185A

and D185N GatCAB variants with ammonium chloride as the substrate are subtle because both of these enzymes are already globally defective in transamidation as demonstrated when glutamine is used as the native substrate (**Figure A.1**). With the D185A mutant, the higher rate of transamidation with ammonium chloride results from the small alanine side chain, which presumably widens the tunnel and allows some ammonia migration to occur in the absence of glutamine bound to GatA. Nevertheless, the D185A mutation still suffers a huge ammonia transfer energy penalty in the absence of the carboxyl group (similar to the D185N variant) as indicated by its low transamidase activity with glutamine as the ammonia donor.

In conclusion, the D185 residue was characterized, and the results revealed a probable step in the ammonia delivery mechanism for GatCAB. The differences between the WT-like D185E GatCAB and the defective D185A and D185N mutants support our hypothesis that D185 acts as an acid/base residue for ammonia transfer during catalysis.

## **A.4 Materials and Methods**

### **A.4.1 Materials**

L-glutamic acid, magnesium chloride, triton X-100, nuclease P1, and PEI-cellulose thin layer chromatography plates were from were purchased from Sigma-Aldrich (St. Louis, MO). All radiolabeled reagents were purchased from American Radiolabeled Chemicals (St. Louis, MO). Ampicillin, chloramphenicol, kanamycin, ethylenediaminetetraacetic acid (EDTA), guanidine thiocyanate, isopropyl  $\beta$ -D-thiogalactopyranoside (IPTG), tris(hydroxymethyl) aminomethane (Tris), and phenylmethanesulfonyl fluoride (PMSF) were from Gold Biotechnology, Inc. (St. Louis,

MO). Sodium chloride (NaCl), and ammonium acetate (NH<sub>4</sub>OAc) were purchased from Fisher Scientific (Hampton, NH).

#### **A.4.2 Overexpression and purification of WT GatCAB and D185 mutants**

WT GatCAB and D185 variants were overexpressed and purified as previously described (71).

#### **A.4.3 *In vivo* transcription and purification of *H. pylori* tRNA<sup>Gln</sup>**

*H. pylori* tRNA<sup>Gln</sup> was overexpressed in *E. coli* MV1184. LB medium supplemented with ampicillin (100 µg/mL) was inoculated with a saturated culture grown from a single colony in the same medium. Cultures were incubated at 37 °C, 200 rpm and overexpression was induced with IPTG (1 mM) when OD<sub>600</sub> reached 0.4-0.6. The cells were pelleted by centrifugation at 4000 rpm at 4 °C for 10 min after 4 hours. The cell pellet was suspended in W1 buffer (50 mM Tris-acetate, pH 7.8, 4 M guanidine thiocyanate, 15 mM β-mercaptoethanol, and 2% triton X-100). After incubating on ice for 15 min, NaOAc (3 M, pH 6.5, 1:1 v/v) was added and the mixture was incubated on ice for an additional 15 minutes. The cell debris was removed by centrifugation at 10,000 g for 20 min. The lysate was isopropanol precipitated and the resulting pellet was dissolved in W4 buffer (10 mM Tris-acetate, pH 7.8 and 1 mM Na<sub>2</sub>EDTA). The solution was phenol/chloroform (1:1 v/v, pH 4.3) extracted several times to remove contaminating proteins. The tRNA sample was isopropanol precipitated and the pellet was resuspended in water and deacylated in 100 mM Tris-HCl (pH 9) for 20 min at 37 °C. These purifications yield tRNA that is enriched with the overexpressed *H. pylori* tRNA<sup>Gln</sup> isoacceptor but also contains total *E. coli* tRNA.

#### **A.4.4 $^{32}\text{P}$ /nuclease P1 GatCAB transamidation assays**

The 3'-end of *H. pylori* tRNA<sup>Gln</sup> was labeled with  $\alpha$ - $^{32}\text{P}$ -AMP and aminoacylated as previously described (149). The plasmid overexpressing the CCA-adding enzyme was provided by Dr. Rebecca Alexander.

The P1 nuclease transamidation assays were performed essentially as described in chapter 5, with the exception of using GatCAB (100 nM),  $^{32}\text{P}$ -labeled Glu-tRNA<sup>Gln</sup> (10  $\mu\text{M}$ ), and  $\text{NH}_4\text{Cl}$  (20 mM) instead of glutamine. The TLC was developed in running buffer (100 mM  $\text{NH}_4\text{OAc}$ , and 5% acetic acid). The plates were imaged overnight and quantified by phosphoimager.

## APPENDIX B

## COPYRIGHTED PERMISSIONS

Rathnayake, U. M.; Wood, W. N.; and Hendrickson, T. L. Indirect tRNA aminoacylation during accurate translation and phenotypic mistranslation. *Curr. Opin. Chem. Biol.* **2017**, *41*, 114-122. DOI: 10.1016/j.cbpa.2017.10.009

4/21/2019

Rightslink® by Copyright Clearance Center



RightsLink®

Home

Create Account

Help



**Title:** Indirect tRNA aminoacylation during accurate translation and phenotypic mistranslation

**Author:** Udumbara M Rathnayake, Whitney N Wood, Tamara L Hendrickson

**Publication:** Current Opinion in Chemical Biology

**Publisher:** Elsevier

**Date:** December 2017

© 2017 Elsevier Ltd. All rights reserved.

## LOGIN

If you're a **copyright.com user**, you can login to RightsLink using your copyright.com credentials. Already a **RightsLink user** or want to [learn more?](#)

Please note that, as the author of this Elsevier article, you retain the right to include it in a thesis or dissertation, provided it is not published commercially. Permission is not required, but please ensure that you reference the journal as the original source. For more information on this and on your other retained rights, please visit: <https://www.elsevier.com/about/our-business/policies/copyright#Author-rights>

BACK

CLOSE WINDOW

Copyright © 2019 [Copyright Clearance Center, Inc.](#) All Rights Reserved. [Privacy statement](#). [Terms and Conditions](#). Comments? We would like to hear from you. E-mail us at [customer@copyright.com](mailto:customer@copyright.com)

Rathnayake, U. M.; and Hendrickson, T. L. Bacterial Aspartyl-tRNA Synthetase Has Glutamyl-tRNA Synthetase Activity. *Genes* **2019**, *10*, 262. DOI: 10.3390/genes10040262.

[Log in](#)

---

## MDPI Open Access Information and Policy

All articles published by MDPI are made immediately available worldwide under an open access license. This means:

- everyone has free and unlimited access to the full-text of *all* articles published in MDPI journals;
- everyone is free to re-use the published material if proper accreditation/citation of the original publication is given;
- open access publication is supported by the authors' institutes or research funding agencies by payment of a comparatively low [Article Processing Charge \(APC\)](#) for accepted articles.

Zhao, L.; Rathnayake, U. M.; Dewage, S. W.; Wood, W. N.; Veltri, A. J.; Cisneros, G. A.; and Hendrickson, T. L. Characterization of tunnel mutants reveals a catalytic step in ammonia delivery by an aminoacyl-tRNA amidotransferase. *FEBS Lett.* **2016**, *590*, 3122-3132. DOI: 10.1002/1873-3468.12347

5/1/2019

Rightslink® by Copyright Clearance Center



RightsLink®

Home

Account  
Info

Help



WILEY

**Title:** Characterization of tunnel mutants reveals a catalytic step in ammonia delivery by an aminoacyl-tRNA amidotransferase

**Author:** Liangjun Zhao, Udumbara M. Rathnayake, Sajeewa W. Dewage, et al

**Publication:** FEBS Letters

**Publisher:** John Wiley and Sons

**Date:** Aug 23, 2016

© Federation of European Biochemical Societies

Logged in as:

Udumbara Rathnayake

Account #:

3001440252

[LOGOUT](#)

### Order Completed

Thank you for your order.

This Agreement between Mrs. Udumbara Rathnayake ("You") and John Wiley and Sons ("John Wiley and Sons") consists of your license details and the terms and conditions provided by John Wiley and Sons and Copyright Clearance Center.

Your confirmation email will contain your order number for future reference.



License Number	4580200873554
License date	May 01, 2019
Licensed Content Publisher	John Wiley and Sons
Licensed Content Publication	FEBS Letters
Licensed Content Title	Characterization of tunnel mutants reveals a catalytic step in ammonia delivery by an aminoacyl-tRNA amidotransferase
Licensed Content Author	Liangjun Zhao, Udumbara M. Rathnayake, Sajeewa W. Dewage, et al
Licensed Content Date	Aug 23, 2016
Licensed Content Volume	590
Licensed Content Issue	18
Licensed Content Pages	11
Type of use	Dissertation/Thesis
Requestor type	Author of this Wiley article
Format	Print and electronic
Portion	Full article
Will you be translating?	No
Title of your thesis / dissertation	Functional characterization of accessory proteins and novel activities in direct and indirect tRNA aminoacylation
Expected completion date	Aug 2019
Expected size (number of pages)	200
Requestor Location	Mrs. Udumbara Rathnayake 910 West Forest Avenue Apartment 10

Silva, G. N.; Fatma, S.; Floyd, A. M.; Fischer, F.; Chuawong, P.; Cruz, A. N.; Simari, R. M.; Joshi, N.; Kern, D.; and Hendrickson, T. L. A tRNA-independent mechanism for transamidosome assembly promotes aminoacyl-tRNA transamidation. *J. Biol. Chem.* **2013**, *288*, 3816-3822. DOI: 10.1074/jbc.M112.441394

#### **Parties who are not authors on the article**

##### **For noncommercial use:**

Parties other than the authors seeking to reuse JBC content for noncommercial purposes are welcome to copy, distribute, transmit and adapt the work at no cost and without permission as long as they attribute the work to the original source using the citation above. Examples of noncommercial use include:

- Reproducing a figure for educational purposes, such as schoolwork or lecture presentations.
- Appending a reprinted article to a Ph.D. dissertation.

**REFERENCES**

1. Ibba, M.; Soll, D., Quality control mechanisms during translation. *Science* **1999**, *286*, 1893-1897.
2. Ribas de Pouplana, L.; Schimmel, P., A view into the origin of life: Aminoacyl-tRNA synthetases. *Cell Mol Life Sci* **2000**, *57*, 865-870.
3. Dale, T.; Uhlenbeck, O. C., Amino acid specificity in translation. *Trends Biochem Sci* **2005**, *30*, 659-665.
4. Mohler, K.; Ibba, M., Translational fidelity and mistranslation in the cellular response to stress. *Nat Microbiol* **2017**, *2*, 17117.
5. Ellis, N.; Gallant, J., An estimate of the global error frequency in translation. *Mol Gen Genet* **1982**, *188*, 169-172.
6. Kurland, C. G., Translational accuracy and the fitness of bacteria. *Annu Rev Genet* **1992**, *26*, 29-50.
7. Jakubowski, H.; Goldman, E., Editing of errors in selection of amino acids for protein synthesis. *Microbiol Rev* **1992**, *56*, 412-429.
8. Ravel, J. M.; Wang, S. F.; Heinemeyer, C.; Shive, W., Glutamyl and glutaminyl ribonucleic acid synthetases of *Escherichia coli* W. Separation, properties, and stimulation of adenosine triphosphate-pyrophosphate exchange by acceptor ribonucleic acid. *J Biol Chem* **1965**, *240*, 432-438.
9. Lee, L. W.; Ravel, J. M.; Shive, W., A general involvement of acceptor ribonucleic acid in the initial activation step of glutamic acid and glutamine. *Arch Biochem Biophys* **1967**, *121*, 614-618.

10. Mehler, A. H.; Mitra, S. K., The activation of arginyl transfer ribonucleic acid synthetase by transfer ribonucleic acid. *J Biol Chem* **1967**, *242*, 5495-5499.
11. Giege, R.; Springer, M., Aminoacyl-tRNA synthetases in the bacterial world. *EcoSal Plus* **2016**, *7*.
12. Ribas de Pouplana, L.; Schimmel, P., Two classes of tRNA synthetases suggested by sterically compatible dockings on tRNA acceptor stem. *Cell* **2001**, *104*, 191-193.
13. Arnez, J. G.; Moras, D., Structural and functional considerations of the aminoacylation reaction. *Trends Biochem Sci* **1997**, *22*, 211-216.
14. Eriani, G.; Delarue, M.; Poch, O.; Gangloff, J.; Moras, D., Partition of tRNA synthetases into two classes based on mutually exclusive sets of sequence motifs. *Nature* **1990**, *347*, 203-206.
15. Ibba, M.; Soll, D., Aminoacyl-tRNA synthesis. *Annu Rev Biochem* **2000**, *69*, 617-650.
16. Woese, C. R.; Olsen, G. J.; Ibba, M.; Soll, D., Aminoacyl-tRNA synthetases, the genetic code, and the evolutionary process. *Microbiol Mol Biol Rev* **2000**, *64*, 202-236.
17. Norris, A. T.; Berg, P., Mechanism of aminoacyl RNA synthesis: Studies with isolated aminoacyl adenylate complexes of isoleucyl RNA synthetase. *Proc Natl Acad Sci U S A* **1964**, *52*, 330-337.
18. Baldwin, A. N.; Berg, P., Transfer ribonucleic acid-induced hydrolysis of valyladenylate bound to isoleucyl ribonucleic acid synthetase. *J Biol Chem* **1966**, *241*, 839-845.

19. Fersht, A. R., Editing mechanisms in protein synthesis. Rejection of valine by the isoleucyl-tRNA synthetase. *Biochemistry* **1977**, *16*, 1025-1030.
20. Ling, J.; Reynolds, N.; Ibba, M., Aminoacyl-tRNA synthesis and translational quality control. *Annu Rev Microbiol* **2009**, *63*, 61-78.
21. Cvetesic, N.; Perona, J. J.; Gruic-Sovulj, I., Kinetic partitioning between synthetic and editing pathways in class I aminoacyl-tRNA synthetases occurs at both pre-transfer and post-transfer hydrolytic steps. *J Biol Chem* **2012**, *287*, 25381-25394.
22. Dock-Bregeon, A. C.; Rees, B.; Torres-Larios, A.; Bey, G.; Caillet, J.; Moras, D., Achieving error-free translation; the mechanism of proofreading of threonyl-tRNA synthetase at atomic resolution. *Mol Cell* **2004**, *16*, 375-386.
23. Silvian, L. F.; Wang, J.; Steitz, T. A., Insights into editing from an Ile-tRNA synthetase structure with tRNA<sup>Ile</sup> and mupirocin. *Science* **1999**, *285*, 1074-1077.
24. Fukai, S.; Nureki, O.; Sekine, S.; Shimada, A.; Tao, J.; Vassylyev, D. G.; Yokoyama, S., Structural basis for double-sieve discrimination of L-valine from L-isoleucine and L-threonine by the complex of tRNA(val) and valyl-tRNA synthetase. *Cell* **2000**, *103*, 793-803.
25. Giege, R.; Sissler, M.; Florentz, C., Universal rules and idiosyncratic features in tRNA identity. *Nucleic Acids Res* **1998**, *26*, 5017-5035.
26. Cantara, W. A.; Crain, P. F.; Rozenski, J.; McCloskey, J. A.; Harris, K. A.; Zhang, X.; Vendeix, F. A.; Fabris, D.; Agris, P. F., The RNA modification database, RNAMDB: 2011 update. *Nucleic Acids Res* **2011**, *39*, D195-201.

27. Gregory, S. T.; Dahlberg, A. E., Effects of mutations at position 36 of tRNA(Glu) on missense and nonsense suppression in *Escherichia coli*. *FEBS Lett* **1995**, *361*, 25-28.
28. Goffeau, A.; Barrell, B. G.; Bussey, H.; Davis, R. W.; Dujon, B.; Feldmann, H.; Galibert, F.; Hoheisel, J. D.; Jacq, C.; Johnston, M.; Louis, E. J.; Mewes, H. W.; Murakami, Y.; Philippsen, P.; Tettelin, H.; Oliver, S. G., Life with 6000 genes. *Science* **1996**, *274*, 546, 563-547.
29. Venter, J. C.; Adams, M. D.; Myers, E. W.; Li, P. W.; Mural, R. J.; Sutton, G. G.; Smith, H. O.; Yandell, M.; Evans, C. A.; Holt, R. A.; Gocayne, J. D.; Amanatides, P.; Ballew, R. M.; Huson, D. H.; Wortman, J. R.; Zhang, Q.; Kodira, C. D.; Zheng, X. H.; Chen, L.; Skupski, M.; Subramanian, G.; Thomas, P. D.; Zhang, J.; Gabor Miklos, G. L.; Nelson, C.; Broder, S.; Clark, A. G.; Nadeau, J.; McKusick, V. A.; Zinder, N.; Levine, A. J.; Roberts, R. J.; Simon, M.; Slayman, C.; Hunkapiller, M.; Bolanos, R.; Delcher, A.; Dew, I.; Fasulo, D.; Flanigan, M.; Florea, L.; Halpern, A.; Hannenhalli, S.; Kravitz, S.; Levy, S.; Mobarry, C.; Reinert, K.; Remington, K.; Abu-Threideh, J.; Beasley, E.; Biddick, K.; Bonazzi, V.; Brandon, R.; Cargill, M.; Chandramouliswaran, I.; Charlab, R.; Chaturvedi, K.; Deng, Z.; Di Francesco, V.; Dunn, P.; Eilbeck, K.; Evangelista, C.; Gabrielian, A. E.; Gan, W.; Ge, W.; Gong, F.; Gu, Z.; Guan, P.; Heiman, T. J.; Higgins, M. E.; Ji, R. R.; Ke, Z.; Ketchum, K. A.; Lai, Z.; Lei, Y.; Li, Z.; Li, J.; Liang, Y.; Lin, X.; Lu, F.; Merkulov, G. V.; Milshina, N.; Moore, H. M.; Naik, A. K.; Narayan, V. A.; Neelam, B.; Nusskern, D.; Rusch, D. B.; Salzberg, S.; Shao, W.; Shue, B.; Sun, J.; Wang, Z.; Wang, A.; Wang, X.; Wang, J.; Wei, M.; Wides, R.; Xiao, C.; Yan, C.; Yao, A.; Ye, J.; Zhan, M.; Zhang,

W.; Zhang, H.; Zhao, Q.; Zheng, L.; Zhong, F.; Zhong, W.; Zhu, S.; Zhao, S.; Gilbert, D.; Baumhueter, S.; Spier, G.; Carter, C.; Cravchik, A.; Woodage, T.; Ali, F.; An, H.; Awe, A.; Baldwin, D.; Baden, H.; Barnstead, M.; Barrow, I.; Beeson, K.; Busam, D.; Carver, A.; Center, A.; Cheng, M. L.; Curry, L.; Danaher, S.; Davenport, L.; Desilets, R.; Dietz, S.; Dodson, K.; Doup, L.; Ferriera, S.; Garg, N.; Gluecksmann, A.; Hart, B.; Haynes, J.; Haynes, C.; Heiner, C.; Hladun, S.; Hostin, D.; Houck, J.; Howland, T.; Ibegwam, C.; Johnson, J.; Kalush, F.; Kline, L.; Koduru, S.; Love, A.; Mann, F.; May, D.; McCawley, S.; McIntosh, T.; McMullen, I.; Moy, M.; Moy, L.; Murphy, B.; Nelson, K.; Pfannkoch, C.; Pratts, E.; Puri, V.; Qureshi, H.; Reardon, M.; Rodriguez, R.; Rogers, Y. H.; Romblad, D.; Ruhfel, B.; Scott, R.; Sitter, C.; Smallwood, M.; Stewart, E.; Strong, R.; Suh, E.; Thomas, R.; Tint, N. N.; Tse, S.; Vech, C.; Wang, G.; Wetter, J.; Williams, S.; Williams, M.; Windsor, S.; Winn-Deen, E.; Wolfe, K.; Zaveri, J.; Zaveri, K.; Abril, J. F.; Guigo, R.; Campbell, M. J.; Sjolander, K. V.; Karlak, B.; Kejariwal, A.; Mi, H.; Lazareva, B.; Hatton, T.; Narechania, A.; Diemer, K.; Muruganujan, A.; Guo, N.; Sato, S.; Bafna, V.; Istrail, S.; Lippert, R.; Schwartz, R.; Walenz, B.; Yooseph, S.; Allen, D.; Basu, A.; Baxendale, J.; Blick, L.; Caminha, M.; Carnes-Stine, J.; Caulk, P.; Chiang, Y. H.; Coyne, M.; Dahlke, C.; Mays, A.; Dombroski, M.; Donnelly, M.; Ely, D.; Esparham, S.; Fosler, C.; Gire, H.; Glanowski, S.; Glasser, K.; Glodek, A.; Gorokhov, M.; Graham, K.; Gropman, B.; Harris, M.; Heil, J.; Henderson, S.; Hoover, J.; Jennings, D.; Jordan, C.; Jordan, J.; Kasha, J.; Kagan, L.; Kraft, C.; Levitsky, A.; Lewis, M.; Liu, X.; Lopez, J.; Ma, D.; Majoros, W.; McDaniel, J.; Murphy, S.; Newman, M.; Nguyen, T.; Nguyen, N.; Nodell, M.; Pan, S.; Peck, J.; Peterson, M.; Rowe, W.;

- Sanders, R.; Scott, J.; Simpson, M.; Smith, T.; Sprague, A.; Stockwell, T.; Turner, R.; Venter, E.; Wang, M.; Wen, M.; Wu, D.; Wu, M.; Xia, A.; Zandieh, A.; Zhu, X., The sequence of the human genome. *Science* **2001**, *291*, 1304-1351.
30. Blattner, F. R.; Plunkett, G., 3rd; Bloch, C. A.; Perna, N. T.; Burland, V.; Riley, M.; Collado-Vides, J.; Glasner, J. D.; Rode, C. K.; Mayhew, G. F.; Gregor, J.; Davis, N. W.; Kirkpatrick, H. A.; Goeden, M. A.; Rose, D. J.; Mau, B.; Shao, Y., The complete genome sequence of *Escherichia coli* K-12. *Science* **1997**, *277*, 1453-1462.
31. Ibba, M.; Soll, D., Aminoacyl-tRNAs: Setting the limits of the genetic code. *Genes Dev* **2004**, *18*, 731-738.
32. Tumbula, D.; Vothknecht, U. C.; Kim, H. S.; Ibba, M.; Min, B.; Li, T.; Pelaschier, J.; Stathopoulos, C.; Becker, H.; Soll, D., Archaeal aminoacyl-tRNA synthesis: Diversity replaces dogma. *Genetics* **1999**, *152*, 1269-1276.
33. Schon, A.; Kannangara, C. G.; Gough, S.; Soll, D., Protein biosynthesis in organelles requires misaminoacylation of tRNA. *Nature* **1988**, *331*, 187-190.
34. Cathopoulis, T.; Chuawong, P.; Hendrickson, T. L., Novel tRNA aminoacylation mechanisms. *Mol BioSyst* **2007**, *3*, 408-418.
35. Becker, H. D.; Kern, D., *Thermus thermophilus*: A link in evolution of the tRNA-dependent amino acid amidation pathways. *Proc Natl Acad Sci U S A* **1998**, *95*, 12832-12837.
36. Curnow, A. W.; Hong, K.; Yuan, R.; Kim, S.; Martins, O.; Winkler, W.; Henkin, T. M.; Soll, D., Glu-tRNA<sup>Gln</sup> amidotransferase: A novel heterotrimeric enzyme



- required for correct decoding of glutamine codons during translation. *Proc Natl Acad Sci U S A* **1997**, *94*, 11819-11826.
37. Rathnayake, U. M.; Wood, W. N.; Hendrickson, T. L., Indirect tRNA aminoacylation during accurate translation and phenotypic mistranslation. *Curr Opin Chem Biol* **2017**, *41*, 114-122.
38. Tumbula, D. L.; Becker, H. D.; Chang, W. Z.; Soll, D., Domain-specific recruitment of amide amino acids for protein synthesis. *Nature* **2000**, *407*, 106-110.
39. Sauerwald, A.; Zhu, W.; Major, T. A.; Roy, H.; Palioura, S.; Jahn, D.; Whitman, W. B.; Yates, J. R., 3rd; Ibba, M.; Soll, D., RNA-dependent cysteine biosynthesis in archaea. *Science* **2005**, *307*, 1969-1972.
40. Wilcox, M.; Nirenberg, M., Transfer RNA as a cofactor coupling amino acid synthesis with that of protein. *Proc Natl Acad Sci U S A* **1968**, *61*, 229-236.
41. Salazar, J. C.; Ahel, I.; Orellana, O.; Tumbula-Hansen, D.; Krieger, R.; Daniels, L.; Soll, D., Coevolution of an aminoacyl-tRNA synthetase with its tRNA substrates. *Proc Natl Acad Sci U S A* **2003**, *100*, 13863-13868.
42. Skouloubris, S.; Ribas de Pouplana, L.; De Reuse, H.; Hendrickson, T. L., A noncognate aminoacyl-tRNA synthetase that may resolve a missing link in protein evolution. *Proc Natl Acad Sci U S A* **2003**, *100*, 11297-11302.
43. Curnow, A. W.; Ibba, M.; Soll, D., tRNA-dependent asparagine formation. *Nature* **1996**, *382*, 589-590.
44. Sheppard, K.; Akochy, P. M.; Salazar, J. C.; Soll, D., The *Helicobacter pylori* amidotransferase GatCAB is equally efficient in glutamine-dependent

- transamidation of Asp-tRNA<sup>Asn</sup> and Glu-tRNA<sup>Gln</sup>. *The Journal of biological chemistry* **2007**, *282*, 11866-11873.
45. Min, B.; Pelaschier, J. T.; Graham, D. E.; Tumbula-Hansen, D.; Soll, D., Transfer RNA-dependent amino acid biosynthesis: An essential route to asparagine formation. *Proc Natl Acad Sci U S A* **2002**, *99*, 2678-2683.
46. Tomb, J. F.; White, O.; Kerlavage, A. R.; Clayton, R. A.; Sutton, G. G.; Fleischmann, R. D.; Ketchum, K. A.; Klenk, H. P.; Gill, S.; Dougherty, B. A.; Nelson, K.; Quackenbush, J.; Zhou, L.; Kirkness, E. F.; Peterson, S.; Loftus, B.; Richardson, D.; Dodson, R.; Khalak, H. G.; Glodek, A.; McKenney, K.; Fitzgerald, L. M.; Lee, N.; Adams, M. D.; Hickey, E. K.; Berg, D. E.; Gocayne, J. D.; Utterback, T. R.; Peterson, J. D.; Kelley, J. M.; Cotton, M. D.; Weidman, J. M.; Fujii, C.; Bowman, C.; Watthey, L.; Wallin, E.; Hayes, W. S.; Borodovsky, M.; Karp, P. D.; Smith, H. O.; Fraser, C. M.; Venter, J. C., The complete genome sequence of the gastric pathogen *Helicobacter pylori*. *Nature* **1997**, *388*, 539-547.
47. Mohan, A.; Padiadpu, J.; Baloni, P.; Chandra, N., Complete genome sequences of a *Mycobacterium smegmatis* laboratory strain (MC<sup>2</sup> 155) and isoniazid-resistant (4XR1/R2) mutant strains. *Genome Announc* **2015**, *3*.
48. Kuroda, M.; Ohta, T.; Uchiyama, I.; Baba, T.; Yuzawa, H.; Kobayashi, I.; Cui, L.; Oguchi, A.; Aoki, K.; Nagai, Y.; Lian, J.; Ito, T.; Kanamori, M.; Matsumaru, H.; Maruyama, A.; Murakami, H.; Hosoyama, A.; Mizutani-Ui, Y.; Takahashi, N. K.; Sawano, T.; Inoue, R.; Kaito, C.; Sekimizu, K.; Hirakawa, H.; Kuhara, S.; Goto, S.; Yabuzaki, J.; Kanehisa, M.; Yamashita, A.; Oshima, K.; Furuya, K.; Yoshino, C.; Shiba, T.; Hattori, M.; Ogasawara, N.; Hayashi, H.; Hiramatsu, K., Whole genome

- sequencing of methicillin-resistant *Staphylococcus aureus*. *Lancet* **2001**, *357*, 1225-1240.
49. Chuawong, P.; Hendrickson, T. L., The nondiscriminating aspartyl-tRNA synthetase from helicobacter pylori: Anticodon-binding domain mutations that impact tRNA specificity and heterologous toxicity. *Biochemistry* **2006**, *45*, 8079-8087.
50. Javid, B.; Sorrentino, F.; Toosky, M.; Zheng, W.; Pinkham, J. T.; Jain, N.; Pan, M.; Deighan, P.; Rubin, E. J., Mycobacterial mistranslation is necessary and sufficient for rifampicin phenotypic resistance. *Proc Natl Acad Sci U S A* **2014**, *111*, 1132-1137.
51. Mladenova, S. R.; Stein, K. R.; Bartlett, L.; Sheppard, K., Relaxed tRNA specificity of the *Staphylococcus aureus* aspartyl-tRNA synthetase enables RNA-dependent asparagine biosynthesis. *FEBS Lett* **2014**, *588*, 1808-1812.
52. Rathnayake, U. M.; Hendrickson, T. L., Bacterial aspartyl-tRNA synthetase has glutamyl-tRNA synthetase activity. *Genes (Basel)* **2019**, *10*.
53. Min, B.; Kitabatake, M.; Polycarpo, C.; Pelaschier, J.; Raczniak, G.; Ruan, B.; Kobayashi, H.; Namgoong, S.; Soll, D., Protein synthesis in *Escherichia coli* with mischarged tRNA. *J Bacteriol* **2003**, *185*, 3524-3526.
54. Becker, H. D.; Reinbolt, J.; Kreutzer, R.; Giege, R.; Kern, D., Existence of two distinct aspartyl-tRNA synthetases in *Thermus thermophilus*. Structural and biochemical properties of the two enzymes. *Biochemistry* **1997**, *36*, 8785-8797.
55. Saad, N. Y.; Schiel, B.; Braye, M.; Heap, J. T.; Minton, N. P.; Durre, P.; Becker, H. D., Riboswitch (t-box)-mediated control of tRNA-dependent amidation in

- Clostridium acetobutylicum* rationalizes gene and pathway redundancy for asparagine and asparaginyl-tRNA<sup>Asn</sup> synthesis. *J Biol Chem* **2012**, *287*, 20382-20394.
56. Nair, N.; Raff, H.; Islam, M. T.; Feen, M.; Garofalo, D. M.; Sheppard, K., The *Bacillus subtilis* and *Bacillus halodurans* aspartyl-tRNA synthetases retain recognition of tRNA(Asn). *J Mol Biol* **2016**, *428*, 618-630.
57. Kim, S. I.; Nalaskowska, M.; Germond, J. E.; Pridmore, D.; Soll, D., Asn-tRNA in *Lactobacillus bulgaricus* is formed by asparaginylation of tRNA and not by transamidation of Asp-tRNA. *Nucleic Acids Res* **1996**, *24*, 2648-2651.
58. Alperstein, A.; Ulrich, B.; Garofalo, D. M.; Dreisbach, R.; Raff, H.; Sheppard, K., The predatory bacterium *Bdellovibrio bacteriovorus* aspartyl-tRNA synthetase recognizes tRNA<sup>Asn</sup> as a substrate. *PLoS One* **2014**, *9*, e110842.
59. Akochy, P. M.; Bernard, D.; Roy, P. H.; Lapointe, J., Direct glutaminyl-tRNA biosynthesis and indirect asparaginyl-tRNA biosynthesis in *Pseudomonas aeruginosa* PAO1. *J Bacteriol* **2004**, *186*, 767-776.
60. Nakamura, A.; Yao, M.; Chimnaronk, S.; Sakai, N.; Tanaka, I., Ammonia channel couples glutaminase with transamidase reactions in GatCAB. *Science* **2006**, *312*, 1954-1958.
61. Sheppard, K.; Soll, D., On the evolution of the tRNA-dependent amidotransferases, GatCAB and GatDE. *J Mol Biol* **2008**, *377*, 831-844.
62. Oshikane, H.; Sheppard, K.; Fukai, S.; Nakamura, Y.; Ishitani, R.; Numata, T.; Sherrer, R. L.; Feng, L.; Schmitt, E.; Panvert, M.; Blanquet, S.; Mechulam, Y.; Soll,

- D.; Nureki, O., Structural basis of RNA-dependent recruitment of glutamine to the genetic code. *Science* **2006**, *312*, 1950-1954.
63. Wilcox, M., Gamma-glutamyl phosphate attached to glutamine-specific tRNA. A precursor of glutaminyl-tRNA in *Bacillus subtilis*. *Eur J Biochem* **1969**, *11*, 405-412.
64. Wilcox, M., Gamma-phosphoryl ester of Glu-tRNA<sup>Gln</sup> as an intermediate in *Bacillus subtilis* glutaminyl-tRNA synthesis. *Cold Spring Harb Symp Quant Biol* **1969**, *34*, 521-528.
65. Thoden, J. B.; Holden, H. M.; Wesenberg, G.; Raushel, F. M.; Rayment, I., Structure of carbamoyl phosphate synthetase: A journey of 96 Å from substrate to product. *Biochemistry* **1997**, *36*, 6305-6316.
66. Chaudhuri, B. N.; Lange, S. C.; Myers, R. S.; Chittur, S. V.; Davisson, V. J.; Smith, J. L., Crystal structure of imidazole glycerol phosphate synthase: A tunnel through a (beta/alpha) 8 barrel joins two active sites. *Structure* **2001**, *9*, 987-997.
67. Larsen, T. M.; Boehlein, S. K.; Schuster, S. M.; Richards, N. G.; Thoden, J. B.; Holden, H. M.; Rayment, I., Three-dimensional structure of *Escherichia coli* asparagine synthetase B: A short journey from substrate to product. *Biochemistry* **1999**, *38*, 16146-16157.
68. Muchmore, C. R.; Krahn, J. M.; Kim, J. H.; Zalkin, H.; Smith, J. L., Crystal structure of glutamine phosphoribosylpyrophosphate amidotransferase from *Escherichia coli*. *Protein Sci* **1998**, *7*, 39-51.
69. Weeks, A.; Lund, L.; Raushel, F. M., Tunneling of intermediates in enzyme-catalyzed reactions. *Curr Opin Chem Biol* **2006**, *10*, 465-472.

70. Kang, J.; Kuroyanagi, S.; Akisada, T.; Hagiwara, Y.; Tateno, M., Unidirectional mechanistic valved mechanisms for ammonia transport in GatCAB. *J Chem Theory Comput* **2012**, *8*, 649-660.
71. Zhao, L.; Dewage, S. W.; Bell, M. J.; Chang, K. M.; Fatma, S.; Joshi, N.; Silva, G.; Cisneros, G. A.; Hendrickson, T. L., The kinase activity of the *Helicobacter pylori* Asp-tRNA(Asn)/Glu-tRNA(Gln) amidotransferase is sensitive to distal mutations in its putative ammonia tunnel. *Biochemistry* **2012**, *51*, 273-285.
72. Dewage, S. W.; Cisneros, G. A., Computational analysis of ammonia transfer along two intramolecular tunnels in *Staphylococcus aureus* glutamine-dependent amidotransferase (GatCAB). *J Phys Chem B* **2015**, *119*, 3669-3677.
73. Zhao, L.; Rathnayake, U. M.; Dewage, S. W.; Wood, W. N.; Veltri, A. J.; Cisneros, G. A.; Hendrickson, T. L., Characterization of tunnel mutants reveals a catalytic step in ammonia delivery by an aminoacyl-tRNA amidotransferase. *FEBS Lett* **2016**, *590*, 3122-3132.
74. Cathopoulis, T. J.; Chuawong, P.; Hendrickson, T. L., Conserved discrimination against misacylated tRNAs by two mesophilic elongation factor tu orthologs. *Biochemistry* **2008**, *47*, 7610-7616.
75. Nunez, H.; Lefimil, C.; Min, B.; Soll, D.; Orellana, O., *In vivo* formation of glutamyl-tRNA(Gln) in *Escherichia coli* by heterologous glutamyl-tRNA synthetases. *FEBS Lett* **2004**, *557*, 133-135.
76. Su, H. W.; Zhu, J. H.; Li, H.; Cai, R. J.; Ealand, C.; Wang, X.; Chen, Y. X.; Kayani, M. U.; Zhu, T. F.; Moradigaravand, D.; Huang, H.; Kana, B. D.; Javid, B., The

- essential mycobacterial amidotransferase gatcab is a modulator of specific translational fidelity. *Nat Microbiol* **2016**, *1*, 16147.
77. Bailly, M.; Blaise, M.; Lorber, B.; Becker, H. D.; Kern, D., The transamidosome: A dynamic ribonucleoprotein particle dedicated to prokaryotic tRNA-dependent asparagine biosynthesis. *Mol Cell* **2007**, *28*, 228-239.
78. Suzuki, T.; Nakamura, A.; Kato, K.; Soll, D.; Tanaka, I.; Sheppard, K.; Yao, M., Structure of the *Pseudomonas aeruginosa* transamidosome reveals unique aspects of bacterial tRNA-dependent asparagine biosynthesis. *Proc Natl Acad Sci U S A* **2015**, *112*, 382-387.
79. Silva, G. N.; Fatma, S.; Floyd, A. M.; Fischer, F.; Chuawong, P.; Cruz, A. N.; Simari, R. M.; Joshi, N.; Kern, D.; Hendrickson, T. L., A tRNA-independent mechanism for transamidosome assembly promotes aminoacyl-tRNA transamidation. *The Journal of biological chemistry* **2013**, *288*, 3816-3822.
80. Huot, J. L.; Fischer, F.; Corbeil, J.; Madore, E.; Lorber, B.; Diss, G.; Hendrickson, T. L.; Kern, D.; Lapointe, J., Gln-tRNA<sup>Gln</sup> synthesis in a dynamic transamidosome from *Helicobacter pylori*, where GluRS2 hydrolyzes excess Glu-tRNA<sup>Gln</sup>. *Nucleic Acids Res* **2011**, *39*, 9306-9315.
81. Ito, T.; Yokoyama, S., Two enzymes bound to one transfer RNA assume alternative conformations for consecutive reactions. *Nature* **2010**, *467*, 612-616.
82. Blaise, M.; Bailly, M.; Frechin, M.; Behrens, M. A.; Fischer, F.; Oliveira, C. L.; Becker, H. D.; Pedersen, J. S.; Thirup, S.; Kern, D., Crystal structure of a transfer-ribonucleoprotein particle that promotes asparagine formation. *EMBO J* **2010**, *29*, 3118-3129.

83. Fischer, F.; Huot, J. L.; Lorber, B.; Diss, G.; Hendrickson, T. L.; Becker, H. D.; Lapointe, J.; Kern, D., The asparagine-transamidosome from *Helicobacter pylori*: A dual-kinetic mode in non-discriminating aspartyl-tRNA synthetase safeguards the genetic code. *Nucleic Acids Res* **2012**, *40*, 4965-4976.
84. Ribas de Pouplana, L.; Santos, M. A.; Zhu, J. H.; Farabaugh, P. J.; Javid, B., Protein mistranslation: Friend or foe? *Trends Biochem Sci* **2014**, *39*, 355-362.
85. Hoffman, K. S.; O'Donoghue, P.; Brandl, C. J., Mistranslation: From adaptations to applications. *Biochim Biophys Acta Gen Subj* **2017**, *1861*, 3070-3080.
86. Rain, J. C.; Selig, L.; De Reuse, H.; Battaglia, V.; Reverdy, C.; Simon, S.; Lenzen, G.; Petel, F.; Wojcik, J.; Schachter, V.; Chemama, Y.; Labigne, A.; Legrain, P., The protein-protein interaction map of *Helicobacter pylori*. *Nature* **2001**, *409*, 211-215.
87. Silva, G. N. Assembly and function of macromolecular complex for accurate tRNA aminoacylation in *Helicobacter pylori*. Ph.D. Dissertation, Wayne State University Detroit, MI, 2014.
88. Marchler-Bauer, A.; Lu, S.; Anderson, J. B.; Chitsaz, F.; Derbyshire, M. K.; DeWeese-Scott, C.; Fong, J. H.; Geer, L. Y.; Geer, R. C.; Gonzales, N. R.; Gwadz, M.; Hurwitz, D. I.; Jackson, J. D.; Ke, Z.; Lanczycki, C. J.; Lu, F.; Marchler, G. H.; Mullokandov, M.; Omelchenko, M. V.; Robertson, C. L.; Song, J. S.; Thanki, N.; Yamashita, R. A.; Zhang, D.; Zhang, N.; Zheng, C.; Bryant, S. H., CDD: A conserved domain database for the functional annotation of proteins. *Nucleic Acids Res* **2011**, *39*, D225-229.
89. Rohl, C. A.; Strauss, C. E.; Misura, K. M.; Baker, D., Protein structure prediction using Rosetta. *Methods Enzymol* **2004**, *383*, 66-93.



90. Goto, M.; Nakajima, Y.; Hirotsu, K., Crystal structure of argininosuccinate synthetase from *Thermus thermophilus* HB8. Structural basis for the catalytic action. *J Biol Chem* **2002**, *277*, 15890-15896.
91. Lemke, C. T.; Howell, P. L., The 1.6 Å crystal structure of *E. coli* argininosuccinate synthetase suggests a conformational change during catalysis. *Structure* **2001**, *9*, 1153-1164.
92. Saraste, M.; Sibbald, P. R.; Wittinghofer, A., The P-loop-a common motif in ATP- and GTP-binding proteins. *Trends Biochem Sci* **1990**, *15*, 430-434.
93. Leipe, D. D.; Koonin, E. V.; Aravind, L., Evolution and classification of P-loop kinases and related proteins. *J Mol Biol* **2003**, *333*, 781-815.
94. Vinayak, M.; Pathak, C., Queuosine modification of tRNA: Its divergent role in cellular machinery. *Biosci Rep* **2009**, *30*, 135-148.
95. Harada, F.; Nishimura, S., Possible anticodon sequences of tRNA<sup>His</sup>, tRNA<sup>Asm</sup>, and tRNA<sup>Asp</sup> from *Escherichia coli* B. Universal presence of nucleoside Q in the first position of the anticodons of these transfer ribonucleic acids. *Biochemistry* **1972**, *11*, 301-308.
96. Morris, R. C.; Elliott, M. S., Queuosine modification of tRNA: A case for convergent evolution. *Mol Genet Metab* **2001**, *74*, 147-159.
97. McCarty, R. M.; Somogyi, A.; Lin, G.; Jacobsen, N. E.; Bandarian, V., The deazapurine biosynthetic pathway revealed: *In vitro* enzymatic synthesis of preQ(0) from guanosine 5'-triphosphate in four steps. *Biochemistry* **2009**, *48*, 3847-3852.

98. Reader, J. S.; Metzgar, D.; Schimmel, P.; de Crecy-Lagard, V., Identification of four genes necessary for biosynthesis of the modified nucleoside queuosine. *J Biol Chem* **2004**, *279*, 6280-6285.
99. Zallot, R.; Ross, R.; Chen, W. H.; Bruner, S. D.; Limbach, P. A.; de Crecy-Lagard, V., Identification of a novel epoxyqueuosine reductase family by comparative genomics. *ACS Chem Biol* **2017**, *12*, 844-851.
100. Lapointe, J.; Duplain, L.; Proulx, M., A single glutamyl-tRNA synthetase aminoacylates tRNA<sup>Glu</sup> and tRNA<sup>Gln</sup> in *Bacillus subtilis* and efficiently misacylates *Escherichia coli* tRNA<sup>Gln1</sup> *in vitro*. *J Bacteriol* **1986**, *165*, 88-93.
101. Suzuki, T.; Yamashita, K.; Tanaka, Y.; Tanaka, I.; Yao, M., Crystallization and preliminary x-ray crystallographic analysis of a bacterial Asn-transamidosome. *Acta Crystallogr F Struct Biol Commun* **2014**, *70*, 790-793.
102. Bailly, M.; Blaise, M.; Lorber, B.; Thirup, S.; Kern, D., Isolation, crystallization and preliminary x-ray analysis of the transamidosome, a ribonucleoprotein involved in asparagine formation. *Acta Crystallogr Sect F Struct Biol Cryst Commun* **2009**, *65*, 577-581.
103. Bezerra, A. R.; Simoes, J.; Lee, W.; Rung, J.; Weil, T.; Gut, I. G.; Gut, M.; Bayes, M.; Rizzetto, L.; Cavalieri, D.; Giovannini, G.; Bozza, S.; Romani, L.; Kapushesky, M.; Moura, G. R.; Santos, M. A., Reversion of a fungal genetic code alteration links proteome instability with genomic and phenotypic diversification. *Proc Natl Acad Sci U S A* **2013**, *110*, 11079-11084.
104. Bullwinkle, T. J.; Ibba, M., Translation quality control is critical for bacterial responses to amino acid stress. *Proc Natl Acad Sci U S A* **2016**, *113*, 2252-2257.

105. Fan, Y.; Wu, J.; Ung, M. H.; De Lay, N.; Cheng, C.; Ling, J., Protein mistranslation protects bacteria against oxidative stress. *Nucleic Acids Res* **2015**, *43*, 1740-1748.
106. Lee, J. Y.; Kim, D. G.; Kim, B. G.; Yang, W. S.; Hong, J.; Kang, T.; Oh, Y. S.; Kim, K. R.; Han, B. W.; Hwang, B. J.; Kang, B. S.; Kang, M. S.; Kim, M. H.; Kwon, N. H.; Kim, S., Promiscuous methionyl-tRNA synthetase mediates adaptive mistranslation to protect cells against oxidative stress. *J Cell Sci* **2014**, *127*, 4234-4245.
107. Ling, J.; Soll, D., Severe oxidative stress induces protein mistranslation through impairment of an aminoacyl-tRNA synthetase editing site. *Proc Natl Acad Sci U S A* **2010**, *107*, 4028-4033.
108. Schwartz, M. H.; Pan, T., Temperature dependent mistranslation in a hyperthermophile adapts proteins to lower temperatures. *Nucleic Acids Res* **2016**, *44*, 294-303.
109. Banerjee, A.; Adolph, R. S.; Gopalakrishnapai, J.; Kleinboelting, S.; Emmerich, C.; Steegborn, C.; Visweswariah, S. S., A universal stress protein (USP) in mycobacteria binds cAMP. *J Biol Chem* **2015**, *290*, 12731-12743.
110. Drumm, J. E.; Mi, K.; Bilder, P.; Sun, M.; Lim, J.; Bielefeldt-Ohmann, H.; Basaraba, R.; So, M.; Zhu, G.; Tufariello, J. M.; Izzo, A. A.; Orme, I. M.; Almo, S. C.; Leyh, T. S.; Chan, J., *Mycobacterium tuberculosis* universal stress protein Rv2623 regulates bacillary growth by ATP-binding: Requirement for establishing chronic persistent infection. *PLoS Pathog* **2009**, *5*, e1000460.
111. Trivedi, A.; Singh, N.; Bhat, S. A.; Gupta, P.; Kumar, A., Redox biology of tuberculosis pathogenesis. *Adv Microb Physiol* **2012**, *60*, 263-324.

112. Nalawansha, D. A.; Pflum, M. K., LSD1 substrate binding and gene expression are affected by HDAC1-mediated deacetylation. *ACS Chem Biol* **2017**, *12*, 254-264.
113. Schimmel, P.; Giege, R.; Moras, D.; Yokoyama, S., An operational RNA code for amino acids and possible relationship to genetic code. *Proc Natl Acad Sci U S A* **1993**, *90*, 8763-8768.
114. Schimmel, P.; Ribas de Pouplana, L., Transfer RNA: from minihelix to genetic code. *Cell* **1995**, *81*, 983-986.
115. Kubyshkin, V.; Acevedo-Rocha, C. G.; Budisa, N., On universal coding events in protein biogenesis. *Biosystems* **2018**, *164*, 16-25.
116. Reynolds, N. M.; Lazazzera, B. A.; Ibba, M., Cellular mechanisms that control mistranslation. *Nat Rev Microbiol.* **2010**, *8*, 849-856.
117. Wiltrout, E.; Goodenbour, J. M.; Frechin, M.; Pan, T., Misacylation of tRNA with methionine in *Saccharomyces cerevisiae*. *Nucleic Acids Res* **2012**, *40*, 10494-10506.
118. Schwartz, M. H.; Pan, T., Determining the fidelity of tRNA aminoacylation via microarrays. *Methods* **2017**, *113*, 27-33.
119. Javid, B.; Sorrentino, F.; Toosky, M.; Zheng, W.; Pinkham, J.; Jain, N.; Pan, M.; Deighan, P.; Rubin, E., Mycobacterial mistranslation is necessary and sufficient for rifampicin phenotypic resistance. *Proc Natl Acad Sci U S A* **2014**, *111*, 1132-1137.
120. Feng, L.; Tumbula-Hansen, D.; Toogood, H.; Soll, D., Expanding tRNA recognition of a tRNA synthetase by a single amino acid change. *Proc Natl Acad Sci U S A* **2003**, *100*, 5676-5681.

121. Feng, L.; Yuan, J.; Toogood, H.; Tumbula-Hansen, D.; Soll, D., Aspartyl-tRNA synthetase requires a conserved proline in the anticodon-binding loop for tRNA(Asn) recognition *in vivo*. *J Biol Chem* **2005**, *280*, 20638-20641.
122. Bernard, D.; Akochy, P. M.; Beaulieu, D.; Lapointe, J.; Roy, P. H., Two residues in the anticodon recognition domain of the aspartyl-tRNA synthetase from *Pseudomonas aeruginosa* are individually implicated in the recognition of tRNA<sup>Asn</sup>. *J Bacteriol* **2006**, *188*, 269-274.
123. Eiler, S.; Dock-Bregeon, A.; Moulinier, L.; Thierry, J. C.; Moras, D., Synthesis of aspartyl-tRNA(Asp) in *Escherichia coli*-a snapshot of the second step. *EMBO J* **1999**, *18*, 6532-6541.
124. Kasai, H.; Oashi, Z.; Harada, F.; Nishimura, S.; Oppenheimer, N. J.; Crain, P. F.; Liehr, J. G.; von Minden, D. L.; McCloskey, J. A., Structure of the modified nucleoside Q isolated from *Escherichia coli* transfer ribonucleic acid. 7-(4,5-cis-dihydroxy-1-cyclopenten-3-ylaminomethyl)-7-deazaguanosine. *Biochemistry* **1975**, *14*, 4198-4208.
125. Sylvers, L. A.; Rogers, K. C.; Shimizu, M.; Ohtsuka, E.; Söll, D., A 2-thiouridine derivative in tRNA<sup>Glu</sup> is a positive determinant for aminoacylation by *Escherichia coli* glutamyl-tRNA synthetase. *Biochemistry* **1993**, *32*, 3836-3841.
126. Varshney, U.; Lee, C. P.; RajBhandary, U. L., Direct analysis of aminoacylation levels of tRNAs *in vivo*. Application to studying recognition of *Escherichia coli* initiator tRNA mutants by glutamyl-tRNA synthetase. *J Biol Chem* **1991**, *266*, 24712-24718.

127. Hasegawa, T.; Himeno, H.; Ishikura, H.; Shimizu, M., Discriminator base of tRNA(Asp) is involved in amino acid acceptor activity. *Biochem Biophys Res Commun* **1989**, *163*, 1534-1538.
128. Nameki, N.; Tamura, K.; Himeno, H.; Asahara, H.; Hasegawa, T.; Shimizu, M., *Escherichia coli* tRNA(Asp) recognition mechanism differing from that of the yeast system. *Biochem Biophys Res Commun* **1992**, *189*, 856-862.
129. Sekine, S.; Nureki, O.; Sakamoto, K.; Niimi, T.; Tateno, M.; Go, M.; Kohno, T.; Brisson, A.; Lapointe, J.; Yokoyama, S., Major identity determinants in the "augmented D helix" of tRNA(Glu) from *Escherichia coli*. *J Mol Biol* **1996**, *256*, 685-700.
130. Sekine, S.; Nureki, O.; Tateno, M.; Yokoyama, S., The identity determinants required for the discrimination between tRNA<sup>Glu</sup> and tRNA<sup>Asp</sup> by glutamyl-tRNA synthetase from *Escherichia coli*. *Eur J Biochem* **1999**, *261*, 354-360.
131. Rodin, S. N.; Ohno, S., Four primordial modes of tRNA-synthetase recognition, determined by the (G,C) operational code. *Proc Natl Acad Sci U S A* **1997**, *94*, 5183-5188.
132. Shimizu, Y.; Inoue, A.; Tomari, Y.; Suzuki, T.; Yokogawa, T.; Nishikawa, K.; Ueda, T., Cell-free translation reconstituted with purified components. *Nat Biotechnol* **2001**, *19*, 751-755.
133. Wilkins, M. R.; Gasteiger, E.; Bairoch, A.; Sanchez, J. C.; Williams, K. L.; Appel, R. D.; Hochstrasser, D. F., Protein identification and analysis tools in the ExPASy server. *Methods Mol Biol* **1999**, *112*, 531-552.

134. Panavas, T.; Sanders, C.; Butt, T. R., SUMO fusion technology for enhanced protein production in prokaryotic and eukaryotic expression systems. *Methods Mol Biol* **2009**, *497*, 303-317.
135. Butt, T. R.; Edavettal, S. C.; Hall, J. P.; Mattern, M. R., SUMO fusion technology for difficult-to-express proteins. *Protein Expr Purif* **2005**, *43*, 1-9.
136. Stathopoulos, P. B.; Scholz, G. A.; Hwang, Y. M.; Rumfeldt, J. A.; Lepock, J. R.; Meiering, E. M., Sonication of proteins causes formation of aggregates that resemble amyloid. *Protein Sci* **2004**, *13*, 3017-3027.
137. Suh-Lailam, B. B.; Hevel, J. M., Efficient cleavage of problematic tobacco etch virus (TEV)-protein arginine methyltransferase constructs. *Anal Biochem* **2009**, *387*, 130-132.
138. Wood, W. N. tRNA aminoacylation: New protein players and new reactions. Ph.D. Dissertation, Wayne State University, Detroit, MI, 2019.
139. Centers for Disease Control and Prevention. Antibiotic / Antimicrobial Resistance (AR / AMR). [https://www.cdc.gov/drugresistance/biggest\\_threats.html](https://www.cdc.gov/drugresistance/biggest_threats.html) (accessed April 29).
140. Chung, G. T.; Yoo, J. S.; Oh, H. B.; Lee, Y. S.; Cha, S. H.; Kim, S. J.; Yoo, C. K., Complete genome sequence of *Nneisseria gonorrhoeae* NCCP11945. *J Bacteriol* **2008**, *190*, 6035-6036.
141. Yang, J.; Yan, R.; Roy, A.; Xu, D.; Poisson, J.; Zhang, Y., The I-TASSER suite: Protein structure and function prediction. *Nat Methods* **2015**, *12*, 7-8.

142. Miles, Z. D.; McCarty, R. M.; Molnar, G.; Bandarian, V., Discovery of epoxyqueuosine (oQ) reductase reveals parallels between halorespiration and tRNA modification. *Proc Natl Acad Sci U S A* **2011**, *108*, 7368-7372.
143. Chan, C.; Pham, P.; Dedon, P. C.; Begley, T. J., Lifestyle modifications: Coordinating the tRNA epitranscriptome with codon bias to adapt translation during stress responses. *Genome Biol* **2018**, *19*, 228.
144. Anderson, K. L.; Roux, C. M.; Olson, M. W.; Luong, T. T.; Lee, C. Y.; Olson, R.; Dunman, P. M., Characterizing the effects of inorganic acid and alkaline shock on the *Staphylococcus aureus* transcriptome and messenger RNA turnover. *FEMS Immunol Med Microbiol* **2010**, *60*, 208-250.
145. Fechter, P.; Rudinger, J.; Giege, R.; Theobald-Dietrich, A., Ribozyme processed tRNA transcripts with unfriendly internal promoter for T7 RNA polymerase: Production and activity. *FEBS Lett* **1998**, *436*, 99-103.
146. Sampson, J. R.; Uhlenbeck, O. C., Biochemical and physical characterization of an unmodified yeast phenylalanine transfer RNA transcribed *in vitro*. *Proc Natl Acad Sci U S A* **1988**, *85*, 1033-1037.
147. Cusack, S., Aminoacyl-tRNA synthetases. *Curr Opin Struct Biol* **1997**, *7*, 881-889.
148. Ruan, B.; Palioura, S.; Sabina, J.; Marvin-Guy, L.; Kochhar, S.; Larossa, R. A.; Soll, D., Quality control despite mistranslation caused by an ambiguous genetic code. *Proc Natl Acad Sci U S A* **2008**, *105*, 16502-16507.
149. Zhao, L. Enzymatic characterization of the ammonia tunnel in *Helicobacter pylori* Asp-tRNA<sup>Asn</sup>/Glu-tRNA<sup>Gln</sup> amidotransferase. Ph.D. Dissertation, Wayne State University, Detroit, MI, 2003.



**ABSTRACT****FUNCTIONAL CHARACTERIZATION OF ACCESSORY PROTEINS AND NOVEL  
ACTIVITIES IN DIRECT AND INDIRECT TRNA AMINOACYLATION**

by

**UDUMBARA MENIKE RATHNAYAKE****August 2019****Advisor:** Dr. Tamara L. Hendrickson**Major:** Chemistry (Biochemistry)**Degree:** Doctor of Philosophy

Indirect tRNA aminoacylation is essential for most bacteria and archaea, particularly when these species do not have genes encoding asparaginyl- and/or glutaminyl-tRNA synthetase (AsnRS and GlnRS). In the absence of AsnRS, the first step in Asn-tRNA<sup>Asn</sup> synthesis involves misacylation of tRNA<sup>Asn</sup> with aspartate to produce Asp-tRNA<sup>Asn</sup>; this reaction is catalyzed by a non-discriminating aspartyl-tRNA synthetase (ND-AspRS). Subsequently, in bacteria, an amidotransferase called GatCAB converts Asp-tRNA<sup>Asn</sup> to Asn-tRNA<sup>Asn</sup>. An analogous, two-step processes exist to produce Gln-tRNA<sup>Gln</sup>. In this case, a non-discriminating glutamyl-tRNA synthetase (ND-GluRS) misacylates tRNA<sup>Gln</sup> to produce Glu-tRNA<sup>Gln</sup>, which is then converted to Gln-tRNA<sup>Gln</sup> by GatCAB. The central hub of the indirect tRNA aminoacylation pathway is the formation of a macromolecular complex called the transamidosome.

In *Helicobacter pylori*, the pathogenic bacterium that causes stomach ulcers and gastric cancers, Asn-transamidosome formation requires a protein partner called Hp0100, to form a stable, tRNA-independent complex. Hp0100 accelerates the GatCAB-catalyzed transamidation of Asp-tRNA<sup>Asn</sup> into Asn-tRNA<sup>Asn</sup> ~35 fold and of Glu-tRNA<sup>Gln</sup>

into Gln-tRNA<sup>Gln</sup> ~3 fold. Our preliminary evidence suggests that Hp0100 contains two mutually exclusive ATP hydrolase domains, which are activated by Glu-tRNA<sup>Gln</sup> and Asp-tRNA<sup>Asn</sup>, respectively.

This dissertation work focusses on four different but connected projects. Chapter 2 discusses the characterization of the *Mycobacterium smegmatis* Asn-transamidosome. Overexpression of GatCAB in *M. smegmatis*, a benign, close relative of *Mycobacterium tuberculosis*, and its purification resulted in the co-purification of ND-AspRS and several other proteins. These results represent the first successful purification of a *Mycobacterial* Asn-transamidosome from its native organism. Efforts to determine if ND-GluRS also co-purified with GatCAB were inconclusive. Two of the unknown proteins that reproducibly co-purify with GatCAB were identified as a universal stress protein (USP) and superoxide dismutase (SOD), which are stress-related proteins. Chapter 3 focuses on the discovery of an unexpected enzymatic activity of AspRSs. We discovered that some bacterial, discriminating AspRS (*E. coli*) and ND-AspRSs (*H. pylori*, *M. smegmatis*, and *Staphylococcus aureus*) are capable of aminoacylating *E. coli* tRNA<sup>Glu</sup> with glutamate to produce correctly aminoacylated Glu-tRNA<sup>Glu</sup> without glutamylating their “natural” tRNAs (tRNA<sup>Asp</sup> and tRNA<sup>Asn</sup>). Chapter 4 summarizes our efforts to optimize the overexpression and purification of Hp100 without a metal-binding tag. Finally, we have identified truncated orthologs of Hp0100 in several other pathogenic bacteria outside this clade. Chapter 5 reports our preliminary characterization of a truncated ortholog of Hp0100 called Sa2591 from *S. aureus*. Sa2591 shares some functional similarities with Hp0100 and may be a sensor for the presence of post-transcriptional modifications in tRNA<sup>Asn</sup>.

## AUTOBIOGRAPHIC STATEMENT

### EDUCATION

- Ph.D. Candidate in Biochemistry** **2012 - present**  
 Department of Chemistry, Wayne State University, Detroit, MI, USA
- Bachelor of Science (B.Sc.)** **2006 - 2010**  
 Special Degree in Chemistry (Second Class Upper Honors)  
 Department of Chemistry, Faculty of Science, University of Peradeniya, Sri Lanka

### RESEARCH EXPERIENCE

- Graduate Research Assistant** **2012 - present**  
 Department of Chemistry, Wayne State University, Detroit, MI, USA  
 Graduate Advisor: Professor Tamara L. Hendrickson
- Undergraduate Researcher** **2009 - 2010**  
 Department of Chemistry, Faculty of Science, University of Peradeniya, Sri Lanka  
 Undergraduate Advisor: Professor R.M.G. Rajapakse
- Researcher** **July - Aug. 2009**  
 Veterinary Research Institute, Peradeniya, Sri Lanka

### AWARDS

- Travel Award (selected by conference organizers)** **2017**  
 11<sup>th</sup> International IUBMB Conference on Aminoacyl-tRNA Synthetases, Clearwater Beach, FL
- Departmental Citation for Excellence in Teaching Service** **2017**  
 Department of Chemistry, Wayne State University, Detroit, MI
- Graduate Student Professional Travel Award (GSPTA)** **2016**  
 Wayne State University, Detroit, MI

### PUBLICATIONS

1. **Udumbara M. Rathnayake**, and Tamara L. Hendrickson, "Some bacterial aspartyl-tRNA synthetases have glutamyl-tRNA synthetase activity." *Genes* 2019, 10(4), 262.
2. T. P. Gamagedara, **Udumbara M. Rathnayake**, and R. M. G. Rajapakse, "Facile synthesis of hydroxyapatite nanoparticles by a polymer-assisted method: morphology, mechanical properties, and formation mechanism." *J. Clin. Invest. Stud.* 2018, 1, 1-5.
3. **Udumbara M. Rathnayake\***, Whitney N. Wood\*, and Tamara L. Hendrickson, "Indirect tRNA aminoacylation during accurate translation and phenotypic mistranslation." *Curr. Opin. Chem. Biol.* 2017, 41, 114-122. \*Authors contribute equally.
4. Liangjun Zhao, **Udumbara M. Rathnayake**, Sajeewa W. Dewage, Whitney N. Wood, Anthony J. Veltri, G. Andrés Cisneros, and Tamara L. Hendrickson, "Characterization of tunnel mutants reveals a catalytic step in ammonia delivery by an aminoacyl-tRNA amidotransferase." *FEBS Lett.* 2016, 590 (18), 3122-32.